Investigation on novel Lewis acids and Lewis bases for Frustrated Lewis Pair chemistry.

F.A.L. Welling

Supervisor: Dr. Matthias Otte

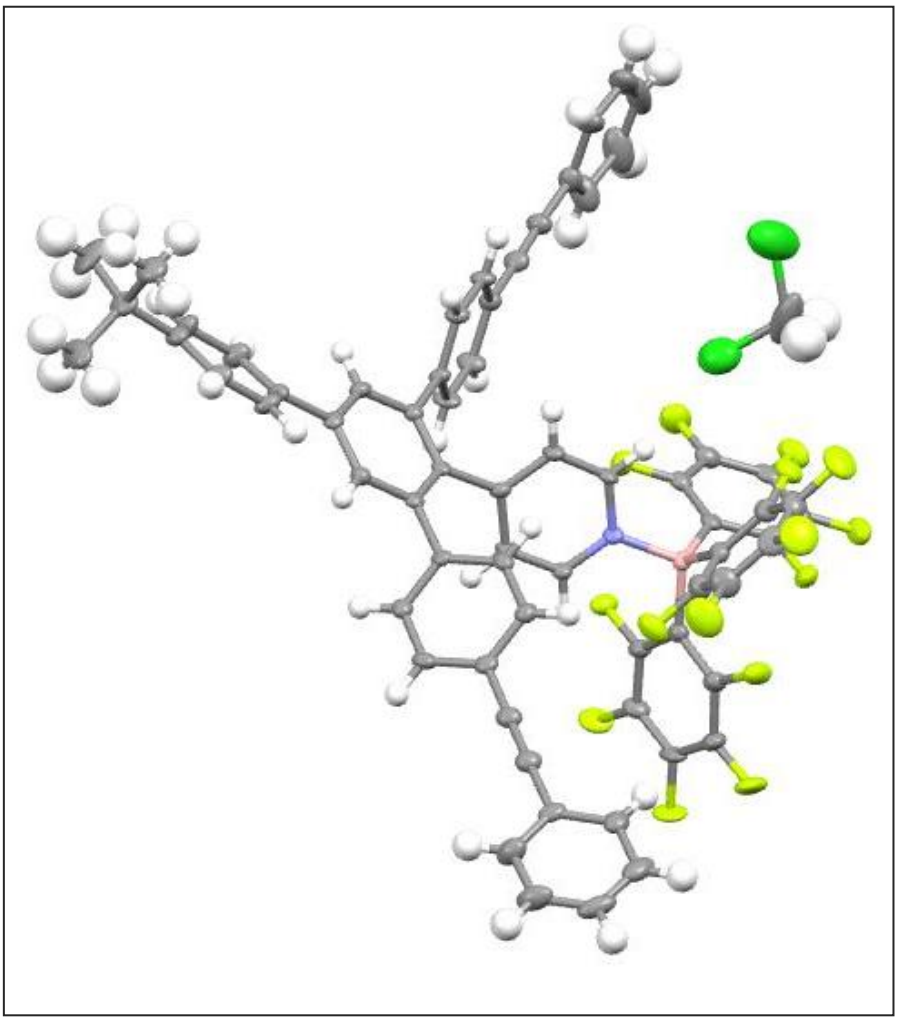

26th of February 2015
Organic Chemistry & Catalysis
Debye Institute for Nanomaterials Science
Utrecht University

Abstract

Hydrogenation reactions are a very common and widely applied in chemistry. As a result catalyzing these reactions has been and continues to be a popular topic in research. However, it remains a field dominated by platinum group transition metals which are in general scares and toxic. In 2006 Stephan et al. showed that a sterically precluded Lewis pair, so called FLP's (Frustrated Lewis Pairs), could activate molecular hydrogen for use in hydrogenation reactions. In general the steric bulk for the Lewis acids and Lewis bases in these FLP's is directly attached to the active center. However exceptions to this trend were reported by Stephan et al. in 2013 using rotaxanes as Lewis bases for FLP chemistry. This showed directly bonding the steric bulk to the active center was not required to attain a viable Lewis base for FLP chemistry.

For this project it was attempted to synthesize Lewis acids and Lewis bases capable for FLP chemistry. The bases and acids would have a comparable rigid organic backbone[39][40]. The concept is to use a large rigid backbone surrounding the active site rather than directly binding the bulk to the active site. The Lewis acids and Lewis bases were designed with the same organic backbone. For the Lewis acid several synthesis routes were explored to attain a BF_2-group as the reactive center. For the Lewis base several approaches were tested to attain a Lewis base for FLP chemistry. The first was a more linear Lewis base, the second a molecular cage and the third a macro cycles. The successfully synthesized base was tested for FLP chemistry.

The compounds that were synthesized were analyzed using Nuclear Magnetic Resonance (NMR) spectroscopy, Electron Spray Ionization Mass Spectroscopy (ESI-MS), Fourier Transform Infra Red spectroscopy (FTIR) and in one case X-Ray Diffraction (XRD).

Table of content

List of abbreviations

General:

ppm	Parts Per Million
g	Gram
mg	Milligram
ml	Milliliter
Hz	Hertz
MHz	Mega Hertz
J	Coupling constant
h	hour
s	singlet
d	doublet
t	triplet
m	multiplet
dd	doublet of doublet
dt	doublet of triplet
HOMO	Highest Occupied Molecular Orbital
LUMO	Highest Unoccupied Molecular Orbital

Analytical:

^{1}H-NMR	Proton Nuclear Magnetic Resonance spectroscopy
^{11}B-NMR	Boron Nuclear Magnetic Resonance spectroscopy
^{13}C-NMR	Carbon Nuclear Magnetic Resonance spectroscopy
^{19}F-NMR	Fluorine Nuclear Magnetic Resonance spectroscopy
APT	Attached Proton Test
COSY	Correlation spectroscopy
HSQC	Heteronuclear Single Quantum Coherence
ESI-MS	Electron Spray Ionization Mass Spectroscopy
FTIR	Fourier Transform Infra Red spectroscopy

Chemicals:

DCM	Dichloromethane
DMF	Dimethylformamide
THF	Tetrahydrofuran
TEA	Triethylamine
PE	Petrolium Ether (40-60˚C)

1. Introduction

Hydrogenation is a cornerstone in organic chemistry for the reduction of unsaturated systems. It's a transformation which is well studied and is known to work for a broad substrate scope: The reduction of ketones[1][2], imines[3][4] and olefins to name a few. A reaction this fundamental has many applications in academic research as well as industrial processes. As a consequence it can be greatly beneficial catalyzing these types of reactions with a novel approach.

1.1 Traditional hydrogenation

Hydrogenation reactions are traditionally catalyzed by platinum group metals. Examples are iridium, platinum, nickel and rhodium catalyzed processes. The metal center in these reactions hetrolytically cleave molecular hydrogen.

The metal catalyst reacts with the hydrogen on a side-on approach. In this approach the LUMO of the transition metal overlaps with the HOMO σ-orbital of molecular hydrogen. This strengthens the bond between the transition metal and molecular hydrogen, while weakening the hydrogen-hydrogen bond at the same time. In addition, the HOMO of the transition metal overlaps with the LUMO σ^*-orbital of the hydrogen (π-backbonding). This also increases the bond strength of the metal hydrogen bond and donates electron density to the anti-bonding orbital of the molecular hydrogen, further decreasing it's bond-order. A depiction of the described orbital overlap is shown in figure 1[6].

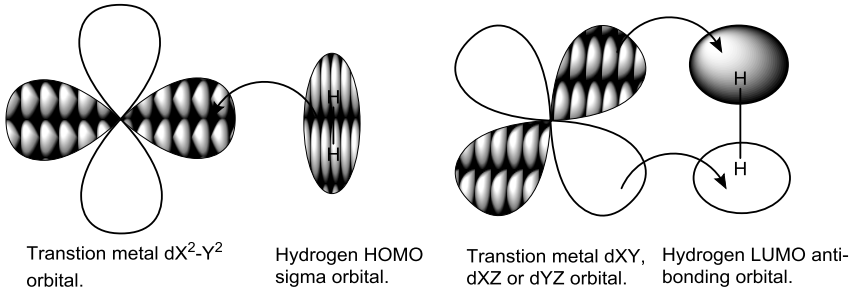

Fig. 1: Transition metal-hydrogen orbital interaction.

The hydrogen-hydrogen bond is cleaved and two hydrides are formed. These hydrides could be viewed as a more reactive or activated form of molecular hydrogen. In its activated form, the hydrogen more readily takes part in hydrogenation reactions. Hydrogenation reactions without a catalyst are possible, however this requires forcing conditions like high temperature and pressure[7][8].

As mentioned platinum group metals are very effective at activating molecular hydrogen. It is a well studied field and as a result catalysts with high turnover numbers, selectivity and stability have been developed. However catalysts based on these platinum group metals also have disadvantages.

The platinum group metals are generally toxic[9]. This can be problematic if the application for the hydrogenation product would be for instance medicine, where even trace amount of toxic metals can be considered too dangerous.
Also the platinum group metals are among the rarest in the earth's crust[10]. This of course makes them expensive but also the global availability of these metals is limited. Some of these metals (osmium and iridium for instance) are so rare that they are obtained as minor side products of the

mining of other metals like for instance platinum[11]. So it would be desirable to develop an alternative to the metals center for catalysis.

1.2 Organocatalysis

Many classic organic reactions can be catalyzed with organocatalysts. Frequently these type of catalysts rely on Lewis acetic or basic center to reversibly bind with functional groups of the substrate[12].

An example of organocatalysis is acyl-transfer reactions between an alcohol and an anhydride catalyzed with a Lewis base catalyst. An example of one of these reactions is shown in figure 2. In this reaction the alcohol is CF_3CH_2OH, the anhydride is **2** and the base is hydroquinidine (anthraquinone-1,4-diyl) (**1**). In the reaction the catalyst coordinates to the α-carbon of the anhydride. This results in the 5-memberd ring opening making it more reactive to the acyl-transfer reaction[13].

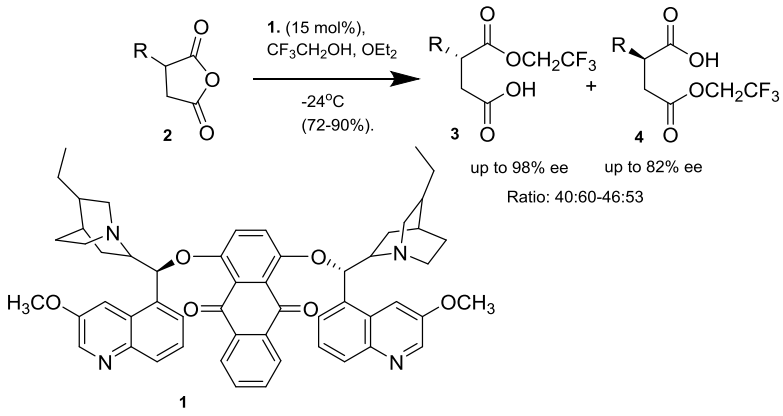

Fig. 2: The acyl-trasfer reaction between an anhydryde (**2**) and an alcohol (CF_3CH_2OH) with a chiral Lewis base (**1**) to form two enantiomerically pure compounds (**3** and **4**).

An example of a Lewis acid functioning as a catalyst is shown in figure 3. Here the Lewis acid (**5**) activates the aldehyde (**6**) by coordinating to the double bonded oxygen of the ester. This makes the aldehyde more electron deprived thus lowering the LUMO. The chiral and enantiomerically enriched nature of **5** results in the enantiomerically pure product (**8**)[14].

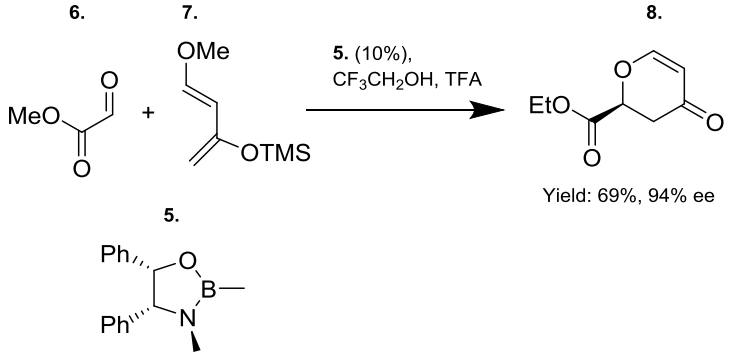

Fig. 3: hetrocyclic reaction between **6** and **7** with a chiral Lewis acid catalyst to form an entiomerically pure compound (**8**).

So both Lewis acids and Lewis bases can be catalytically active. Bases increasing the electron density on the substrate and Lewis acids decreasing the electron density on the substrate. In an ideal situation one could imagine a reaction where the Lewis base increases the HOMO of one reactant and the Lewis acid decreases the LUMO of another reactant. In this reaction the Lewis base and acid

would work in tandem to increase reactivity. Unfortunately when a "normal" Lewis acid an base are mixed they form a so called Lewis adduct quenching much of potential reactivity the pair might have had (figure 4)[15].

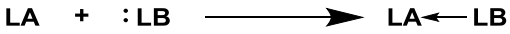

Fig. 4: Lewis adduct fromation.

1.3 Frustrated Lewis Pairs

It is however possible to prevent adduct formation of a Lewis acid and base. In 1942 Brown *et. al.* discovered that lutidine combined with BMe_3 did not form the expected Lewis adduct (figure 5)[16]. The unexpected result was contributed to the bulkiness of the lutidine and BMe_3. Several other research groups noticed similar behavior of Lewis pairs with bulky substituent. However the reactivity of these Lewis pairs was not examined further at that time[16-19].

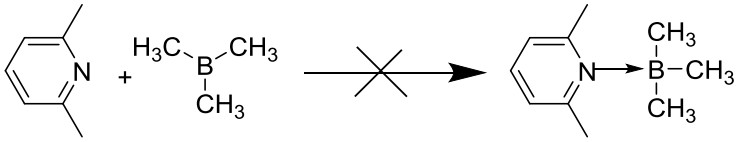

Fig. 5: Inability of lutidine to form a Lewis adduct with $B(Me)_3$.

In 2006 Stephan *et. al.* synthesized and tested the reactivity of one of these sterically hindered Lewis pairs (Frustrated Lewis Pairs) (**9**) shown in figure 6. The compound includes a sterically basic an acetic center in a single structure. The compound was shown to be able to activate molecular hydrogen[20].

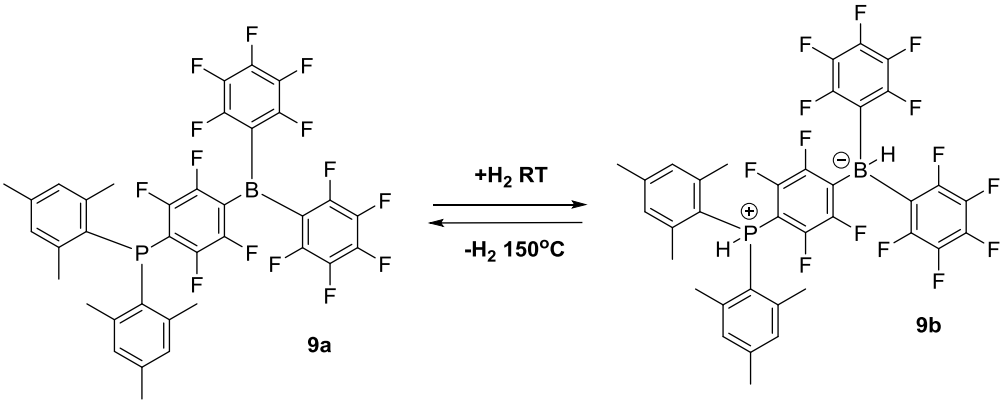

Fig. 6: The initial FLP reported by stephan et al. (**9a**) reacting with hydrogen to form **9b**.

The orbital interaction of the activation of the hydrogen with a Frustrated Lewis Pair is shown in figure 7. For this interaction the HOMO p-orbital of the Lewis base interacts with the σ^*-orbital of H_2 and the LUMO of the Lewis acid interacts with the σ-bonding orbital of the H_2[21][22]. The result is the hetrolytic cleavage of the hydrogen-hydrogen bond into a proton on the Lewis base and a hydride on the Lewis acid. This is a significant deviation from the interaction shown in figure 1 for most known transition metals.

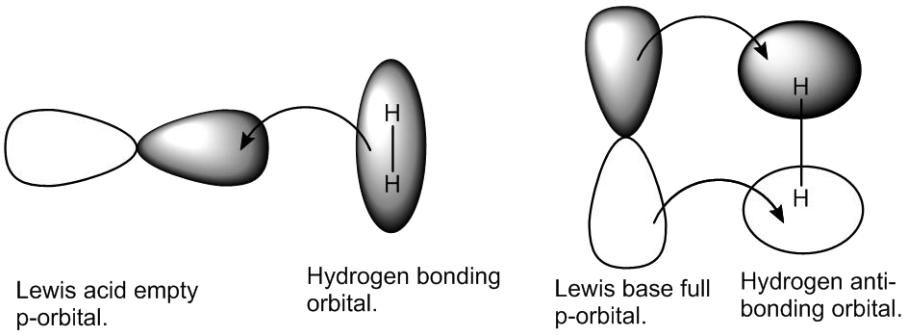

Fig. 7: Orbital overlap of a Frustrated Lewis Pair (FLP) with molecular hydrogen.

Other intra-molecular FLP's similar to **9** have been developed [23][24] and have been shown to be able to activate molecular hydrogen and subsequently catalyze a variety of reduction reactions. However these intra-molecular FLP's are not the only approach towards FLP chemistry. Alternatives are inter-molecular FLP's. In these FLP's the Lewis basic and Lewis acetic centers are in different molecules. This will now be discussed in greater detail.

The Lewis acids currently reported for FLP chemistry have a similar makeup where a boron center with 2 or 3 pentafluorophenyl-groups are used. The most commonly used is tris(pentafluorophenyl)borane (**10**) it is commercially available. Another Lewis acid is (pentachlorophenyl)bis(pentafluorophenyl)borane (**11**) unlike **10** it is reported to be air stable and is more tolerant of for instance solvents like THF[25]. The Lewis acids **10** and **11** are shown in figure 8.

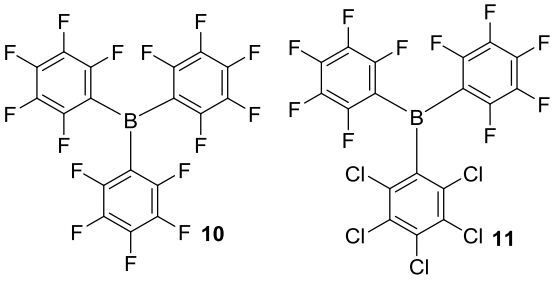

Fig. 8: A commercially available Lewis acid for FLP chemistry (**10**) and a more air stable derivative of this acid (**11**).

The bases reported to take part in FLP chemistry are more diverse. For FLP chemistry with **10** several FLP bases have been developed[26-28]. An example of such a FLP base is shown in figure 9[27]. It has been shown that this base (**12**) in combination with the commercially available Lewis acid (**10**) can activate molecular hydrogen to form (**13**). **13** has been shown to be able to catalytically reduce silyl enol ethers in the presence of molecular hydrogen[27].

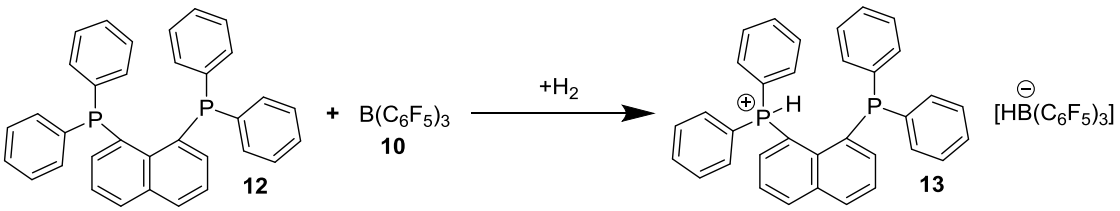

Fig. 9: A phosphine based Lewis base (**12**) reacting with a **10** and H_2 to form **13**.

In some catalytic reactions the substrate itself can be used as the base. Steric bulk does need to be present on the Lewis base in order for the substrate to be suitable. The Lewis acid used in reactions

reported so far is often **10**. The example shown in figure 10 is the reduction of an imine (**14**) followed by the activation of molecular hydrogen using the formed amine (**15**) to form **16**. Note that the amine initially forms an adduct with **10**. With more forcing conditions this adduct can still activate molecular hydrogen[29].

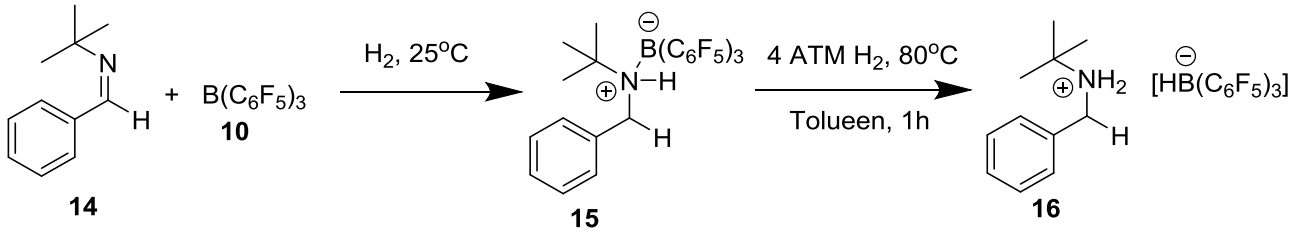

Fig. 10: The reduction of an imine (**14**) with H_2 catalyzed by **10** to form **15.** Also the subsequent reaction of **15** and **10** with H_2 to form **16**.

Another approach is to use the solvent as the Lewis base. In the example shown in figure 11 the solvent used is diethyl ether which in the presence of hydrogen and **10** can catalytically convert ketones to alcohols[30]. It is surprising diethyl ether is a viable Lewis base for FLP chemistry. Diethylether is traditionally not considered to be very sterically demanding.

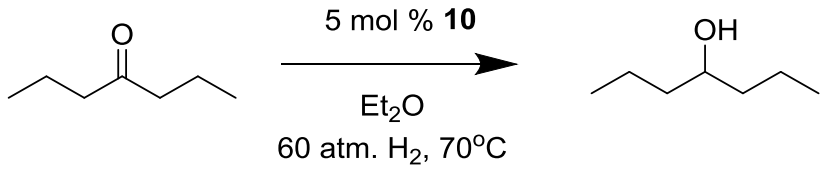

Fig. 11: Reduction of 4-heptanone with H_2 catalyzed by **10** to form 4-hetanol

In the examples of figures 9, 10 and 11 different approaches are used to achieve FLP chemistry, but also different basic centers are used. In figure 9 phosphorus is used, in figure 10 nitrogen and in figure 11 oxygen.

As mentioned earlier lutidine does not form the expected Lewis adduct with BMe_3[16]. In 2009 Stephan *et. al.*[31] showed that lutidine formed with **10** an adduct. The boron-nitrogen bond length was significantly elongated compared to unsubstituted pyridine. A similar effect was observed for other *ortho* substituted pyridine derivatives. *Para* substituted pyridine rings however did not yield the same elongation observed for the *otho* substituted derivatives (figure 12)[31].

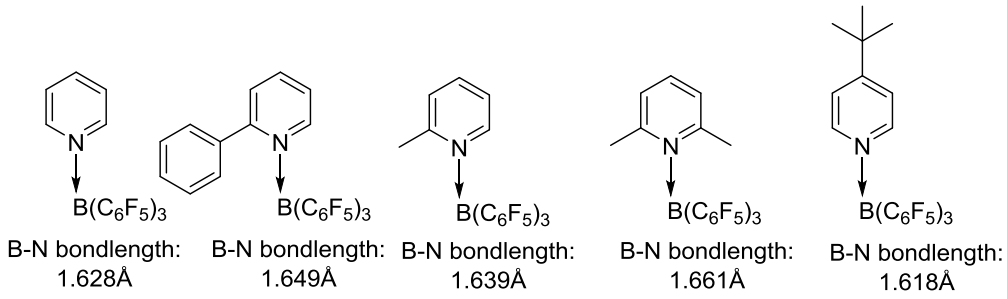

Fig. 12: B-N bond lengths of pyridine derivatives with $B(C_6F_5)_3$.[31]

Lutidine does not form an adduct with BMe_3. However, BMe_3 is not acetic enough to facilitate the activation of H_2[32]. Though lutidine does form an adduct with **10** this mixture can still activate hydrogen due to the elongated B-N bond[31].

There is an example to be noted where rotaxanes are used as the Lewis base in FLP chemistry. Rotaxanes are compounds where a macrocyclic compound (in this case a crown ether) encircles a liniar molecule (an amine in this case). The macrocycle is kept in place by steric bulk on the ends of the linear molecule. Both **17** and **18** have been shown to be able to activate moleculair hydrogen with **10** as the Lewis acid (figure 13). The difference between **17** and **18** is that **17** has a crown ether that has two more carbon atoms in its backbone. It was reported that **18** more readily reacted with H_2 and that the amine without the crown ether formed a Lewis adduct with **10**. That **17** was less reactive than **18** was contributed to the increased steric bulk of the larger crown ether[33].

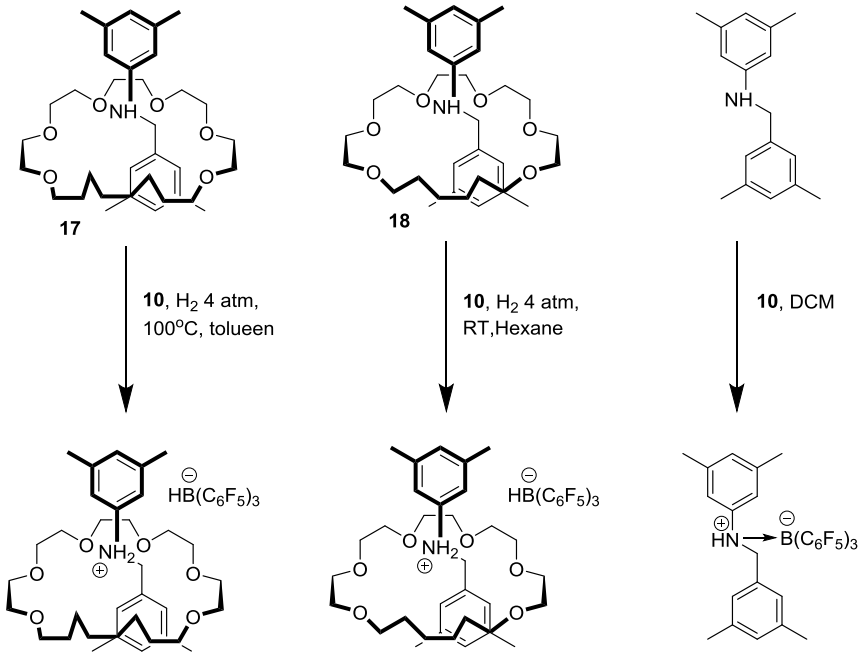

Fig. 13: FLP bases **17** and **18** with crown ethers as steric bulk (rotaxanes).

Like mentioned before ethers and also crown ethers in particular have been shown to be able to activated molecular hydrogen without the amine[34]. When hydrogen is activated with the rotaxanes it is reported that the hydrogen is observed on the nitrogen in ^{1}H-NMR[33]. However the possibility that the crown ether is somehow involved in the activation of H_2 cannot be excluded. These rotaxanes show that the steric bulk of an FLP does not have to be attached directly to the basic center in order to form a viable FLP. Moreover it is the first example of a supramolecular Lewis base suitable for FLP chemistry.

1.4 Macro cycle and molecular cage synthesis.

The crown ethers used in these rotaxanes are so called macro cycles. Macro cycles are large molecular rings. A molecular cage is similar to this, but rather encloses a space in three dimensions rather than two. Shape persistent macro cycles and cages are of particular interest as they are less likely to deform. An example of a molecular cage and a macro cycle (shape persistent) are shown in figure 14[35][36].

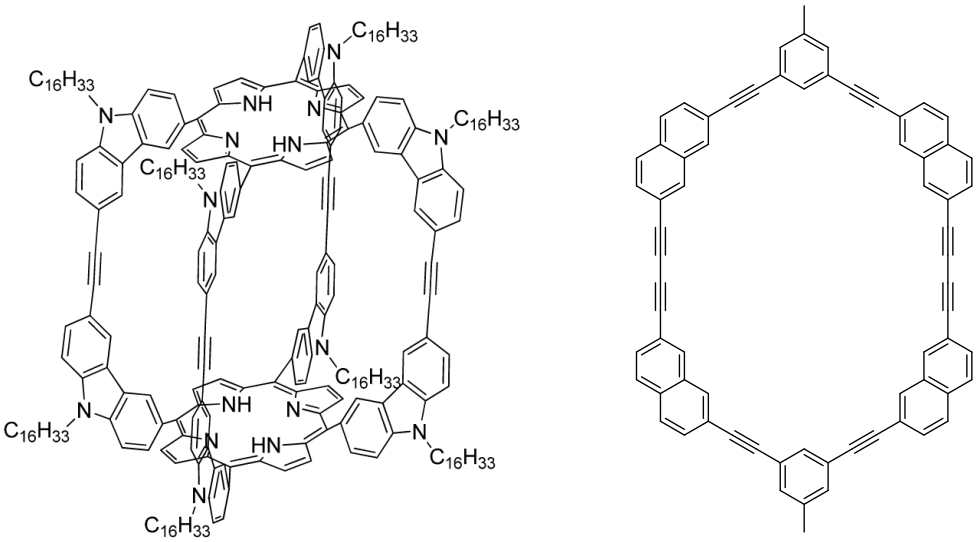

Fig. 14: On the left an example of a molecular cage[35]. On the right an example of a macro cycle[36].

Molecular cages and macro cycle synthesis can be categorized into two different approaches. The first is using a kinetic controlled or irreversible reaction and the second is a thermodynamic controlled or reversible reaction. Each of the approaches will be discussed in more detail.

Thermodynamically controlled synthesis have less difficulty with oligomerization than the kinetic controlled reactions. Several molecular cages and macro cycles have been synthesized using thermodynamically controlled reactions[37-39]. A disadvantage of this is that if the desired product is not the thermodynamic product the reaction will not work. Often unexpected/undesired cages or macro cycles are synthesized rather than the expected/desired cage or macro cycle. Also the scope of reversible reactions that can form carbon-carbon bonds is limited. In addition less work has been done on thermodynamic controlled synthesis of shape persistent macro cycles and cages. An example of a non shape persistent macro cycle synthesized with a thermodynamically controlled reaction is shown in figure 15[38].

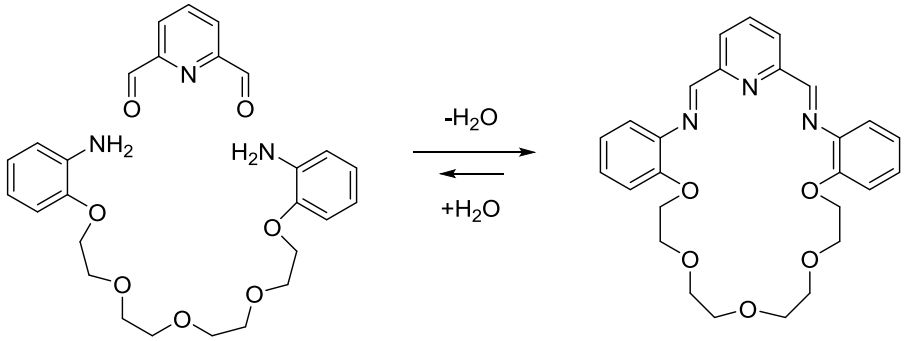

Fig. 15: Synthesis of a macro cycle using imine condensation[38].

The synthesis shown in figure 15 is an imine condensation. The resulting cycle contains two imine functionalities. This highlights a final disadvantage for the use of thermodynamically controlled reactions for the synthesis of Lewis acids and bases for FLP chemistry. Imines and most other functionalities left by thermodynamically controlled reactions are known to take part in FLP chemistry.

Most commonly used reactions to form carbon-carbon bonds are irreversible reactions and therefore kinetic controlled, for example palladium cross coupling reactions and Grignard reactions. The major disadvantage of synthesizing molecular cages or macro cycles with kinetic controlled reactions is there tendency to form oligomers. In order to prevent this high dilution and the slow dosing of building blocks are often used to minimize the oligomer formation[40][41]. An advantage of kinetic controlled reactions is that more work has been reported on the synthesis of shape-persistent macro cycles and cages. Both the examples shown in figure 14 are synthesized using Glaser cross coupling, a kinetic controlled reaction. In figure 16 the synthesis of the shape persistent macro cycle of figure 14 is shown. The reaction shown is a Glaser cross coupling reaction.

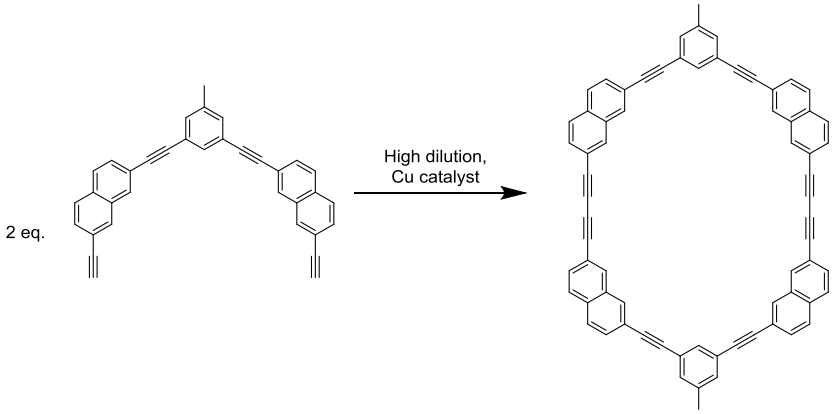

Fig. 16: Glaser cross coupling reaction to form a shape persistent macro cycle.

Macro cycles that have been reported that are of particular interest are the macro cycles developed by Höger et al. The reported shape-persistent macro cycle is synthesized using a kinetic controlled reaction[42][43]. Although the macro cycle itself will not be used in this project the precursors of these macro cycles will be.

2. Aim of the project

The goal of this project is to develop new Lewis acids and bases capable of FLP chemistry. The steric bulk should not be directly attached to the active center. This would be achieved by attaching the reactive center to a large shape persistent organic backbone. The desired effect would be that this would leave the reactive center more open to smaller molecules like H_2 and CO_2 while leaving it inaccessible to larger molecules like **10**. A graphic representation of a "traditional" FLP base, a rotaxane and the proposed FLP base are shown in figure 17.

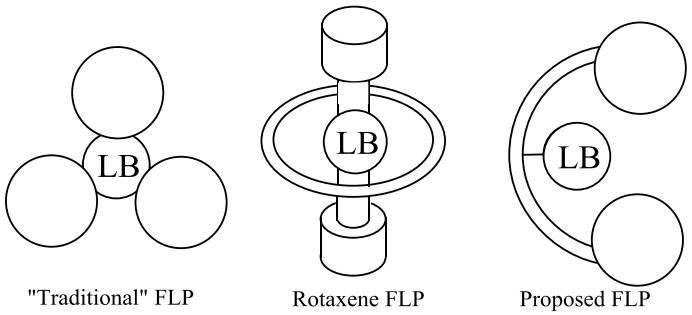

Fig. 17: Graphic representation of a traditional, rotaxene and the proposed FLP's base.

The first sub goal of the project is to synthesize the Lewis base. The basic structure of the proposed Lewis base and a 3D model of this base is shown in figure 18. The basic structure of the base is derived from a precursor of a shape-persistent macrocycle reported by Höger *et al*[42][43]. These structures were chosen for their rigid backbone. If the backbone is not rigid enough the steric bulk might simply move out of the way of approaching Lewis acids. The basic backbone shown in figure 18 could be functionalized on the positions marked by R and R' to increase the steric congestion around the pyridine ring.

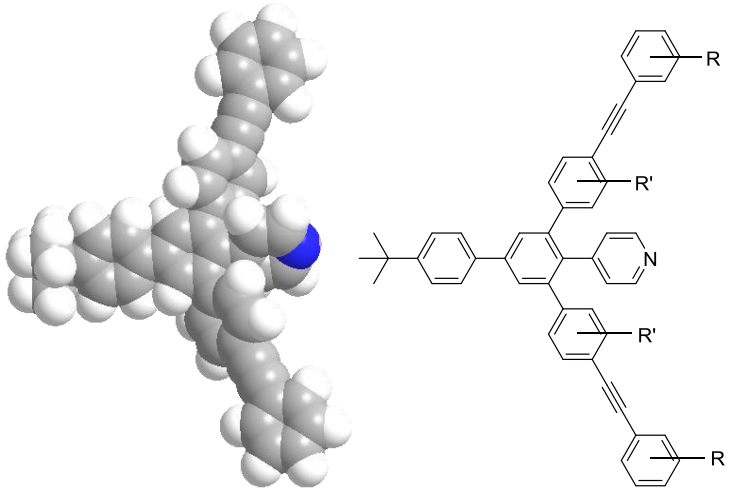

Fig. 18: The proposed FLP base and a 3D model of this base.

The second sub goal of the project is to develop a Lewis acid based on the same backbone as the proposed base (figure 19). The introduction of the BF_2-group would be an additional challenge to synthesize compounds like these.

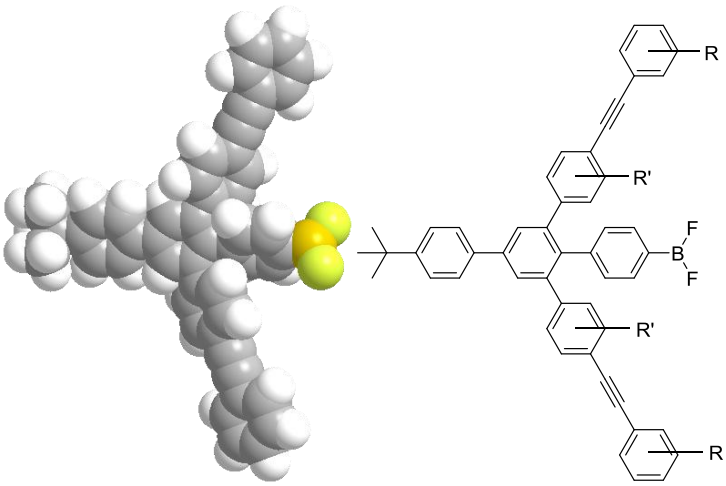

Fig. 19: The proposed Lewis acid and 3D of this acid.

If any Lewis bases or Lewis acids are successfully synthesized they have to be tested for activity in FLP chemistry. The first thing that has to be determined is if adduct formation occurs with known Lewis acids and bases capable of FLP chemistry. For Lewis bases the adduct formation would be tested with **10** and for the acid for instance 2,6-biphenylpyridine could be used, but other Lewis bases might also be viable.

If adduct formation does not occur, the Lewis acid and base mixture might be capable of activating molecular hydrogen. If it does form an adduct it might still be able to activate molecular hydrogen. So regardless of the results of the test with adduct formation, tests will be done in order to determine if the mixture is capable of activating hydrogen. This will be done by exposing the mixture in solution to a hydrogen atmosphere.

3. Results and discussion

3.1 Lewis acid synthesis

The synthesis route chosen for the proposed Lewis acid was first to synthesis the organic backbone and later introduce the BF_2-group. It was expected the BF_2-group would be to sensitive to expose to a long synthesis route and likely degrade during following reactions. In order to introduce the BF_2 functionality later a functional group needed to be present that could be replaced with the BF_2-group later. Bromide was chosen because it is known to be able to be replaced by boronic esters[44] and even BF_2[45].

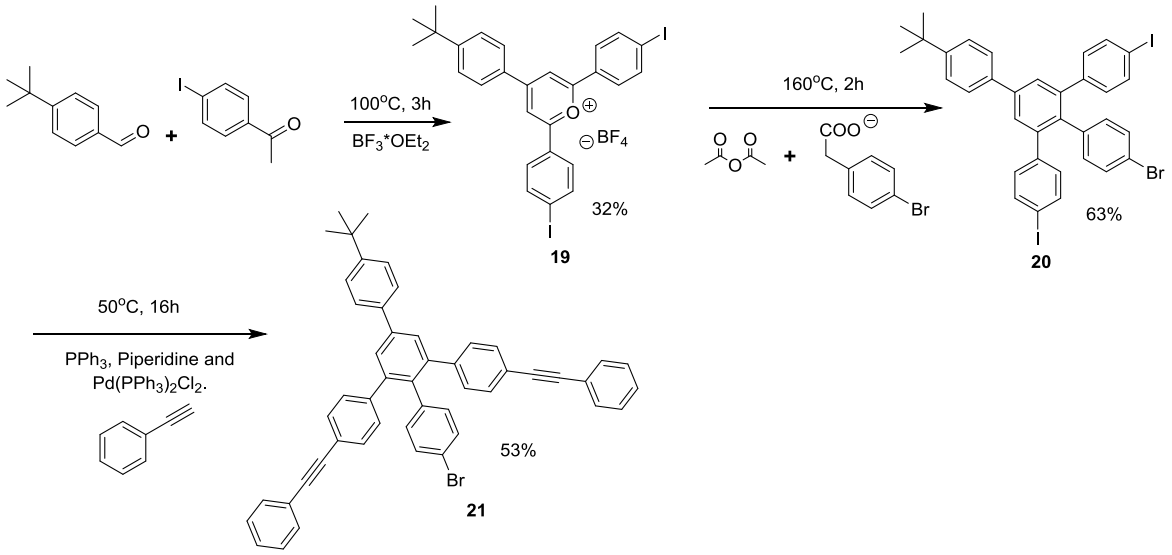

Fig. 20: Synthesis route of **21** via **19** and **20**.

An overview of the reaction pathway to **21** is shown in figure 16. The first reaction is an aldol reaction between 4-tert-butylbenzaldehyde and 4-iodoacetophenone in BF_3*OEt_2. The BF_3 binds to the aldehyde oxygen which allows for easier nucleophilic attack by the 4-iodoacetophenone. The product of a 2:1 reaction between 4-iodoacetophenone and 4-tert-butylbenzaldehyde at 100 ˚C in BF_3*OEt_2 is **19** in a 32% yield. This compound was synthesized before and tested with ^{1}H-NMR in CD_2Cl_2 by dr. Matthias Otte. His results matched literature values. The compound was used without further analysis.

The next reaction is between **19** and sodium-(4-bromophenyl)acetate. The racemic mixture of **19** with sodium-(4-bromophenyl)acetate in acetic anhydride at 160 ˚C generates **21** (63% yield). The reaction generates CO_2, which can be observed as bubbles evolving from the reaction mixture. ^{1}H-NMR was done and verified with known literature values[42].

The formed diiodo-compound (**20**) was then subjected to a Sonogashira cross coupling reaction with a palladium/copper catalyst. The amount of phenyl acetylene was decreased from an access to stochiometric amounts. This was done in order to prevent overreaction on the bromide.

The purification of **21** proved to be challenging. Several techniques where tested amongst which extraction, recrystallization and column chromatography. The eventual method that proved most effective included a column with a $CHCl_3$/PE eluence. Generally, if the PE concentration increased the separation increased as well. However as the PE concentration increased the solubility decreased to a point where it is no longer a valid eluence for a column. It was found that if a ratio of 1/3 $CHCl_3$/PE was used, a pure product could be obtained. However the separation was not ideal and the solubility

was poor. On numerous occasions the product was obtained in two fraction of which one had to be columned a second time in order to attain a pure compound.
The next reaction (the introduction of a boron center) was expected to be difficult, so this compound was analyzed more extensively. ^{1}H-NMR, ^{13}C-NMR, ^{1}H-^{1}H COSY-NMR, ^{1}H-^{13}C HSQC-NMR, APT-NMR, FTIR and ESI-MS were done.

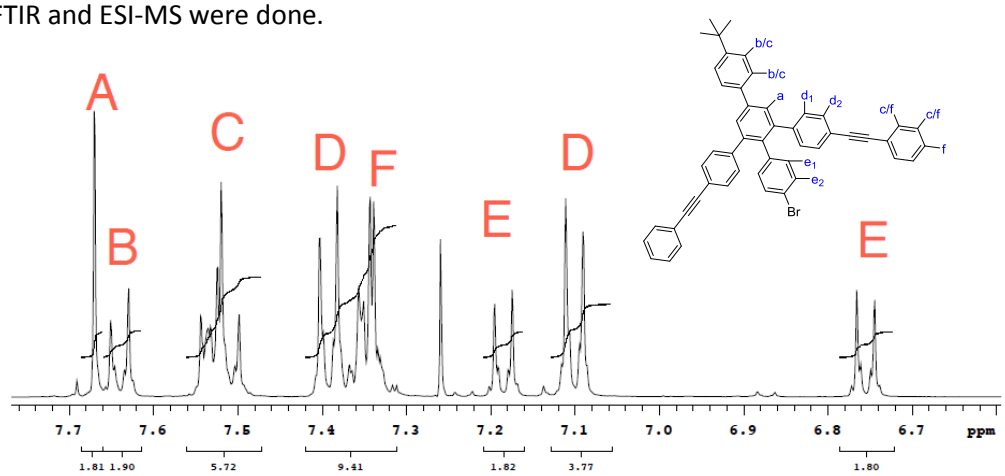

Fig. 21: A zoom in of the ^{1}H-NMR spectrum of **21**.

In the ^{1}H-NMR most peaks are in the aromatic region as it is to be expected (a zoom in of the aromatic region is shown in figure 21). At 1.38 ppm the tert-butyl-group can be identified as a singlet corresponding to 9 protons.
The bromide can donate one of its lone pairs to the phenyl ring increasing the electron density at the *ortho* postion. The protons at the *ortho* position would then be more shielded and in the ^{1}H-NMR spectrum shift up field. Therefore the peak most up field in the aromatic region (at 6.75 ppm) can be allocated to the protons at the *ortho* position with respect to the bromide (**e1**). With the COSY-NMR (figure 22) the protons that couple to those protons on the *meta* postion of that ring can be identified near 7.2 ppm (**e2**), these are marked **E** in the spectrum.

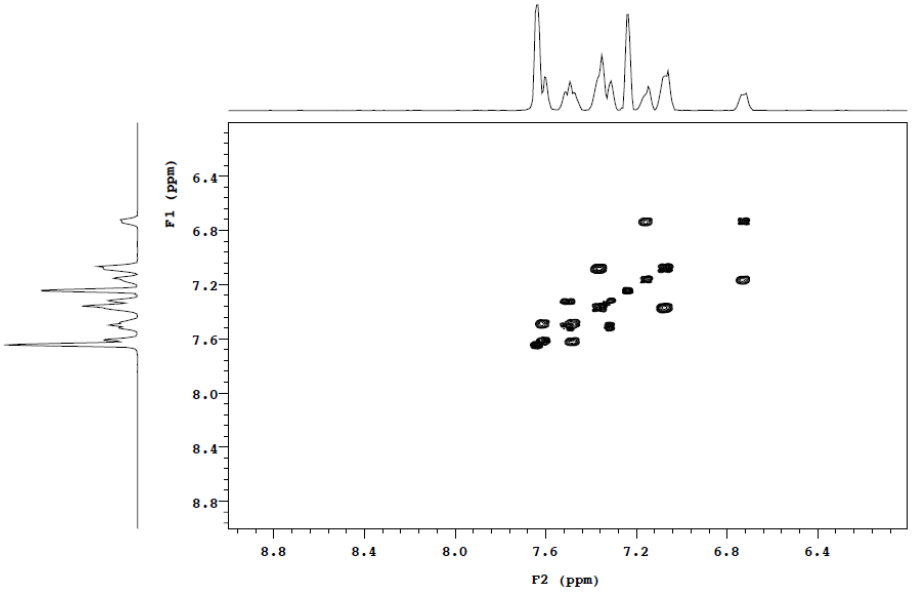

Fig. 22: COSY-NMR of the arromatic region of **21**.

The signal at 7.26 is the solvent signal of $CDCl_3$ which leaves one other singlet at 7.67 ppm. These aromatic protons do not undergo any coupling and can therefore only be the proton marked **a** in the

structure.
With integration it was determined the doublet at 7.64 ppm corresponded to 2 protons. The protons marked **b/c** could generate the doublet at 7.64 ppm (^{3}J-coupling with the neighboring hydrogen for the doublet and symmetry makes the left and right side of the phenyl ring identical to NMR) . One other doublet like the doublet marked **B** would be expected because each site marked **b/c** in the structure is expected to generate a distinguishable peak. With COSY-NMR it could be determined that one of the sites marked with **b/c** are part of the multiplet marked **C** in the spectrum.
The peaks marked **D** in the spectrum each correspond to four protons. Also each of the peaks is a doublet and with aid of the COSY-NMR it could be determined they only couple with each other. As a result these protons can only be the protons marked **d1** and **d2** in the structure.
The protons on the terminal phenyl groups still need to be allocated. Only the two multiplets remain to allocate these protons to. The first multiplet (marked by **C** in the spectrum) contains six hydrogen's of which two have already been allocated to the protons marked **b/c** in the structure. This leaves four hydrogen's in the first multiplet and six hydrogens in the second multiplet. The *ortho*, the *meta* and the *para* position of the phenyl ring would in theory each generate a distinguishable signal in the spectrum, the *ortho* and *meta* with four protons and the *para* with two. As a result the second multiplet (marked by **F** in the spectrum) must contain the protons on the *para* position and either the protons on the *meta* or the protons on the *ortho* postion. The multiplet marked **C** must then also contain the signal of either the *ortho* or the *meta* position. COSY-NMR verified that coupling occurs between multiplet **C** and **F**.
^{13}C-NMR, FTIR and ESI-MS spectra were also obtained. In the ^{13}C-NMR spectrum 2 clear signals near 90 ppm could be observed, these can be attributed to the carbon atoms in the triple bond. Formic acid and pyridine in DCM were used to attain a charged complex of **21** that could be measured with ESI-MS. In the spectrum the expected isotope distribution of pyridine^{+}+H+**21** is observed between 796-802 g/mol. Also the isotope distribution of pyridine^{+}+H+2***21** was observed between 1512-1520 g/mol.

The next step is introducing the boron group. For the first approach the goal is to convert the bromide intermediate (**21**) directly into the desired Lewis acid (**22**). This is shown in figure 23. First **21** had to lithiated, to achieve this *n*-BuLi was used. The *n*-BuLi was added at -78˚C to form (**23**). After the lithiation step, BF_3*OEt_2 was added at -78˚C with the goal to replace the Li with BF_2[45]. After the first attempt the starting material was retrieved. The most logical cause of the failed reaction was the failing of the lithiation step. If the lithiation step succeeded it would have been highly unlikely the bromide would have re-attached.

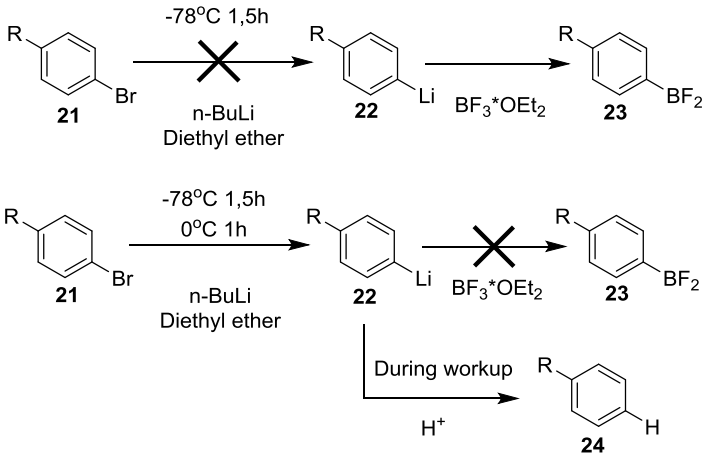

Fig. 23: The attempted conversion of **21** to the desired Lewis acid (**23**).

For the second attempt the relative amount of *n*-BuLi and BF_3*OEt_2 was increased. Also after the addition of *n*-BuLi and the reaction had stirred at -78˚C for 1.5 hours the reaction temperature was increased to 0˚C and stirred for another hour. Then the BF_3*OEt_2 was added and this was allowed to heat up to room temperature overnight. After workup ^{1}H-NMR showed clear differences with the starting material. ESI-MS did not show the expected peaks, but did show peaks that would correlate with a protonated product (**24**). It was determined the reaction had failed. The formation of **24** can be explained by a reaction with a proton of for instance water during the workup.

For the second approach **21** first had to be converted to a boronic ester (**25**) with bis(pinacolato)diboron and a palladium catalyst with PPh_3 to activate the catalyst and potassium acetate as a base (figure 24)[44].

The first attempt used dried and degassed dioxane as a solvent, a two times excess of bispinacolatodiboron and had a reaction temperature of 80˚C. A crude ^{1}H-NMR spectra showed a very cluttered aromatic region and a multiplet between 1.2-1.4 ppm. Based on this data, it would seem the reaction product contains several pinacol groups with slightly different electronic properties.

The solvent was changed to DMF so the reaction temperature could be raised to 105˚C. The initial reaction temperature would likely have been too low to facilitate the desired reaction with **21** as a substrate. It is possible the increased steric bulk of **21** makes the desired reaction more difficult. However the ^{1}H-NMR of this compound still showed a cluttered aromatic region and a multiplet between 1.2-1.4 ppm. It was attempted to purify this compound, however this was not successful. It was likely some sort of secondary reaction was occurring. The triple bonds, being the only other functionality in the structure would be the most likely candidate[46].

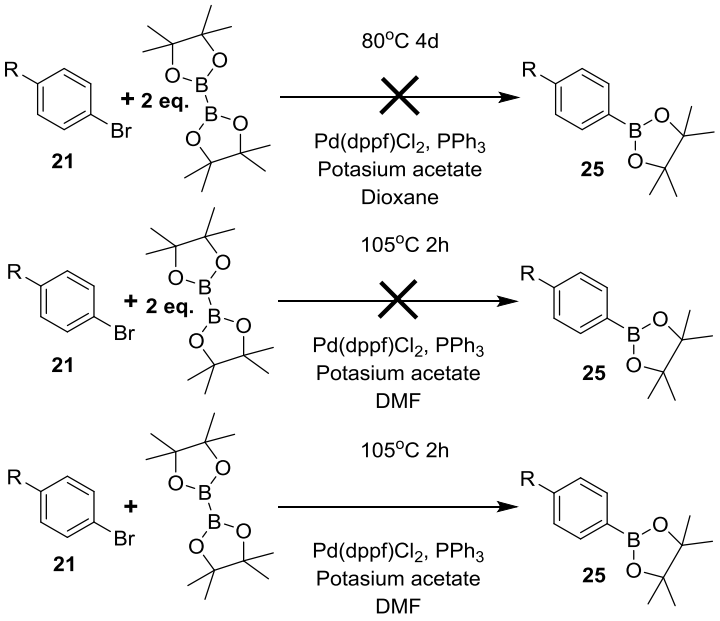

Fig. 24: The synthesis of **25** from **21** using a palladium catalyzed reaction with bispinacolatodiboron.

In the reactions so far a two times excess of the diboron compound was added. If this compound can than react with the triple bonds, several different compounds can be formed even if the reaction with the bromide occurs first because two triple bonds are also present. This would explain the cluttered ^{1}H-NMR spectra.

It is possible that the reaction has no preference to either the bromide or the alkyne functionality. If this is the case, either the triple bond cannot be present in the structure or a different reaction has to be used. If however the reaction has a preference to the bromide functionality reducing the amount of the diboron compound to stochiometric amounts would result in a more pure product. This was attempted and the resulting crude product was tested with ^{1}H-NMR (figure 25). The spectrum showed two clear peaks between 1.2 and 1.4 ppm, which is expected (one for the pinacol group and one for the *tert*-butyl group).

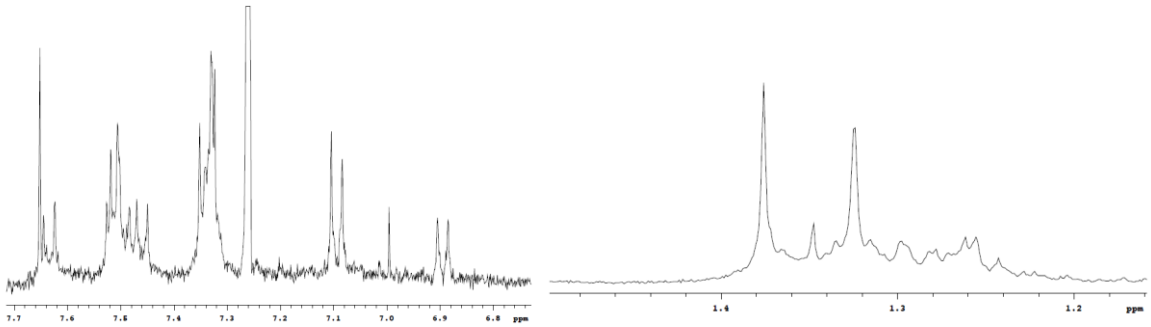

Fig. 25: A zoom in of the arromatic region and the region between 1.2-1.4 ppm of the third synthesis attempt of **25**.

Figure 25 shows that the compound is still not pure, but one major product appeared to have formed. If the major product was a reaction on the triple bonds, more major peaks are expected in the region between 1.2-1.4 ppm. Also the peaks in figure 21 that were labeled **E** (at 7.18 and 6.75 ppm) belonging to the protons on the bromophenyl-group are not present in the spectrum of **25**. This points to a reaction on the bromide and that the desired reaction occurred. It would therefore seem likely the desired product (**25**) had been formed.

During the workup a column was attempted in order to purify the sample. During the column the sample got stuck on the column. Eventually the sample was recovered from the column, however ^{1}H-NMR showed a drastically different compound. The boronic ester likely oxidized to formed a boronic acid on the column.

The synthesizing and purifying of precursors for the Lewis acid was very time consuming and the backbone was as of yet untested in FLP chemistry. The Lewis base is less challenging to synthesize. So developing a Lewis base that can successfully take part in FLP chemistry would most likely also be easier and less time consuming. Ones the Lewis base is synthesized and proven to work for FLP chemistry, the backbone can be used for the Lewis acid. This would improve the chances of the Lewis acid working in FLP chemistry on the first try and decrease the time required to develop the backbone for the Lewis acid. It was therefore decided to develop the Lewis base first before resuming the development of the Lewis acid. Unfortunately, due to time constraints, the synthesis of the FLP acid was not attempted again.

3.2 Non cyclic base synthesis

The first reaction in the synthesis of the base is identical as the first reaction of the acid: the aldol reaction between 4-tert-butylbenzaldehyde and 4-iodo-acetophenone. Therefore this reaction will not be explained further.

The second reaction of the base synthesis is similar to the second reaction of the acid synthesis. The reaction is between **19** and sodium-(4-pyridyl)acetate. The racemic mixture of **19** with sodium-(4-pyridyl)acetate in acetic anhydride at 160 ˚C yields **26** (96% yield). The reaction generates CO_2, which can be observed as bubbles froming in the reaction mixture. ^{1}H-NMR was done and verified with known literature values[43].

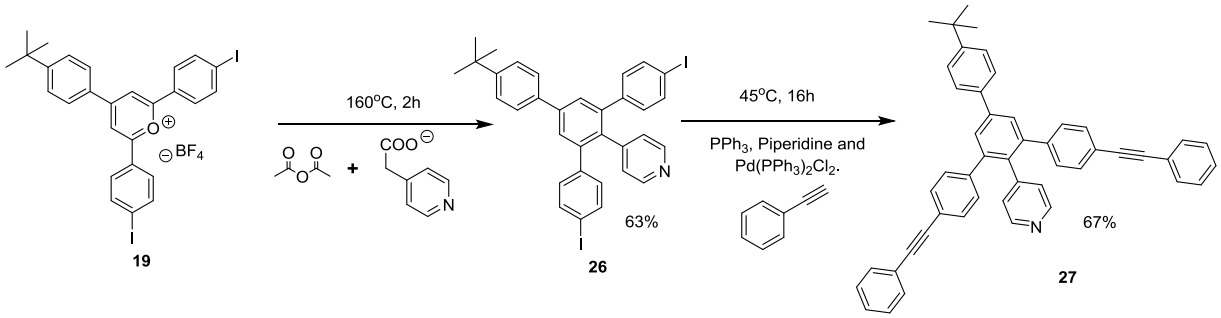

Fig. 26: Synthesis route to **27**. First the aldol reaction to form **19**, followed by the introduction of the pyridine ring and finally the Sonogashira reaction with phenylacetylene to form **27**.

To obtain **27** a Sonogashira reaction with **26** and phenylacetylene was done. The reaction conditions were similar compared to the Sonogashira reaction used in the synthesis of **21**. The overall reaction pathway is shown in figure 26. **27** was isolated with a 67% yield and analysed with ^{1}H-NMR, ^{13}C-NMR, ESI-MS and FTIR. ^{13}C-NMR shows two signals near 90 ppm. Which again can be allocated to the carbon atoms in the triple bonds.

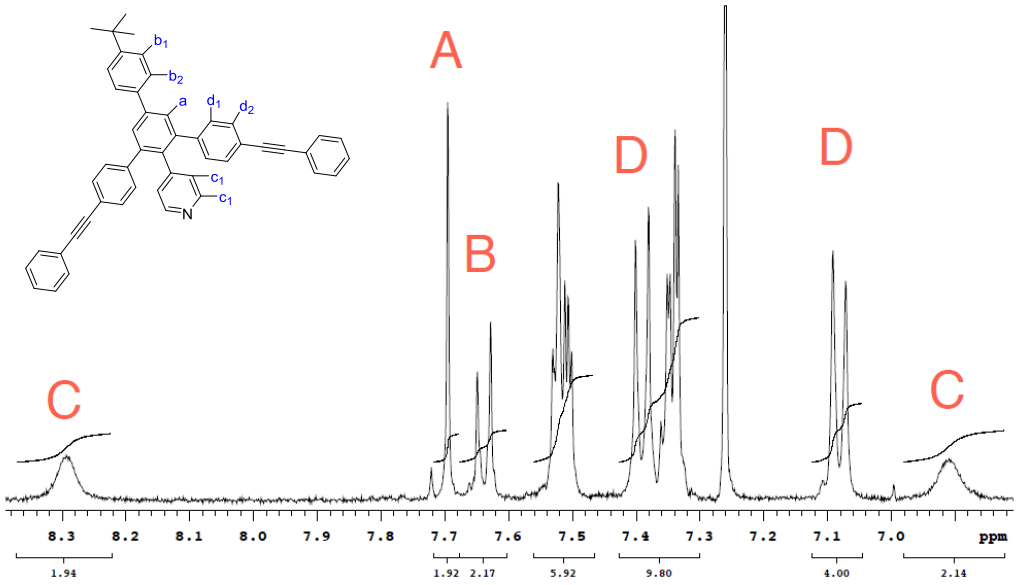

Fig. 27: A zoom in of the aromatic region of the ^{1}H-NMR spectrum of **27**.

The aromatic region of the ^{1}H-NMR spectrum is shown in figure 27. The structure of **27** is comparable to the structure of **21**. The spectrum seems to reflect this and protons marked **a**, **b** and **d** as well as the *tert*-butyl group protons can be allocated in a similar fashion to the protons of **21** (figure 21). Though it must be noted no COSY-NMR was done for this compound.
The peaks marked by **C** are significant deviation of the spectrum of **21** (figure 21) and it can be concluded that these must then belong to the protons of the pyridine ring. The nitrogen in the pyridine ring can accept electrons from the ring deactivating the *ortho* position on the ring resulting in an down field shift. The meta position of the ring however is not affected by this due to resonance and the signals of these protons would be expected significantly up field compared to the *ortho* position. Doublets are expected for the pyridine protons (^{3}J-coupling with each other) , however the broadness of the peaks masks any coupling. The broadness of the peaks also points to the pyridine ring because the pyridine ring is a Lewis base and can therefore interact with a proton. This is interaction of the pyridine ring with a proton is an equilibrium and over the NMR timescale this is observed as a broadening of the peaks.

FTIR and ESI-MS spectra were also obtained. Formic acid in DCM was used in order to protonate the sample for ESI-MS. The ESI-MS spectrum showed the expected peak pattern of M^{+}+H between 640-644 g/mol. Compound **27** was tested for FLP chemistry with the commercially available FLP Lewis acid (**10**). These results will be discussed in the next paragraph.

In order to synthesize a more sterically precluded derivative of **27** a more bulky terminal benzyl group can be used. It was attempted to introduce such a terminal group using compound **30**. The synthesis route that was attempted to attain this compound is shown in figure 28.
The synthesis route of Yamamoto et al[47] was used to attain 1-bromo-4-chloro-2,6-diiodobenzene (**29**). In the first reaction silversulfate and iodine is added to 4-chloroaniline to form 4-chloro-2,6-diiodoaniline (**28**). The silver sulfate dissociates into 2*Ag^{+} and SO_4^{2-} of which the Ag^{+} crashes out of solution with iodide as AgI. This leaves I^{+} and SO_4^{2-} in solution of which the I^{+} can undergo electrophylic aromatic substitution on the 2 and 5 positions of 4-chloro-aniline. These positions are favored because of the activating nature of amine and deactivating nature of the chlorine on the ring.
The second step the of the reaction is a Sandmeyer reaction with $CuBr_2$ and a *t*-BuONO catalyst. The *t*-BuONO generates NO^{+} which forms a aryl diazonium salt with **28**. This can then react with $CuBr_2$ to form 1-bromo-4-chloro-2,6-diiodobenzene (**29**). For the third step a Sonogashira cross coupling reaction with the reaction conditions of the synthesis of **21** to form **30** has been used.

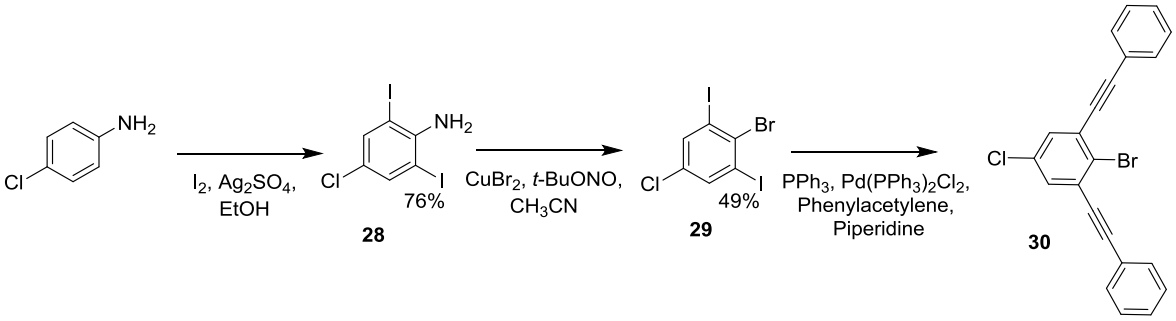

Fig. 28: Synthesis of **30** via **28** and **29**.

^{1}H-NMR of **28** and **29** were compared to literature values. These matched and **28** and **29** were used without further analysis. Though the initial synthesis of **28** was successful, in the group further attempts to synthesize **28** have failed either resulting in a mono substituted product or no reaction at all.

30 was analyzed with ^{1}H-NMR, ^{13}C-NMR, FTIR and ESI-MS. ESI-MS did not show the expected peaks. This could mean the reaction did not occur. It is however also possible the sample simply could not be charged and therefore not measured.

^{1}H-NMR was cluttered and it is likely several compounds were present. Attempts to further purify the compound failed. ^{13}C-NMR showed two peaks to many, one near 81 ppm and one near 74 ppm.

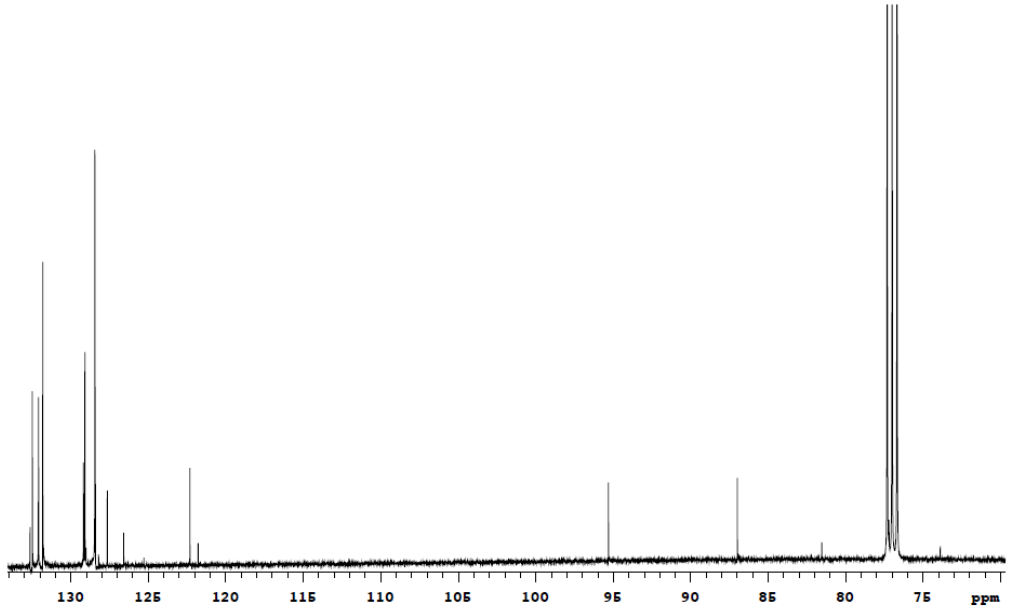

Fig. 29: ^{13}C-NMR of **30**.

In figure 29 a section of the ^{13}C-NMR is included. It can be seen a peak at 81.5 ppm and a peak at 73.9 ppm are present in the spectrum. These perfectly match values reported by Mack *et al*[48]. for the homo coupling product of phenyl acetylene. The other ^{13}C-NMR peaks reported were 121.8, 128.4, 129.2 and 132.5 ppm[48]. Peaks are also present at these values in the obtained spectrum however if these peaks are of the homo coupling product one peak must overlap with one of the peaks of **30**. If the homo coupling occurred it would be via a Glaser cross coupling reaction. These type of side reactions have been reported for Sonogashira reactions[49]. The impure **30** was used without further purification in the subsequent Sonogashira reaction with the assumption the impurity was the homo coupling product.

In order to use **30** in a Sonogashira reaction an acetylene functionality had to be introduced to **26**. To achieve this a Sonogashira reaction with **26** and TMS-acetylene was done followed by a deprotection with potassium carbonate. Initially the deprotection was done over 5 hours, however a crude ^{1}H-NMR showed the reaction was incomplete and the reaction time was increased to 16 hours. The longer reaction time is most likely caused by the pour solubility of **31** in methanol. The overall reaction is shown in figure 30.

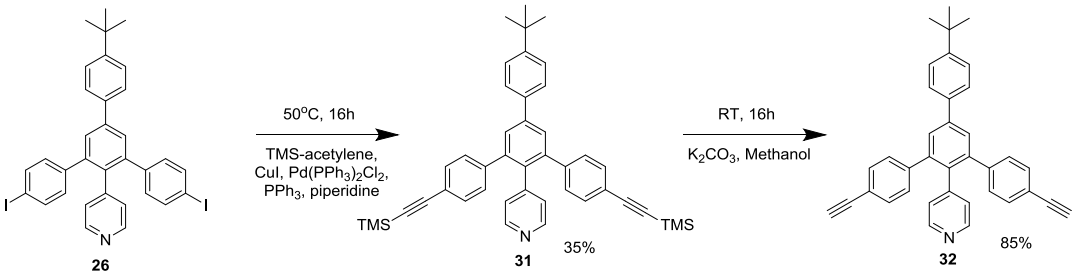

Fig. 30: The synthesis of **32** via **31**.

With both the product of the Sonogashira reaction (**31**) and the deprotection (**32**) difficulties were encountered during the column. Roughly one hour into the column of both compounds, the compounds got stuck on the column. For the product of the Sonogashira reaction switching the eluence from a $CHCl_3$/PE mixture to pure $CHCl_3$ released it form the column.
For the deprotection two columns were done, the first was with CH_2Cl_2. The sample got stuck and the solvent was switched to $CHCl_3$ to release the product from the column. The product was still impure, so a second column was done with $CHCl_3$. However the product again got stuck and 1% TEA had to be added to the eluence in order to release it again.

An overlay of the aromatic region of the ^{1}H-NMR spectrum of **31** with **26** is shown in figure 26. In the figure the purple graph is **26** and the green graph is **31**. It can also be seen the pyridine peaks are very broad in **31**. This would indicate a relatively large amount of protons in the sample of **31** with which the pyridine ring can interact. It would therefore seem likely **31** got stuck on the column because it got protonated by either the chloroform or the silica gel itself.

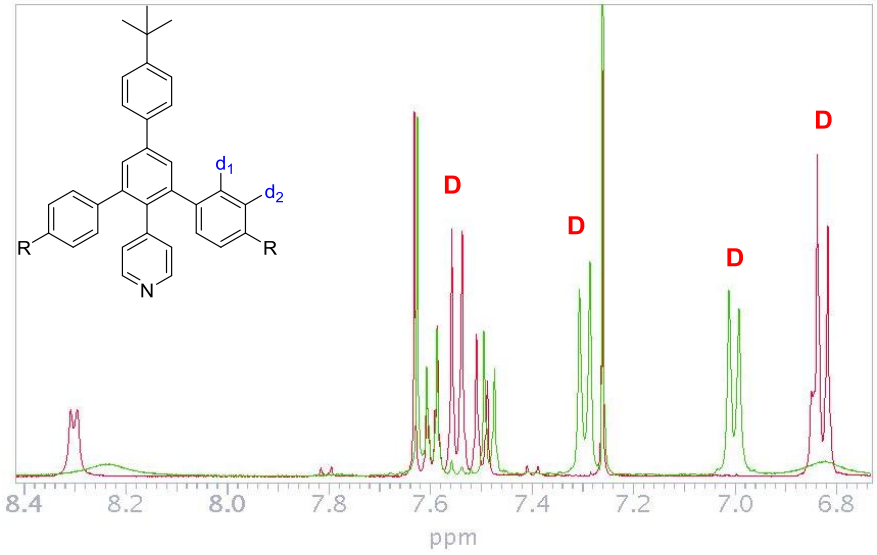

Fig. 31: Overlay of the arromatic region of the ^{1}H-NMR spectrum of **31** (green) and **26** (purple).

The spectrum of **26** and **31** can be compared to the spectrum of the previously synthesized FLP base (**27**). The most notable peaks in the spectrum are the larger doublets (marked by **D**) that can be assigned to the protons marked **d1** and **d2**. These are the rings containing the iodine and it is therefore expected that these protons show the greatest shift compared to the staring material. This is indeed what is observed as the more down field peak shifts up field and the more up field peak shifts down field. This fits expectations as the iodine can donate its long pairs to increase electron density on the *ortho* position whilst the electron withdrawing nature of the iodine reduces the

electron density on the *meta* position. The loss of the iodine would shift the signal of the proton on the *ortho* position down field and shift the signal of the proton on the *meta* postion up field. This due to increasing and decreasing shielding around the mentioned protons.
A minor amount of impurities, presumably the starting material due to the shift, can be observed near 7.57 ppm. However the amount was presumed negligible and the deprotection was carried out without further purification.

The aromatic region of the ^{1}H-spectrum of **32** is shown in figure 27. In the figure the small impurity observed in the spectrum of **31** is no longer present. Also the pyridine signals are not broad in the spectrum due to the small amount of TEA used to release the product from the column.

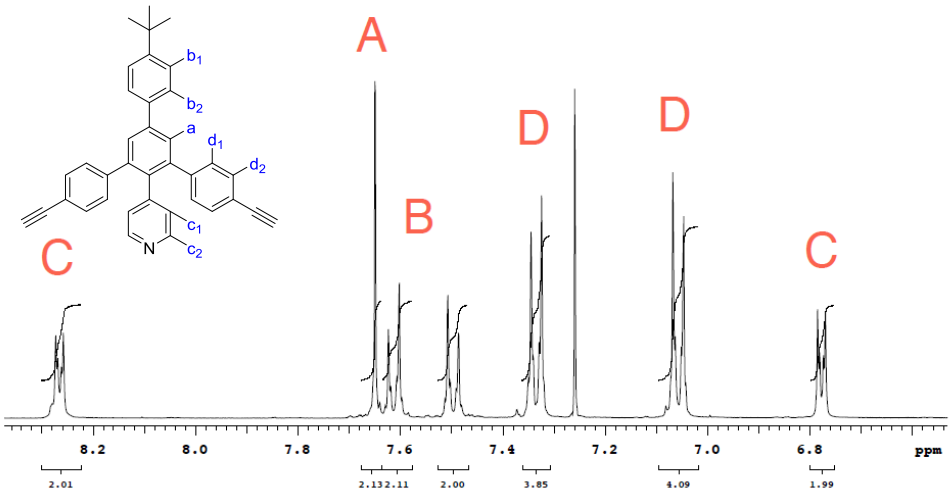

Fig. 32: A zoom in of the aromatic region of the 1H-NMR spectrum of **32**.

A small shift of the peaks belonging to the phenyl ring *ortho* compared to the pyridine ring (marked **D** in the figure) can be noted. Both shift slightly down field, which would point to a loss in electron density on these protons. This is not an unexpected result considering the loss of the electron donating TMS-group. It is however also possible the changed electronic environment of the pyridine due to the protonation is effecting the peaks in the spectrum elsewhere in the structure. Other peaks worth noting are the disappearance of the TMS peak near 0.2 ppm and the appearance of a peak near 3 ppm. With integration it was determined the peak near 3 ppm accounted for 2 protons. This peak can be attributed to the newly introduced acetylene protons and confirm the successful deprotection.

Besides ^{1}H-NMR, ^{13}C-NMR, FTIR and ESI-MS were done in order to verify the formation of the correct compound. Two peaks near 80 ppm were observed in the ^{13}C-NMR spectra pointing to the carbon attoms in the acetylene functionality. ESI-MS showed the expected peaks between an m/z value of 488-491 g/mol for the M^{+}+H signal as well as the expected peaks between an m/z value of 975-979 g/mol for the M_2^{+}+H signal. Formic acid was used to protonate the sample for the ESI-MS and the solvent was DCM.

As the bromine is less reactive then iodine in a Sonogashira reaction, modified reaction conditions had to be employed. The reaction conditions chosen were a $Pd(PPh_3)_2Cl_2$ (2 mol %) and CuI (1 mol %)

catalyst, with TEA as a solvent. These conditions were chosen because of its high reported yield in the transformations of related substrates[50]. The reaction between **30** and **32** is shown in figure 28.

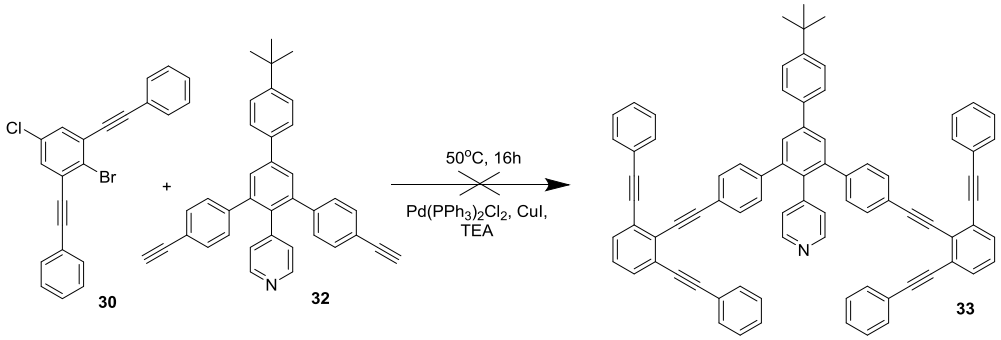

Fig. 33: Synthesis of **33** using **30** and **32** with a Sonogashira reaction.

This reaction however failed, an insoluble white solid was obtained and the starting material (**30**) was recovered. It is possible the homo coupling product coordinated to the catalyst and made it inactive. The reference paper uses bromo-benzaldehydes as substrates. It is possible that the reaction conditions were not sufficient to facilitate a reaction for a substrate without the benzaldehyde functionally[50]. What is also possible is that the synthesis of **30** was unsuccessful and the incorrect compound was used in the synthesis. The insoluble solid are likely oligomers formed by the homo coupling of **32**.

In order to increase reactivity It was attempted to substitute the bromine on **30** with iodine using *n*-BuLi and I_2 (figure 34)[51]. At -78˚C *n*-BuLi was added to a solution of **30** in THF. This turned the solution purple, pointing to a reaction occurring in solution. I_2 was added and the solution turned red-brown which is to be expected for Iodine in solution. The solution was stirred for 2 hours at -78˚C and 1 hour at RT.

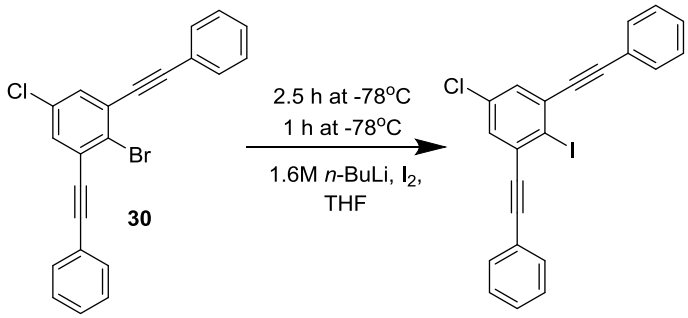

Fig. 34: Reation of **30** with *n*-BuLi and I_2.

After workup a crude ^{1}H-NMR was done. The obtained spectrum was cluttered and was still a mixture of compounds. It is likely more than one compound was formed in the reaction. It would seem likely the initial synthesis of **30** was unsuccessful and that this is caused both this synthesis as well as the synthesis of **33** to fail. It is however also possible a side reaction occurred with the chlorine in the structure of **30**.

An attempt was also made to synthesize a derivative of **30** that substitutes the chlorine with a *tert*-butyl group. A different reaction was used to introduce the iodine on the phenyl ring than was used for **28**[52]. The different reaction was used because of the problem encountered reproducing the

initial results. Also the chosen reaction is a direct reproduction of literature which would not be the case if the reaction condition were used from the synthesis of **28**.

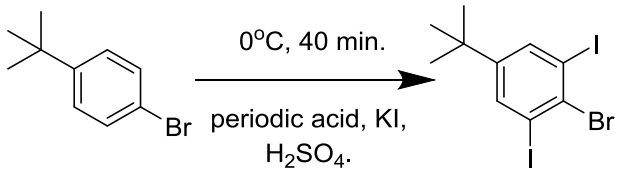

Fig. 35: Introduction of iodine into 1-Bromo-4-*tert*-butylbenzene.

Periodic acid was dissolved in sulfuric acid and KI was added. The solution turned purple and a crust formed on the surface that could not be redissolved. Reaction was continued by cooling to 0˚C followed by the addition of 4-*tert*-butyl-1-bromobenzene. This was stirred for 40 minutes at 0˚C. After workup ^{1}H-NMR showed the starting material. It is likely the crust that formed on the reaction surface before adding the 4-*tert*-butyl-1-bromobenzene prevented the reagents from mixing properly, causing the reaction to fail.

3.3 FLP experiments

The base (**27**) that was successfully synthesized was tested on its FLP behavior. In order to do this the test was split up into two parts. The first part was to compare the NMR spectra of the mixed Lewis pair of (**27**) with the commercially available Lewis acid (**10**) with the NMR spectra of the unmixed compounds. The second part is to see if the mixture of **27** and **10** can activate hydrogen.

For the first part **27** and **10** were mixed in stochiometric quantities in toluene-d8. This was done under an inert atmosphere to prevent the Lewis acid from coordinating to moisture in the air. Toluene was used because this is a solvent commonly used in literature for FLP chemistry. This makes it possible to compare the attained data with literature. The ^{1}H-NMR, ^{19}F-NMR and ^{11}B-NMR spectra of the mixed and unmixed base and acid were compared.

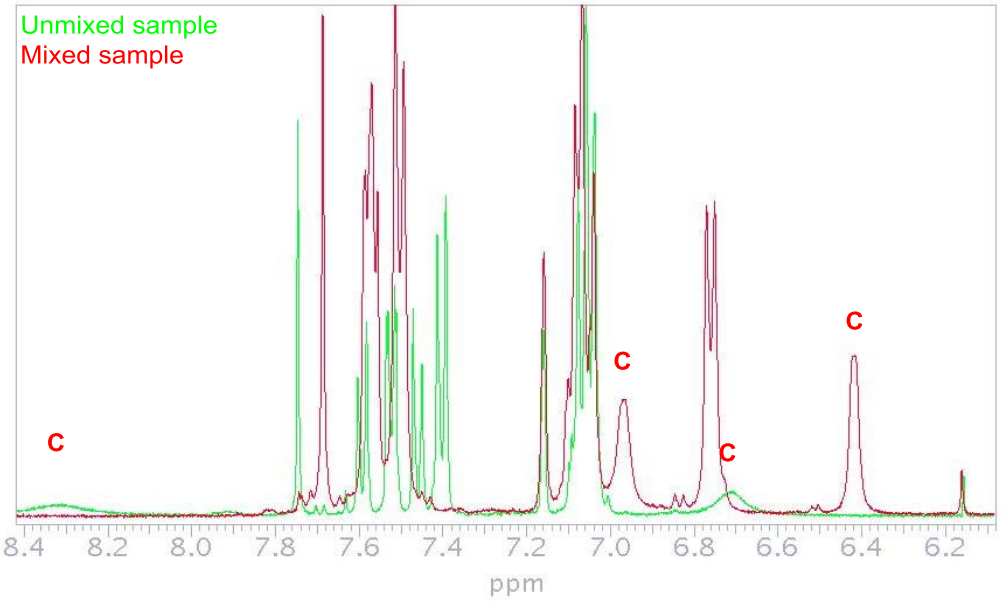

Fig. 36: The overlay ^{1}H-NMR spectrum of **27** with (red) and without (green) **10**.

In figure 36 the overlay of the aromatic region of the ^{1}H-NMR spectra are shown. In the overlays the green line is of the unmixed **27** and the red line is of the mixed sample. The main peaks of intrest are the peaks corresponding to the pyridine proton. If the nitrogen of the pyridine coordinates to **10** these peaks would shift significantly. The ^{1}H-NMR spectrum indeed shows significant shifts of the broad pyridine peaks in the spectrum (marked **C**) which indicates adduct formation. Other peaks also shift, however these are difficult to allocate due to the toluene solvent signals.

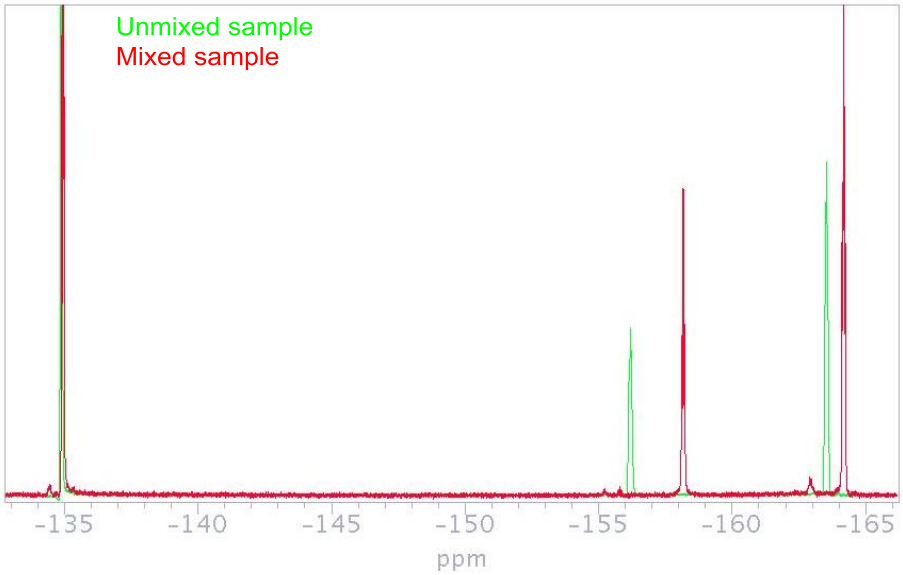

Fig. 37: Stacked ^{19}F-NMR of unmixed **10** (green) and **10** and **27** mixed (red).

An overlay of the ^{19}F-NMR spectrum of **10** (green) and **10** mixed with **27** (red) is shown in figure 37. This spectrum also shows clear shifts of two of the three peaks. It is therefore likely an adduct is formed.

16 hours after the mixing of the sample, hydrogen was added and the sample was measured again. A hydrogen peak was observed in the ^{1}H-NMR, but also a new set of peaks appeared in the ^{19}F-NMR. The sample was measured several times over the next 12 days and it was observed the new peaks grew larger whilst the existing peaks grew smaller. The ^{19}F-NMR spectrum of the sample with hydrogen after 16 hours, 40 hours and 12 days (green, red and black respectively) is shown in figure 38.

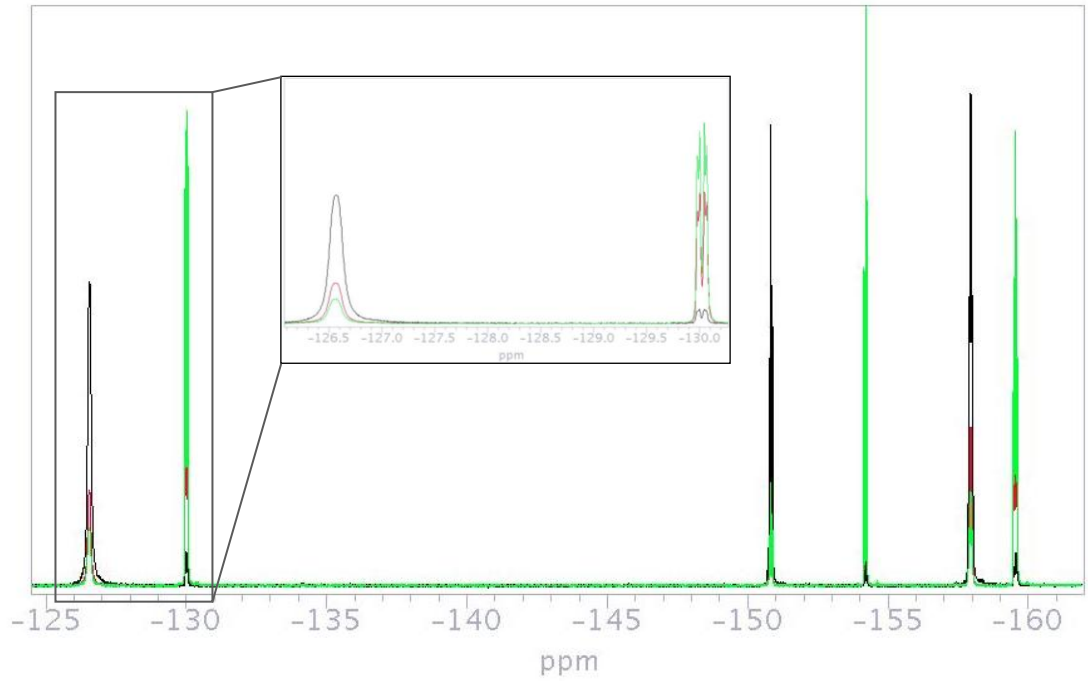

Fig. 38: Mixture of **27** and **10** over time.

To test if the effect was caused by the hydrogen, the reaction was repeated without hydrogen over one day. The same new peaks were observed, also several other minor peaks formed in the sample without hydrogen. This is however most likely because a regular NMR tube was used instead of a J. Young tube. The regular tube is not as well sealed and thus the sample gets exposed to air.
This was an unexpected result as no real explanation could be given for the formation of the new peaks in absence of hydrogen. The obtained ^{19}F-NMR spectrum of the Lewis acid was compared to reported spectra[53]. The reported values for ^{19}F-NMR spectrum of **10** are -161, -144 and -128. This is clearly different from the obtained spectrum (the green line in figure 30). Also a peak in the ^{11}B-NMR is expected near 60 ppm which is not present. It is likely the batch of **10** that was used had interacted with some sort of Lewis base (possibly moisture from the atmosphere), effectively quenching any reactivity. The change in the ^{19}F-spectrum before and after mixing might be an exchange of the Lewis base attached to **10**.

The experiment was repeated in CD_2Cl_2 with a new batch of **10**. The compound was first tested with ^{19}F-NMR and ^{11}B-NMR to check if the correct compound was used[53]. CD_2Cl_2 was used instead of toluene so it could be used as a reference for other compounds synthesized within our group.
Again upon mixing of **27** and **10** significant changes could be observed in the ^{1}H-NMR and ^{19}F-NMR spectra. Also a minor broad peak in the ^{11}B-NMR disappeared near 60 ppm. All of which point to the formation of an adduct. To check if a slow conversion like the one observed with the previous batch of **10** occurs the sample was tested again after two days. This time no new peaks were observed. The ^{19}F-NMR spectrum of **10** mixed and unmixed with **27** are shown in figure 39.

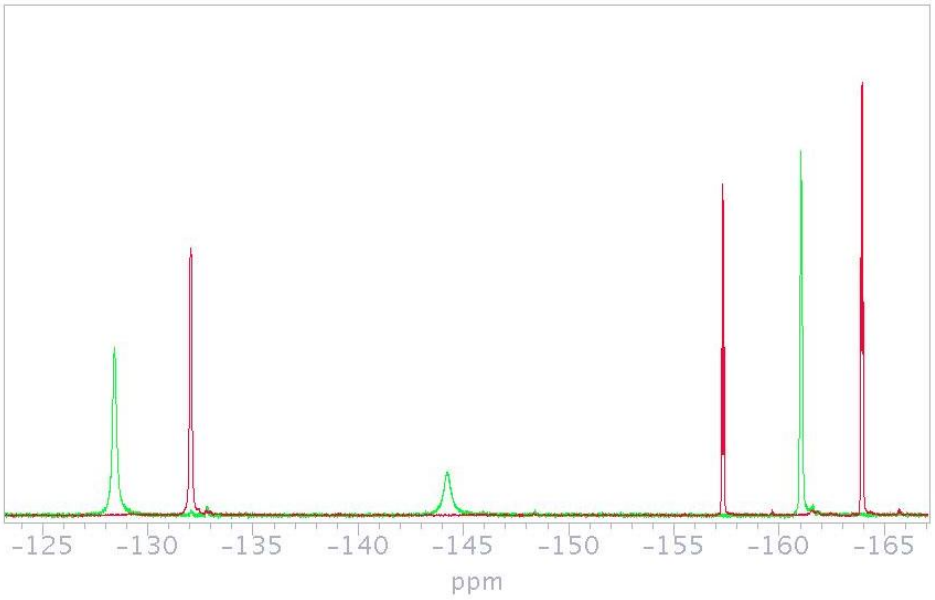

Fig. 39: ^{19}F-NMR of **10** mixed with **27** (red) and unmixed (green).

Hydrogen was added to the sample and the sample was tested with ^{1}H-NMR, ^{19}F-NMR and ^{11}B-NMR. Only a minor hydrogen peak was observed in the ^{1}H-NMR spectrum. The sample was kept in a J. Young tube under an H_2 atmosphere. In order to ensure optimal amounts of hydrogen in solution the solution was agitated periodically. No new peaks were observed in the ^{19}F-NMR or the ^{11}B-NMR. Though only a small amount of hydrogen dissolved, if the sample is able to activate hydrogen some new peaks are expected in the ^{19}F-NMR and ^{11}B-NMR.

After three days crystals were observed in solution. XRD analysis was done on these crystals and the obtained crystal structure is shown in figure 40. The bond length of the nitrogen-boron bond is 1.629 Å which is a normal bond length for an unhindered Lewis adduct of pyridine with **10**[31].

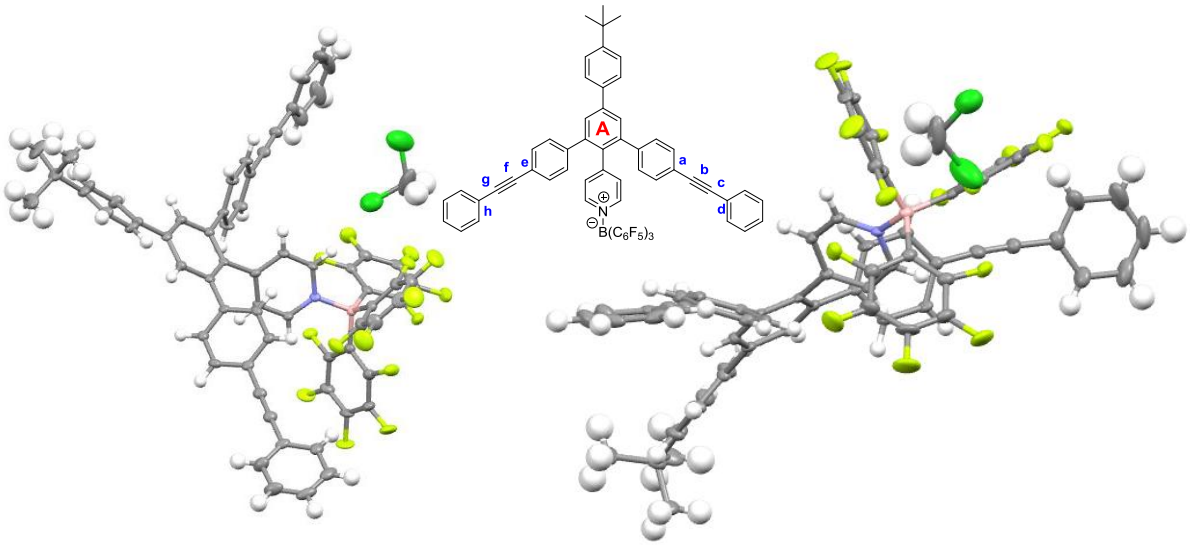

Fig. 40: The drawn structure and obtained crystal structure of the mixture of **10** and **27**.

In figure 40 several atoms are labeled. The bond angle between these labeled atoms is for **a**, **b** and **c** 174.9˚, between **b**, **c** and **d** 175.6˚, between **e**, **f** and **g** 179.1˚ and between **f**, **g** and **h** 177.1˚. So all triple bonds bend slightly away from the approaching Lewis acid.
The crystal structure also shows the phenyl rings around the phenyl ring marked **A** are at an angle rather than in plane with **A**. This is probably due to the steric congestion around **A**.

Though **33** (the derivative of **27** that was attempted to be synthesized in the last paragraph) would be more sterically precluded than **27**, the nitrogen in the pyridine ring is still relatively open to attack from the front. Given that **27** does not increase the bond length of the nitrogen-boron bond, it is unlikely the increased steric bulk of **33** will be sufficient to active in FLP chemistry either. It was therefore decided to change the design of the backbone for the Lewis base.

3.4 Molecular cage Lewis base synthesis

In order to reduce the number of approach angles for the Lewis acid, a new concept for the FLP base was devised. A molecular cage was designed in the hope that if the compound could be synthesized the backbone would hinder the basic center from as many as possible approach angles as possible. A 3D model of the proposed structure is shown in figure 41.

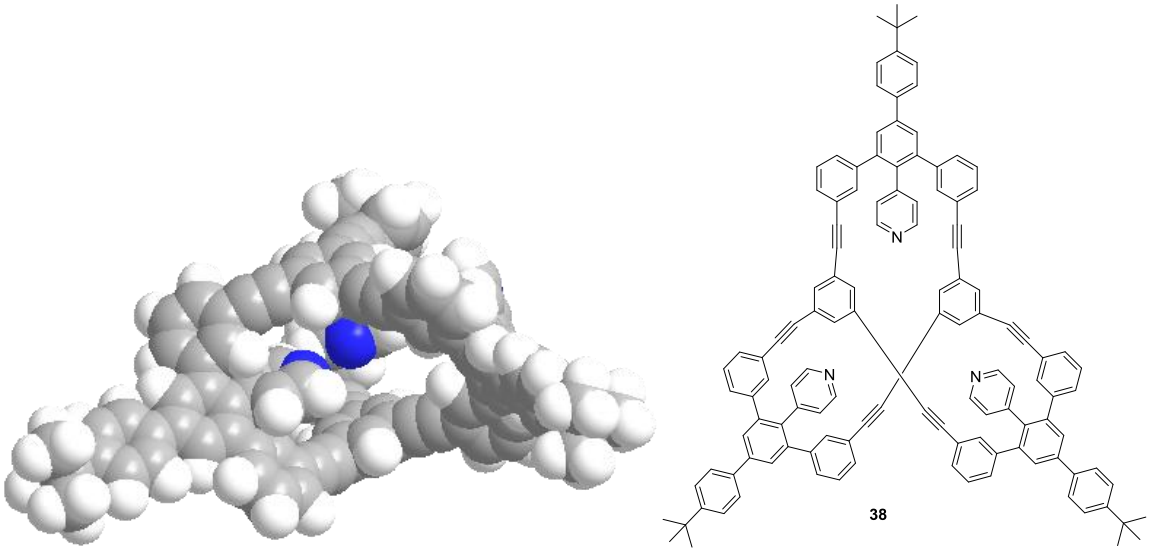

Fig. 41: Proposed molecular cage for FLP chemistry.

The first approach of synthesizing this cage (figure 42) was by using a derivative of **27** (**35**) and 1,3,5-triiodobenzene (synthesized and purified by Dr. Matthias Otte). To synthesize **34** 4-*tert*-butylbezaldehyde and 3-bromo-acetophenone were used with similar reaction conditions as the synthesis of **19**. **34** was attained at a 34% yield and was used without further purification.

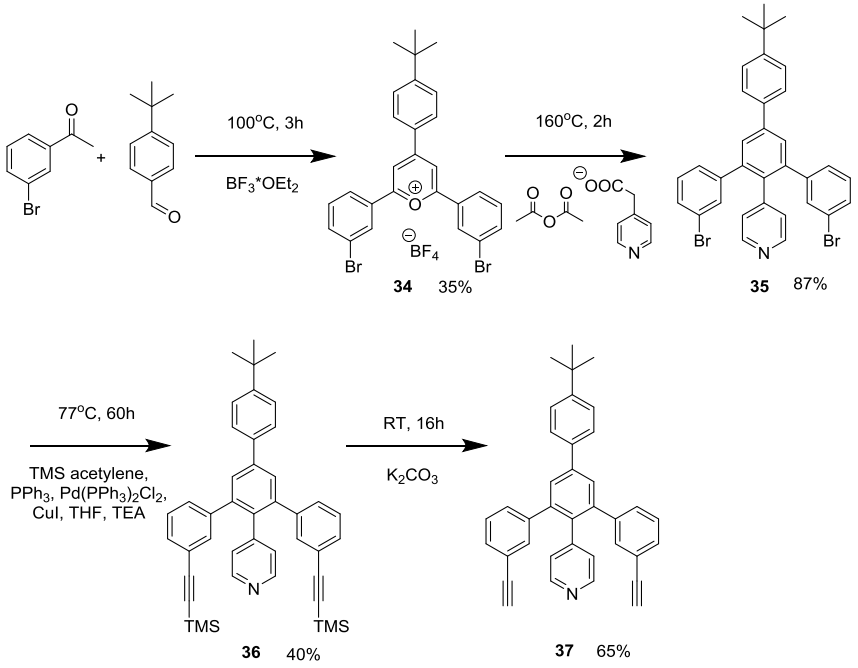

Fig. 42: Synthesis of **37** via **34**, **35** and **36**.

Subsequent reaction with sodium-(4-pyridyl)acetate to form **35** was preformed as with **26**. **35** was obtained at a yield of 87% and was analyzed using ^{1}H-NMR, ^{13}C-NMR, ESI-MS and FTIR. A zoom in of

the aromatic region ^{1}H-NMR spectrum is shown in figure 43. The peaks marked **A**, **B** and **C** could be assigned as before with **27**.

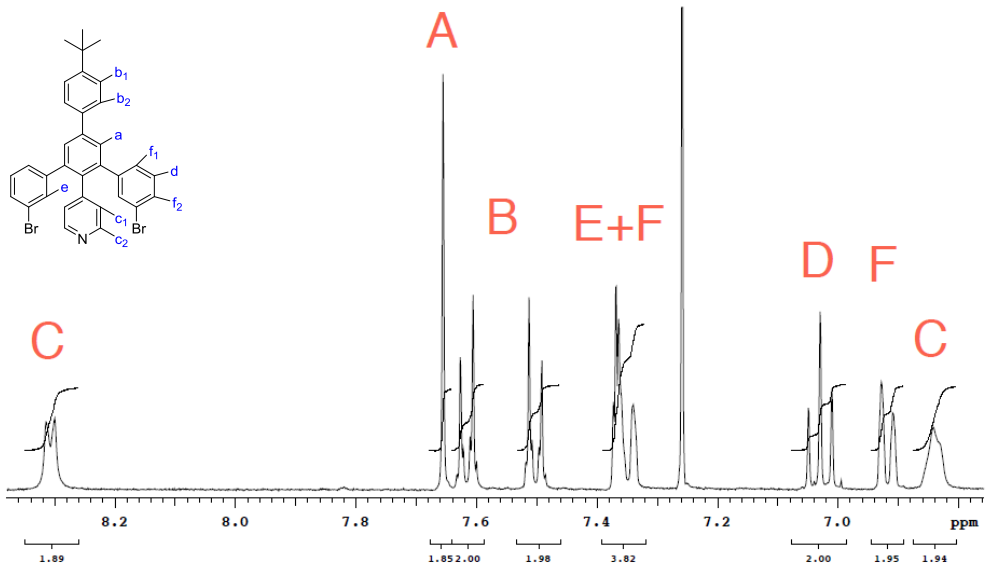

Fig. 43: A zoom in of the aromatic region of the ^{1}H-NMR spectrum of **35**.

For the protons marked **d1** and **d2** in the structure a doublet of doublet is expected as the ^{3}J-coupling of the protons at the two sites marked **f1** and **f2** in the structure are expected to be electronically different. However in the spectrum no doublet of doublet is observed. Instead what looks like a triplet is observed. Upon closer inspection the ratio of the peaks in the "triplet" marked **D** is 1:2:1. This is consistent for a doublet of doublets where two of the peaks overlap. This would be caused by an identical coupling constant from the protons marked **f1** and **f2**. The protons marked **d** can therefore be allocated to the peak marked **D**. The doublet at 6.92 ppm can be assigned to protons of one of the sites marked **f1** or **f2** in the structure. One more doublet is expected of the protons marked with **f** in the structure. Also protons marked **e** in the structure are expected to show in the spectrum as a singlet. Only the multiplet at 7.35 ppm remains and must then contain the signals still expected from **f** and **e**.
^{13}C-NMR, FTIR and ESI-MS was also done for the compound. In order to attain the charged particle required for ESI-MS formic acid was in DCM was used to protonate **35**. The obtained spectrum showed the expected peak pattern between an m/z value of 595-603 g/mol for M^{+}+H.

For the reaction conditions of the Sonogashira with bromine new reaction conditions were applied[54]. These are more forcing conditions, which might be required for the substitution of the less reactive bromine. The reaction temperature was 77˚C. In order to attain a pure compound the crude product had to be columned three times using a $CHCl_3$ eluence with 1% TEA. The TEA was used to prevent the compound getting stuck on the column like **31**.

The aromatic region of the ^{1}H-NMR spectrum of **36** is shown in figure 44. Peak marked **E** shifted significantly down field compared to **35**. The doublet that was still visible in the spectrum of **35** shifted up field and now overlaps with one of the pyridine signals. Near 0.2 ppm a singlet is observed of the TMS group. **36** was used without further analysis.

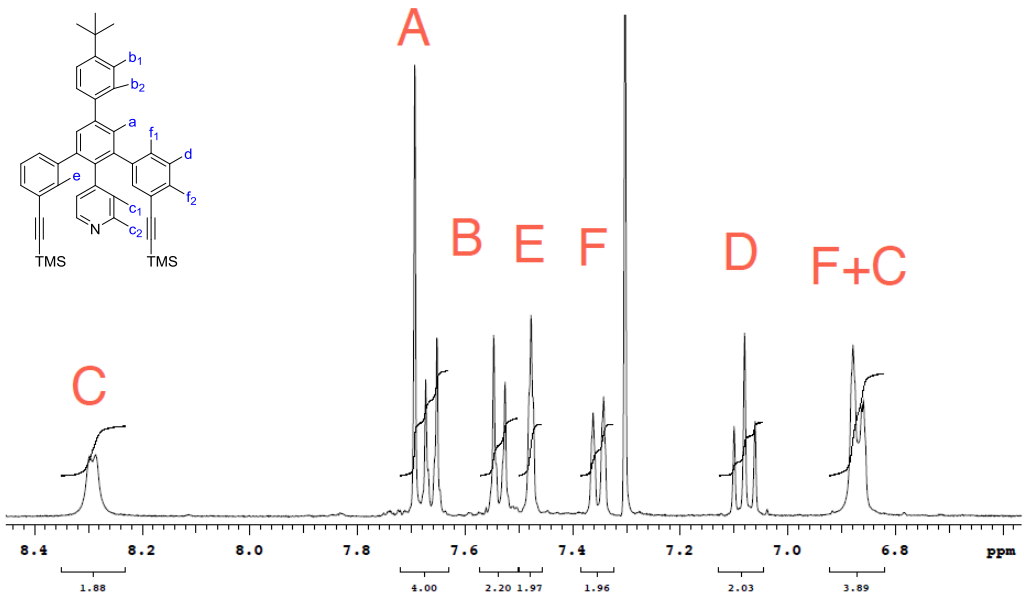

Fig. 44: A zoom in of the arromatic region of the ^{1}H-NMR spectrum of **36**.

For the deprotection the solvent was switched from pure methanol (as with **32**) to methanol/THF 1/1. This was done in order to increase solubility of the starting material and to increase reactivity. However due to practical issues, the reaction time was not decreased and the reaction was left to stir for 16 hours at RT to form **37**.

A zoom in of the aromatic region of **37** is shown in figure 45. Slight up field shifts of the peak at 6.96 and the peak at 7.38 is observed. This is slightly counter intuitive considering the electron donating TMS group has been eliminated in favor of the hydrogen. However the pyridine peaks are also significantly less broad in this spectrum compared to the spectrum of **36**. This could point to a slightly different electronic environment at the pyridine ring. It is possible other protons in the structure are affected.

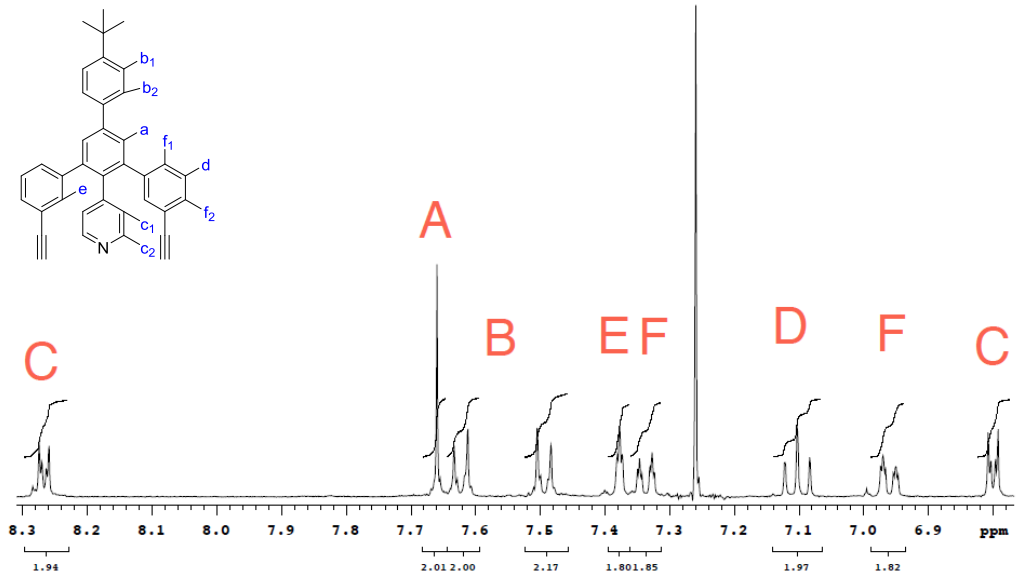

Fig. 45: A zoom in of the ^{1}H-NMR spectrum of **37**.

It can also be observed the peaks marked **E**, **F** and **C** are affected by some sort of small coupling. A similar coupling can be observed in the spectrum of **36** (figure 44) however the coupling constant is not large enough to be observed with the resolution of the measurement. Due to the small coupling

constant of the coupling of **E**, **F** and **C** it is likely the coupling is not caused by ^{3}J-coupling, but rather an interaction over a larger distance. An example would be the interaction between the pyridine protons and the protons marked **e** and **f** on the structure. How the protons marked **f1** on the *ortho* postion compared to the acetylene can interact with the pyridine protons is unclear.

Outside of the aromatic region a singlet appeared near 3 ppm corresponding to two protons that can be allocated to the acetylene protons. Also the singlet near 0.2 ppm is no longer present showing no residual starting material is left.

^{13}C-NMR showed some unusual activity near 80 ppm where the two peaks of the acetylene carbons are expected. The one signal that can easily be observed is up field compared to the acetylene signals of **32**. Also only one clear signal can be observed where two would be expected from the structure. The red arrow in figure 46 points to, what appears to be a signal overlapping with the solvent peaks, however it cannot be identified with certainty.

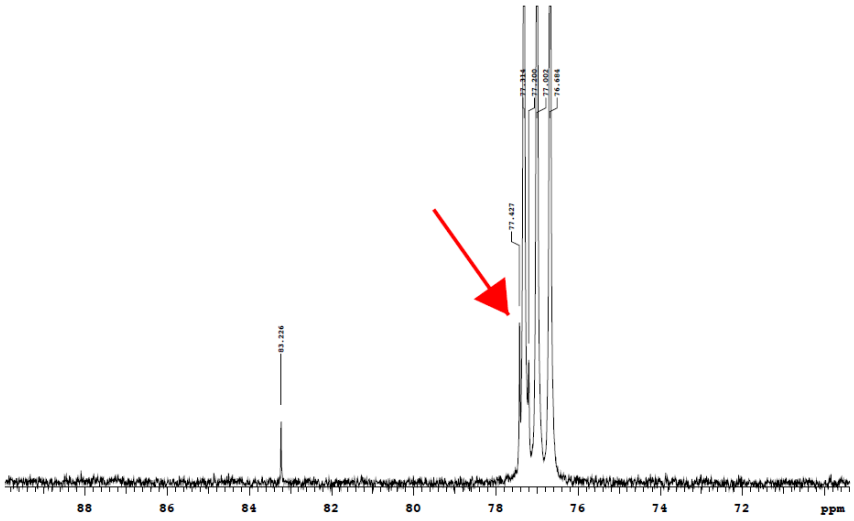

Fig. 46: A zoom in of a section of the ^{13}C-NMR spectrum of **37**.

FTIR and ESI-MS spectra were also obtained for **37**. For the ESI-MS the sample was protonated with formic acid in DCM. The expected peak pattern of M^{+}+H was observed between an m/z value of 487-491 g/mol and the expected peak pattern of M_2^{+}+H was observed between an m/z value of 972-979 g/mol.

With **37** in hand the desired cage synthesis got into the focus. Though kinetic controlled cross coupling reaction have been used in the past to synthesize macrocycles and some molecular cages, non are similar enough to the desired molecular cage to use reaction conditions from these papers. So reaction conditions had to be devised using these papers as a guide.
In general the reactions are highly diluted (4 mM for instance[40]), this is to prevent oligomerization of the reactants. As the dilution increases the chances for an intermolecular reaction decreases as well. This promotes intramolecular reactions, which is favored given a cage is the desired product. However when the reaction mixture is diluted the catalyst concentration drops as well. In order to maintain reactivity in the reaction mixture the catalyst loading is often increased.

The reaction conditions of the synthesis of **27** were adapted because these reaction conditions proved effective in the Sonogashira reaction of a iodo-phenyl compound with a phenyl acetylene (figure 47). The dilution was increased (7.7 mM) and the PPh_3, CuI and $Pd(PPh_3)_2Cl_2$ amounts were increased with it, as mentioned before.

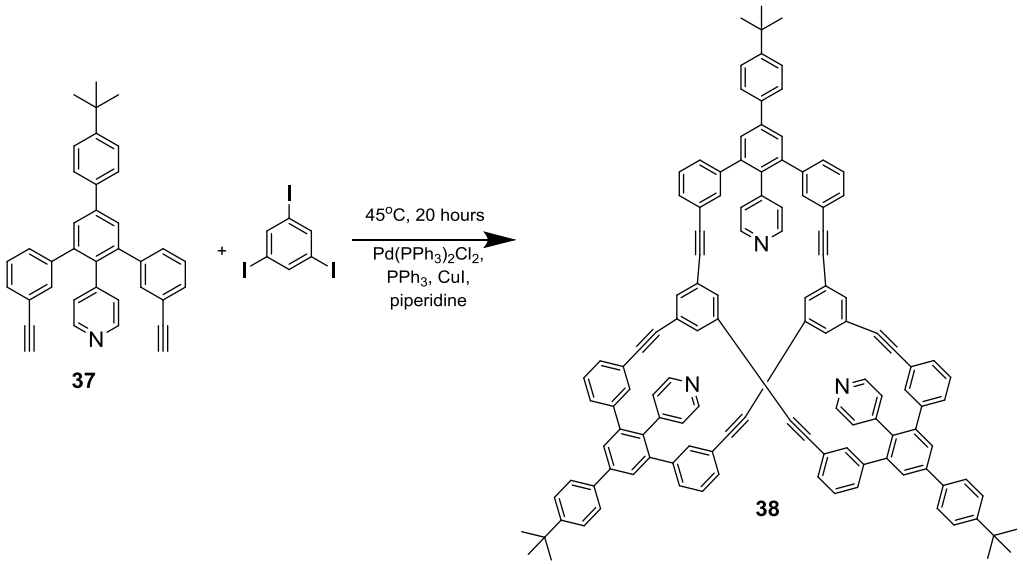

Fig. 47: Synthesis of **38** using **37** and 1,3,5-triiodobenzene.

The major product of the reaction was an insoluble white solid. A minor amount of a brown solid was obtained (roughly 15 mg) that could be dissolved in $CDCl_3$. A ^{1}H-NMR was done of this and showed a very cluttered aromatic region. It is possible that the minor amount of brown solid contains **38**. If so, it was too little to be isolate and analyzed. It is also possible that the minor products was a combination of smaller oligomers that were still soluble.

For the next approach it was attempted to convert **35** with a Finkelstein reaction to the corresponding iodine (**39**) (figure 48)[55]. The iodine would have been more reactive in a Sonogashira reaction than bromide. **39** could then be used in combination with the commercially available 1,3,5-triethynylbenzene in a Sonogashira reaction to attain the desired cage (**38**).

For the synthesis of **39** that was attempted, a very small amount of N,N-dimethylethelynediamine (9 mg) had to be added. A small error was made in the addition of this liquid and instead 25 mg was added.

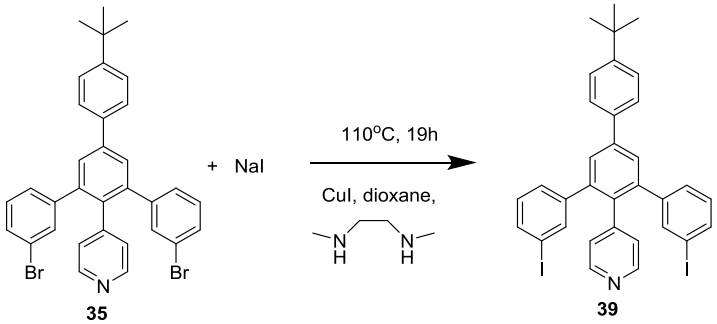

Fig. 48: Finckelstein reaction of **35** to **39**.

A ^{1}H-NMR spectrum would not be ideal to determine if the reaction was successful instead an ESI-MS spectrum was obtained. The change from a two bromine too two iodine should result in a significantly larger mass as well as a different isotopic pattern. Formic acid in DCM was used in order to protonate the sample. The obtained spectrum showed a clear peak pattern between an m/z value of 595-603 g/mol corresponding to the protonated starting material. A smaller peak pattern was observed between an m/z value of 643-649 g/mol corresponding to the protonated mono substituted product. Where the product peaks are expected (between an m/z value of 691-695 g/mol) only very small peaks could be observed.
Though ESI-MS is not a viable method to determine the relative quantities of each of the compounds it does show the reaction was incomplete. It is possible that the substrate had to compete with the ligand for room on the metal center of the catalyst because of the extra ligand added. This would slow down the reaction speed.

It was decided to use **35** with 1,3,5-triethynylbenzene in a Sonogashira reaction to form **38** (figure 49). For this reaction the reaction conditions of the synthesis of **36** were modified.
For this reaction the dilution was increased further than with the previous attempt of synthesizing **38** (catalyst loading was also increased as before with the previous approach). Also a solution of 1,3,5-triethynylbenzene was slowly dosed to the reaction mixture. This minimizes the amount of the 1,3,5-triethynylbenzene in the reaction. This together with the dilution further reduces the chance of oligomerization but also the homo coupling reaction from occurring. For the initial synthesis it was attempted to dose the 1,3,5-triethynylbenzene over 24 hours. However the apparatus used malfunctioned and no 1,3,5-triethynylbenzene was actually introduced to the reaction mixture. The apparatus was reset and the dosing time was decreased to 4 hours so it could be monitored. This time the dosing was preformed as planned.

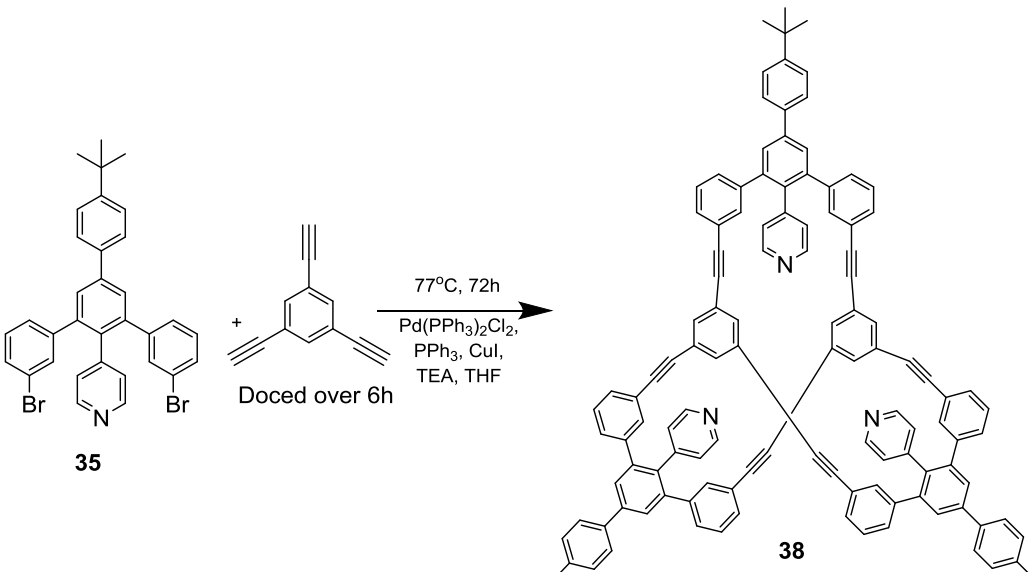

Fig. 49: Synthesis of **38** using **35** and 1,3,5-triethynylbenzene.

Again an insoluble solid was obtained also a small amount of an pyridine organic compound was obtained (checked by a crude ^{1}H-NMR). However this was still a mixture and was even less than with the previous attempt (roughly 3 mg). This was too little to purify further.

Unfortunately no useful analytical data could be obtained of the insoluble solid, as most of these techniques require a dissolved sample (NMR, ESI-MS). With no other pyridine containing products obtained it can be concluded that the major product of the reaction is this insoluble solid. One possibility is that the initially obtained brown solid was the product of homo coupling. With the dosing of the 1,3,5-triethynylbenzene over time this no longer occurred to the same degree and the small amount of brown material was not obtained.
What is however also possible is that the designed cage (**38**) is sterically too strained to form. If this is the case the measures taken to prevent oligomerization would at best succeed at creating a better defined oligomer rather than the cage. For example: If in the initial reaction a mixture of oligomers ranging between 7-3 repeating elements/monomers were formed, the oligomers containing 3 monomers might still dissolve. If the change in reaction conditions succeeded at creating a better defined oligomer it might only have created oligomers consisting out of 5 monomers, all of which insoluble.
The final possibility is that the measures taken to prevent oligomerization worked exactly as intended and more of **38** was formed in the second reaction than the first. But that the cage that is formed is itself insoluble. Unfortunately without any further analytical data it is not possible to determine which of the earlier mentioned scenarios is accurate.

With the failed second attempt and without clear analytical data to determine why it failed, a change in strategy was necessary. The molecular cage **38** was designed to sterically hinder approaching FLP acids from as many angles as possible. The most important angle to hinder would be the angle where the lone pair orbital of the pyridine nitrogen is located. This orbital pointing directly outwards in plain with the pyridine ring. Figure 50 shows how this would roughly look like. In order to hinder this angle a macrocycle was designed.

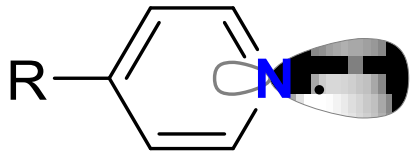

Fig. 50: Orientation of the pyridine lone pair orbital.

3.5 Macro cycle Lewis base synthesis

If a macro cycle is to be used to hinder the approach of an FLP acid, the macro cycle in question would have to be shape persistent. In other words the macro cycle needs to be rigid enough so that it cannot move out of the way of the approaching FLP acid. The synthesis routes used so far were for a large part based on work by Höger et al.[42][43]. In the reference paper compounds very similar to the ones already synthesized in this project were used to synthesize just the kind of shape persistent macro cycles that could be useful for FLP chemistry. However these macro cycles were synthesized over a large number of synthesis steps and would take a lot of time and materials to make in any significant quantity for catalytic testing.

Although a direct reproduction of the of the macro cycles by Höger at al. was not a practical option, it does show the potential for the already synthesized compounds to be building blocks for a macro cycle synthesis. To minimize the time required to synthesize the macro cycle itself, a reaction pathway was designed based on a already synthesized compound. Also it was attempted to minimize the reaction steps required to get to the desired product in order to make it attractive as a possible FLP catalyst. The proposed structure and the proposed synthetic route for the macro cycle is shown in figure 51.

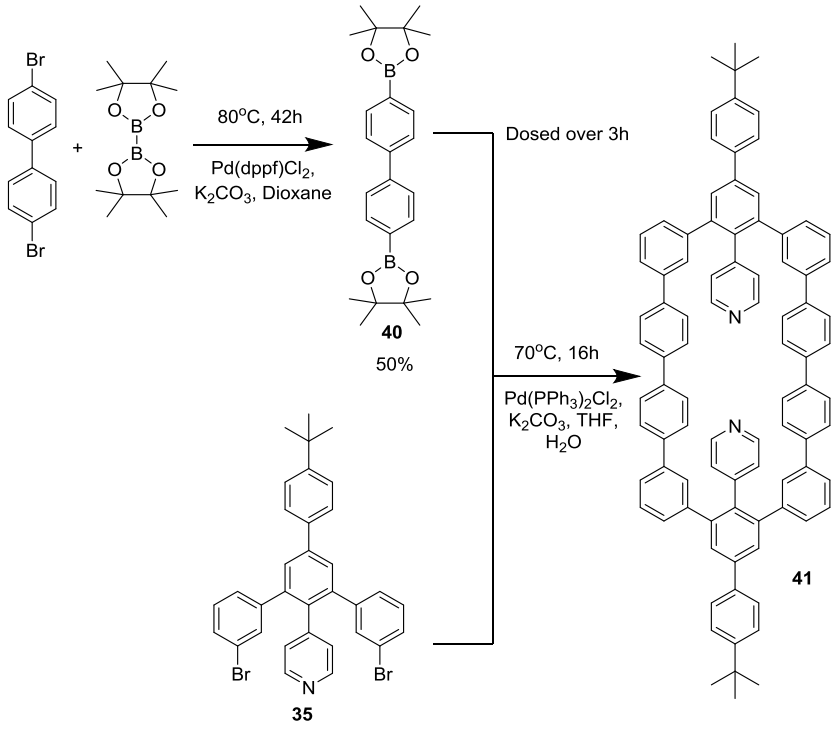

Fig. 51: Synthesis of **41** via **35** and **40**.

The proposed reaction to form **41** is the Suzuki cross coupling reaction between **35** and **40**. This reaction was chosen because it would result in a product without triple bonds which could make any future synthesis of a Lewis acid less difficult. The Lewis acid without the triple bond would not undergo the same side reaction observed for the synthesis of **25** (figure 24). It also only takes one reaction step to synthesize a viable reaction partner for **35** from commercially available chemicals.

The Suzuki cross coupling is from a mechanistic point of view similar to the Sonogashira reaction. The oxidative addition of the phenyl-bromine bond occurs over the palladium center followed by a trans

metallation with the boron and a reductive elimination of the product. In this reaction the base (K_2CO_3) is added to displace the bromide from the metal center after oxidative addition of the phenyl-bromine bond.

The synthesis of **40** was done using the reaction conditions for the initial attempt to synthesize the brooronic ester precursor of the Lewis acid (**25**)[44]. These reaction conditions are expected to work for this reaction because unlike **21**, no triple bonds are present in the structure.
The synthesis was completed with a 50% isolated yield and was tested with ^{1}H-NMR. The obtained spectrum was compared to known literature values[56]. These values matched and **40** was used without further analysis.

For the synthesis of **41** literature was found that used Suzuki cross coupling reactions to synthesize a macro cycle[41]. However this paper used a catalyst that was not commercially available. Concentrations of the macro cycle synthesis where used, however a different reference was used to for the relative concentrations of chemicals[57]. In order to maintain reactivity the catalyst loading was increased to match the concentration of the catalyst in solution of the work of Grazulevicius et al.[57] Also **40** was dosed over 3 hours into the reaction mixture to minimize oligomerization.

After the reaction an insoluble solid was obtained and 50 mg of brown solid. A crude ^{1}H-NMR was done and this showed a mixture of organic compounds. The spectrum also showed peaks where pyridine signals would be expected.
A TLC test was done in order to determine if the brown solid could be columned. The best separation was attained using chloroform, where a one spot was visible at an R_f value of 0.89. Also a spot was visible that did not move at all on the TLS plate. If the first spot with an R_f value of 0.89 contained pyridine functionality it could have been the macro cycle. Even if it is not the macro cycle, information could be gained about the reaction. If however the spot stuck on the TLC plate is the fraction containing a compound with a pyridine functionality, it would most likely be lost on the column. A small scaled column was done with a portion of the brown solid. However no fractions containing any pyridine signals in the ^{1}H-NMR spectrum could be obtained.
In order to determine if the brown solid contained **41** an ESI-MS spectrum was obtained using formic acid in DCM. The spectrum did not show any peaks that could correspond to the desired macro cycle.

The synthesis of **41** was split up into two steps as shown in figure 52. The first reaction would use an excess of **40** in the presence of **35** as in the reference reaction[57]. The second reaction, should the first succeed would have the same dilution of the previous attempt at synthesizing **41**.

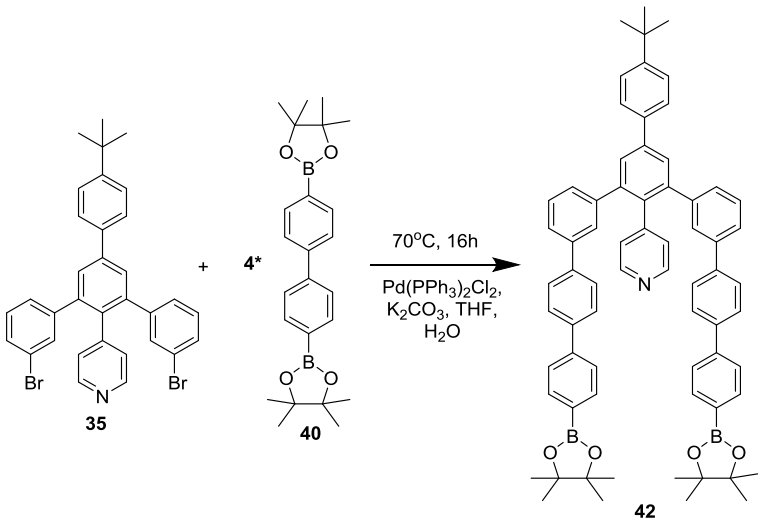

Fig. 52: Synthesis of **42** via **40** and **35**.

An amount of isoluble solid was obtained and 80 mg of a brown solid. A crude ^{1}H-NMR was done of the brown solid and very cluttered spectrum was obtained. A TLC test was done in order to determine if a column would be a viable option for purifying the compound. Spots were observed at an R_f value of: 0.02, 0.11, 0.23, 0.32, 0.48, 0.75 and 0.91. To obtain a pure compound out of this would likely require several successive columns. It is unlikely enough material would be left after the further purification to continue with the second reaction. That is assuming the correct compound was formed. The small amounts of dirty unknown compound did not appear promising, so different approach was devised.

The reaction used so far to synthesize either cages or macro cycles were under kinetic controle. The disadvantage with this is when the wrong bond is formed that molecule can never become the desired compound. For instance with the cage synthesis (figures 47 and 49) 6 bonds had to formed in order to successfully synthesize the desired cage. This means 6 bonds have to be formed in succession without one incorrect bond formation in order to attain the desired product. This means that even if a kinetic controlled cage or macro cycle synthesis is successful the yield is generally poor.

There are however reaction that are reversible that can be used for macro cycle and cage synthesis. In such a case the reaction would be controlled by what is thermodynamically favorable rather than what gets formed first as the bonds can break and reform until the most favorable structure is obtained. This means that in theory, if the desired product is the thermodynamically favorable, it can be formed at very high yields. Indeed such reactions have been reported[37-39]. Unfortunately the scope of reversible reactions that form carbon-carbon bonds is limited. More often these reactions form for instance carbon-nitrogen bonds like in imine condensation.
Olefin metathesis reactions however do form a carbon-carbon bond reversibly. This reaction leaves the product with a double bond which is why it initially was not considered, because FLP's can potentially reduce the double bonds in the presence of the hydrogen. However if a macro cycle can be synthesized using olefin metathesis reaction this might still be interesting. If the macro cycle can be synthesized and the double bonds do get reduced this would prove the initial macro cycle was capable of activating hydrogen. Also the reduced macro cycle might still be capable of FLP chemistry.

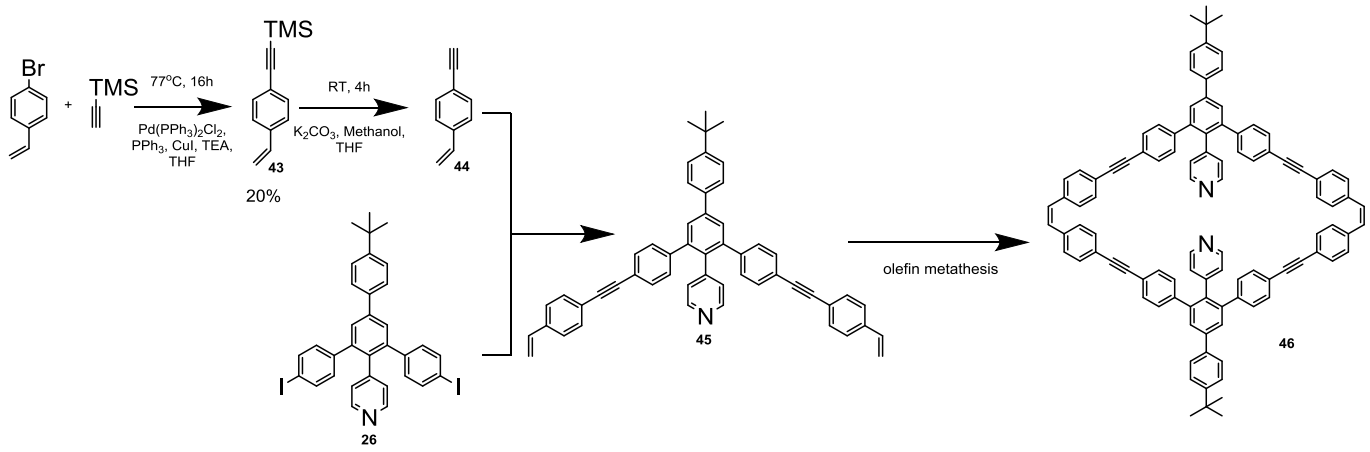

Fig. 53: Synthesis of **46** via **43**, **44**, **26**, and **45**.

So a synthesis route for a macro cycle was devised (figure 53) that would make use of olefin metathesis reaction. **26** will be used as starting point for the synthesis. A Sonogashira coupling would then need to be done with 4-ethynyl-styrene (**44**). **44** would have to be synthesized form 4-bromo-styrene and TMS-acetylene followed by a deprotection. The product of reaction between **44** and **26** could be used in an olefin metathesis reaction.

The first reaction was carried out as intended using the reaction conditions used for **36**. The compound was purified and measured with ^{1}H-NMR. The attained spectrum was compared to known literature values and this matched[58]. The deprotection of **43** to form **44** was done like the synthesis of **37**. However this compound could not be purified in the remaining time of the project.

4. Conclusions

The synthesis of the Lewis acid (**23**) was unsuccessful because the BF_2-group could not be introduced. For introducing this BF_2-group for directly converting it using *n*-butyl-lithium and BF_3*OEt_2 under the applied reaction conditions is not possible. No reaction occurred for the first reaction, as the starting material was recovered. The second reaction did not yield a compound that could be the desired acid. However a reaction did occur making it likely the lithiation step worked and the reaction with BF_3*OEt_2 did not.

Thought the reaction preformed to synthesize **25** itself was inconclusive, the synthesis of **40** was. The same reaction conditions that gave a very messy reaction for **25** did give a selective reaction for **40**. The only functionality in **25** that could generate a side reaction to explain the very messy ^{1}H-NMR spectrum is the triple bond, which is absent in **40**. It can therefore be concluded the triple bond undergoes an undesired side reaction under the applied reaction conditions. In order to determine the details of this side reaction more research would have to be done.

The synthesis of **27** was successful however when this base is mixed with **10** (the commercially available Lewis acid) an adduct is obtained. This can be observed in the form of shifting peaks in the ^{19}F-NMR, ^{1}H-NMR, ^{11}B-NMR and the obtained crystal structure. The mixture of **27** and **10** can therefore not be considered a FLP.

Upon addition of hydrogen to this mixture in CD_2Cl_2 no change could be observed in ^{19}F-NMR and ^{11}B-NMR. So it can be concluded the mixture is not capable of activating molecular hydrogen under the given reaction conditions. It is also unlikely it would be able to activate molecular hydrogen under any conditions considering no elongation of the boron-nitrogen bond is observed in the crystal structure. The possibility can however not be fully excluded.

Given this lack of the elongation of the boron-nitrogen bond in **27** it is unlikely a modification on the terminal phenyl group like the one used in **33** would be sufficient to form an FLP with **10**. Also the crystal structure showed the triple bonds can bend. This means the terminal phenyl group more mobile than originally intended further decreasing the likely hood of attaining a FLP by increasing the steric bulk on these groups. The bending of the triple bonds could however be a sign that there is a steric interaction between **10** and the terminal phenyl group even if it is not significant enough to elongate the nitrogen-boron bond.

It is difficult to draw any definitive conclusions based on the molecular cage and macrocycle synthesis. Due to the large amount of insoluble solid obtained in each of the reactions the formed compounds cannot be identified. However considering even the synthesis of **42** yielded a mixture of many compounds, it is highly unlikely the synthesis of **41** resulted in the formation of the desired macro cycle. All these reaction were under kinetic control and none of these reactions yielded any significant amount of the desired product. The irreversible carbon-carbon bond formation is therefore an unpractical approach towards synthesizing the desired cages and maco cycles. A promising alternative would be by using reversible reactions for the cage/macro cycle synthesis.

Also the obtained crystal structure shows the rings on the 1,2 and 6 position on the central phenyl ring are out of plain and at an angle compared to the central phenyl ring. In order for the molecular cage (**38**) and the macro cycle (**41**) to form the rings would have to flatten out otherwise the linking molecules would not line up. Based on the angle at which the rings are in the structure it is highly unlikely this would be possible. Therefore it is unlikely the synthesis of **41** or **38** would be possible.

5. Outlook

If macro cycles/molecular cages are explored further for FLP chemistry it would be advisable to start from an existing cage or macro cycle. This would save time on the development of the molecular cage/macro cycle which are known to be difficult to synthesize. **46** however remains an interesting compound. Synthesizing **46** and compounds like it using olefin metathesis is still a promising approach to obtaining useful catalysts for FLP chemistry. In general employing thermodynamic controlled reactions for the synthesis of cages and macro cycles would be a good approach for the continuation of this research.

A general trend during the project was when the compounds started to become larger the isolation of these compounds became more difficult. This is to be expected as a modification on a large molecule has less effect than a modification on a small molecule. For the reaction pathways in this project, the aldol reaction that formed **19** and **34** was always done first. What might be a viable alternative for compounds with more reaction steps is to postpone this reaction to as late as possible in the overall reaction pathway. An example for the synthesis of **27** is shown in figure 54.

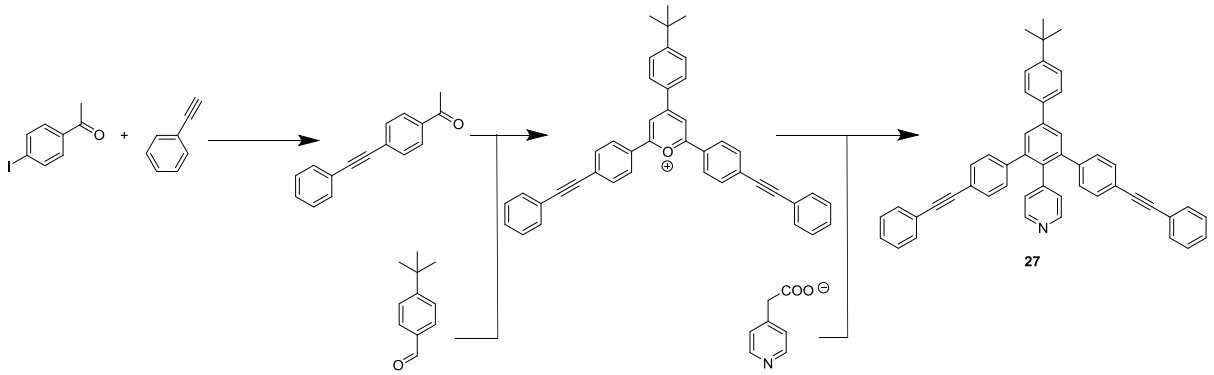

Fig. 54: Possible variation in the synthesis of **27** postponing the aldol reaction.

For any compound that is designed contain BF_2-group it would be highly advisable to avoid the use of triple bonds in these structures. This would allow for the introduction of a boronic ester with the reaction conditions used for **40**[41]. Also this would ensure no reaction can occur with itself should a palladium catalyst be used later on in the synthetic pathway. As a result a Sonogashira reaction cannot be used for the synthesis of these compounds, however Suzuki cross coupling could be used as an alternative. The Suzuki cross coupling reaction would replace the triple bond with a phenyl ring. A phenyl ring is also rigid and it could therefore be a good alternative for the triple bond.

A different strategy for achieving a Lewis base (or acid) based on the structure of **27** would be to introduce the steric bulk on the phenyl rings on the 1 and 6 position on the central phenyl ring. This would put the bulk more close to the pyridine nitrogen. This would also put less bonds between the nitrogen and the steric bulk, meaning less bonds can bend to allow adduct formation.
^{1}H-NMR of **37** did point to a larger amount of steric congestion on these phenyl rings compared to **32**. If this is an accurate assumption it might be difficult to synthesize compounds with large steric bulk on the mentioned phenyl groups.

Also for this project only pyridine was used as a base. In the background (chapter 1) an example was used were an ether was used as a Lewis base. Among the ethers used was dioxane which is compared to for instance **27** not very heavily sterically hindered. In dioxane the oxygen is the basic

center rather than nitrogen. Also the nitrogen is part of an aromatic ring. It is possible the adduct formation of compound containing an aromatic nitrogen happens more readily than for a compound with oxygen. It would be interesting to test the behavior of bases with different basic centers based on a similar structure.

Ideally a crystal structure could be compared between each of the bases mixed with **10**. Also to test the reactivity of each of these bases to see what different basic centers have for an effect on the reactivity of FLP's.

6. Experimental section

General

Where an inert atmosphere was required, N_2 was used and standard Schlenck techniques. Where necessary the M200B M-Braun glovebox system was used under an N_2 atmosphere. Dioxane was degassed, distilled over Na and stored over 4 Å molecular sieves and THF was degassed and distilled over sodium before use. Piperidine, TEA and DMF were degassed before used. Acetonitrile was dried using the MBraun SPS-800. Other commercially available chemicals were used as they were.

For ^{1}H-NMR a MRF400 or VNMRS400 was used (both 400 MHz). For ^{19}F-NMR the MRF400 was used (376 MHz). For ^{11}B-NMR the MRF400 was used (128 MHz). ^{13}C-NMR was done with the MRF400 or VNMRS400 (100 MHz). For recording FTIR spectra, Perkin Elmer Spectrum One FT-IR spectrometer and Perkin Elmer Spectrum two FT-IR spectrometer were used. For obtaining the ESI-MS spectra, a Micromass MS technologies LCT Premier XE was used.

Synthesis of **19**.[43]

Under a N_2 atmosphere 25 ml BF_3*OEt_2 were added to a mixture of 8.12 g 4-*tert*-butylbenzaldehyde and 24.9 g 4-iodoacetophone. The mixtrue was stirred at 100 ˚C for 3 hours. Reaction mixture was allowed to cool to room temperature and was added to approximately 250 ml of diethyl ether. The yellow solid was filtrated off and washed with more diethyl ether. The crude product was further purified by refluxing in 1,2-dichloroethane for 2 hours. The product was obtained as a yellow powder and used as it was (11.396 g, 16.2 mmol, 32%).

Synthesis of **20**.[42]

960 mg NaOH were dissolved in 50 ml MeOH. 5.16 g (24 mmol) 4-bromophenylacetic acid were added to this and stirred at room temperature for 15 min. The solvent was then removed under vacuum and a white solid was obtained. To this 4.22 g (6 mmol) **19** were added and 18 ml acetic anhydride. The mixture was stirred under nitrogen (no schlenck techniques used, just an N_2 flow) for 2 hours at 160 ˚C. Afterwards the mixture was cooled to room temperature, diethylether and water were added. The organic and water layers were separated and the organic layer was washed with water and brine. The organic layer was dried over $MgSO_4$ and solvent was removed under vacuum. The solid was dissolved in chloroform and recrystallized using an excess of methanol. Compound **20** was obtained as a white powder (2.92 g, 3.81 mmol, 63%). ^{1}H-NMR matched literature values[42]: (400 MHz, $CDCl_3$, 25 ˚C): δ = 7.60-7.57 (m, 4H), 7.53 (d, ^{3}J(HH) = 8.44 Hz, 4H), 7.48 (d, ^{3}J(HH) = 8.44 Hz, 2H), 7.18 (d, ^{3}J(HH) = 8.41 Hz, 2H), 6.83 (d, ^{3}J(HH) = 8.31 Hz, 4H), 6.71 (d, ^{3}J(HH) = 8.41 Hz, 2H), 1.37 (s, 9H). ^{13}C-NMR also matched literature values[42]: (100 MHz, $CDCl_3$, 25˚C): δ = 151.0, 141.3, 140.9, 140.8, 137.7, 137.0, 136.1, 133.1, 131.7, 130.9, 128.4, 126.8, 125.9, 120.7, 92.5, 34.6, 31.3.

Synthesis of **21**.[43]

Under a N_2 atmosphere 1,00 g (1.30 mmol) of compound **20**, 130 mg of CuI, 259 mg of PPh_3, 259 mg of $Pd(PPh_3)_2Cl_2$ and 60 ml piperidine were added to a dried Schlenck flask. To this 279 mg (2.73 mmol) phenylacetylene were added. The solution was stirred 16 hours at 50 ˚C. Afterwards the solution was cooled to RT diethyl ether and water were added. The organic layer was separated, washed with water, 10% acetic acid(aq), water and brine and dried over $MgSO_4$. The solvent was removed using vacuum. The obtained yellow solid was further purified using column chromatografie using a chloroform/petroleum (40-60) 1/4 eluence (R_f = 0.71). Compound **9** was obtained as a white

solid (487 mg, 0.689 mmol, 53%). ^{1}H-NMR (400 MHz, $CDCl_3$, 25 ˚C): 7.66 ($s^{(broad)}$,2H), 7.63 (d, ^{3}J(HH) = 8.23 Hz, 2H), 7.54-7.48 (m,6H), 7.40-7.32 (m,10H), 7.18 (d, ^{3}J(HH) = 8.60 Hz), 7.09 (d, ^{3}J(HH) 8.42 Hz, 4H), 6.75 (d, ^{3}J(HH) = 8.22 Hz, 2H), 1.38 (s, 9H). ^{13}C-NMR (100 MHz, $CDCl_3$, 25˚C): 150.9, 141.7, 141.5, 140.6, 137.9, 137.1, 136.3, 133.2, 131.6, 131.1, 130.8, 129.9, 128.4, 128.3, 128.3, 126.8, 125.9, 123.2, 121.4, 120.6, 89.8, 89.2, 34.6, 31.3. (ESI-MS): *m/z* 798.2573 g/mol [M+pyridine^{+}+H].

Synthesis of **23**.[45]
Under a N_2 atmosphere **21** (107mg, 0.15 mmol) was dissolved in 5 ml of diethylether (dried in the MBraun SPS-800). The reaction mixture was cooled to -78˚C and 0.14 ml of 1.6 M *n*-BuLi solution in *n*-hexane (0.23 mmol) was added. The mixture was stirred at -78˚C for 1,5 hours. 32 mg (0.225 mmol) of $BF_3{\cdot}OEt_2$ was added and the reaction mixture was allowed to heat up to room temperature overnight. 5 ml water were added. Organic layer was separated and dried over $MgSO_4$. Solvent was evaporated and the obtained white solid was analyzed using ^{1}H-NMR.

Under a N_2 atmosphere **21** (107mg, 0.15 mmol) was dissolved in 7.5 ml of diethylether (dried in the MBraun SPS-800). The reaction mixture was cooled to -78˚C and 0.28 ml of 1.6 M *n*-BuLi solution in *n*-hexane (0.45 mmol) was added. The mixture was stirred at -78˚C for 1,5 hours. 128 mg (0.225 mmol) of $BF_3{\cdot}OEt_2$ was added and the reaction mixture was allowed to heat up to room temperature overnight. 5 ml water were added. Organic layer was separated and dried over $MgSO_4$. Solvent was evaporated and the obtained white solid was analyzed using ^{1}H-NMR.

Synthesis of **25**.[44]
1.4 ml were dioxane was added to 122 mg (0.17 mmol) **21**, 117 mg (1.19 mmol) potassium acetate, 128 mg (0.51 mmol) bispinacolatodiboron and 6.8 mg (0.06 mmol) Pd(dppf)Cl_2. The mixture was stirred at 80˚C for 4 days. Water was added and the mixture was extracted with dichloromethane. The organic layer was dried with $MgSO_4$ and solvent was removed under vacuum. The obtained white solid was analyzed with ^{1}H-NMR.

2 ml dioxane were added to 106 mg (0.15 mmol) **21**, 90 mg (0.90 mmol) potassium acetate, 87.1 mg (0.33 mmol) bispinacolatodiboron and 5.7 mg (7.5 µmol) Pd(dppf)Cl_2. The mixture was stirred at 105˚C for 2 days. Water was added and the mixture was extracted with dichloromethane. The organic layer was dried with $MgSO_4$ and solvent was removed under vacuum. The obtained white solid was analyzed with ^{1}H-NMR.

2 ml dioxane were added to 107 mg (0.15 mmol) **21**, 89 mg (0.90 mmol) potassium acetate, 38.9 mg (0.15 mmol) bispinacolatodiboron and 5.8 mg (7.5 µmol) Pd(dppf)Cl_2. The mixture was stirred at 105˚C for 2 days. Water was added and the mixture was extracted with dichloromethane. The organic layer was dried with $MgSO_4$ and solvent was removed under vacuum. The obtained white solid was further purified using column chromatografie using a chloroform/petroleum (40-60) 1/2 eluence.

Synthesis of **26**.[43]
1.89 g NaOH were dissolved in 90 ml MeOH. 3.95 g 4-piridylacetic acid (28.80 mmol) were added to the mixture and stirred at room temperature for 15 min. The solvent was removed under vacuum and a white solid was obtained. To the solid, 4.00 g (5.69 mmol) **19** were added and 19 ml acetic

anhydride. The mixture was stirred under a N_2 atmosphere (no Schlenck techniques used, just an N_2 flow) for 2 hours at 160 ˚C. Afterwards the mixture was cooled to room temperature and diethylether and water were added. The organic and water layers were separated and the organic layer was washed with water and brine. The organic layer was dried over $MgSO_4$ and the solvent was removed under vacuum. Further purification was achieved with column chromatography using a chloroform eluence (R_f = 0.37)[43]. Compound **26** was obtained as a white powder (3.8287g, 5.54 mmol, 97%). ^{1}H-NMR was compared to known literature values and matched[43]. (400 MHz, $CDCl_3$, 25 ˚C): δ = 8.30 (d, ^3J(HH) = 5.46 Hz, 2H), 7.63 (s, 2H), 7.60 (d, ^3J(HH) = 8.44 Hz, 2H), 7.58 (d, ^3J(HH) = 8.44 Hz, 4H), 7.50 (d, ^3J(HH) = 8.44 Hz, 2H), 6.86-6.80 (m, 6H), 1.37 (s, 9H).

Synthesis of **27**.[43]
Under an N_2 atmosphere, 560 mg (0.81 mmol) compound **26**, 88.7 mg of CuI, 160 mg PPh_3 and 163 mg $Pd(PPh_3)_2Cl_2$ were dissolved in 40 ml piperidine. To the mixtrue 182 mg (1.78 mmol) phenylacetylene were added. The solution was stirred 16 hours at 50 ˚C. After the solution was cooled to room temperature and diethyl ether and water were added. The organic layer was separated, washed with water, 10% acetic acid(aq), water and brine and dried over $MgSO_4$. The solvent was removed using vacuum. The obtained yellow solid was further purified using column chromatografie using a chloroform eluence (R_f = 0.32). Compound **27** was obtained as a slightly yellow solid (347.2 mg, 0.54, 67%). ^{1}H-NMR (400 MHz, $CDCl_3$, 25˚C): δ = 8.30 (s (broad), 2H), 7.70 (s, 2H), 7.64 (d, ^3J(HH) = 8.42 Hz, 2H), 7.54-7.49 (m, 6H), 7.39 (d, ^3J(HH) = 8.25 Hz, 4H),7.37-7.32 (m, 6H), 7.08 (d, ^3J(HH) = 8.07 Hz, 4H), 6.91 (s (broad), 2H), 1.38 (s, 9H). ^{13}C-NMR (100 MHz, $CDCl_3$, 25˚C): δ = 151.2, 141.5, 141.3, 140.9, 136.9, 131.6, 131.2, 129.8, 128.5, 128.3, 128.3, 126.9, 129.9, 123.1, 121.9, 90.0, 89.0, 34.6, 31.3. MS (ESI-MS): *m/z* 640.3003 g/mol [M^++H].

Testing of **27** for FLP chemistry.
In the gloverbox, 20 mg (0.04 mmol) of **10** and 16 mg (0.04 mmol) of **27** were dissolved in 0,5 ml of toluene-d8 or CD_2Cl_2. Two other samples were prepared, each with either **10** or **27** in toluene-d8 or CD_2Cl_2. The samples were compared using ^{1}H-NMR, ^{19}F-NMR and ^{11}B-NMR.

10 in toluene-d8: ^{19}F-NMR (376 MHz, toluene-d8, 25˚C): -130.0 (dd, 24.3 Hz and 8.73 Hz), -151.3 (t, 22.5 Hz), -158.6 (dt, 22.5 Hz, 8.73 Hz).
27 in toluene-d8: ^{1}H-NMR (400 MHz, toluene-d8, 25˚C): 8.29 ($s^{(broad)}$, 2H), 7.71 (s, 2H), 7.55 (d, ^3J(HH) = 8.67 Hz, 2H), 7.48 (d, ^3J(HH) = 8.48 Hz, 4H), 7.42 (d, ^3J(HH) = 8.48 Hz, 2H), 7.36 (d, ^3J(HH) = 7.71 Hz, 4H), 7.07-6.95 (m), 6.68 ($s^{(broad)}$, 2H), 1.34 (s, 9H).
Mixture in toluene-d8: ^{1}H-NMR (400 MHz, toluene-d8, 25˚C): 7.65 (s, 2H), 7.58-7.42 (m, 10H), 7.09-6.97 (m), 6.93 ($s^{(broad)}$, 2H), 6.72 (d, ^3J(HH) = 7.57 Hz, 4H), 6.37 ($s^{(broad)}$, 2H), 1.34 (s, 9H). ^{19}F-NMR (376 MHz, toluene-d8, 25˚C): -135.5 (dd, 24.5 Hz and 7.17 Hz), -158.7 (t, 20.3 Hz), -164.4 (dt, 21.5 Hz and 7.17 Hz).
New peaks formed in mixture after 12 days: ^{19}F-NMR (376 MHz, toluene-d8, 25˚C): -126.6 ($s^{(broad)}$), -150.9 (t, 20.9 Hz), -158.0 (t, 20.4 Hz).

10 (new batch) in CD_2Cl_2: ^{19}F-NMR (376 MHz, CD_2Cl_2, 25˚C): -132.1 ($s^{(broad)}$), -157.4 ($s^{(broad)}$), -161.1 ($s^{(broad)}$). ^{11}B-NMR (128 MHz, CD_2Cl_2, 25˚C): 56.4 ($s^{(broad)}$).
27 in CD_2Cl_2: ^{1}H-NMR (400 MHz, CD_2Cl_2, 25˚C): 8.29 ($s^{(broad)}$, 2H), 7.73 (s, 2H), 7.69 (d, ^3J(HH) = 7.64 Hz, 2H), 7.58-7.50 (m, 6H), 7.45-7.34 (m, 10H), 7.15 (d, 7.64 Hz, 4H), 6.89 ($s^{(broad)}$, 2H), 1.39 (s, 9H).

Mixture in CD_2Cl_2: ^{1}H-NMR (400 MHz, CD_2Cl_2, 25˚C): 8.20 ($d^{(broad)}$, 6.12 Hz, 2H), 7.83 (s, 2H), 7.70 (d, ^3J(HH) = 8.57 Hz, 2H), 7.63-7.54 (m, 6H), 7.47-7.36 (m, 10H), 7.16-7.06 (m, 6H), 1.39 (s, 9H). ^{19}F-NMR (376 MHz, CD_2Cl_2, 25˚C): -132.1($s^{(broad)}$), -157.4 (t, 20.0 Hz), -164.0 (dt, 23.0 Hz and 8.15 Hz).

Synthesis of **28.**[47]

Under a N_2 atmosphere, 2.88 g (11.3 mmol) iodine and 3.49 g of silversulfate were dissolved in 40 ml of ethanol. 508 mg (3.98 mmol) 4-chloroaniline were added to the solution and the mixture was stirred for 1 hour at room temperature. The mixture was filtrated and the filtrate was concentrated under vacuum. The sample was dissolved in approximately 100 ml of ethylacetate and washed two times with a 100 ml of saturated sodiumthiosulfate(aq). The organic fase was collected and the solvent was removed under vacuum. Product was obtained as a black solid (1.16 g, 3.05 mmol,76%). ^{1}H-NMR was done and matched literature values[47]. ^{1}H-NMR (400 MHz, $CDCl_3$, 25˚C): 7.61 (s, 2H)

Synthesis of **29**.[47]

Under an N_2 atmosphere, 1.05 g (2.76 mmol) **28** was dissolved in 50 ml of acetonitrile. 3.06 g (13.7 mmol) $CuBr_2$ and 0.52 ml *t*-butyl-nitrite were added to the solution. This was stirred at 50˚C for 16 hours. 50 ml saturated $HNaCO_3$(aq) were added and an extraction was done with three times 50 ml of ethylacetate. Organic layer was washed with 100 ml of saturated sodiumthiosulfate(aq). Organic layer was separated and dried using $MgSO_4$. The obtained black solid was further purified using column chromatografie DCM as an eluence (R_f = 0.90). Product was obtained as a black solid (596 mg, 1.34 mmol, 49%). ^{1}H-NMR was compared to known literature values and matched[47]. (400 MHz, $CDCl_3$, 25˚C): 7.84 (s, 2H). ^{13}C-NMR (100 MHz, $CDCl_3$, 25˚C): 139.5, 134.6, 133.8, 99.6.

Synthesis of **30**.[43]

Reaction conditions of **21** were used to attain the crude product. The obtained brown solid was further purified using column chromatography using a toluene eluence (R_f = 0.81). Compound **9** was obtained as an impure yellow solid (219 mg). ^{1}H-NMR (400 MHz, $CDCl_3$, 25˚C): 7.62-7.57 (m), 7.55-7.52 (m), 7.49 (s), 7.41-7.31 (m). ^{13}C-NMR (100 MHz, $CDCl_3$, 25˚C): 132.7, 132.5*, 132.1, 131.8, 129.2*, 129.1, 128.46, 128.4*, 127.7, 126.6, 125.3, 122.3, 121.8*, 95.3, 87.0, 81.5*,73.9*. *= Matches the homo coupling product of phenyl acetylene[48].

Synthesis of **31**.[43]

Under an N_2 atmosphere, piperidine (24 ml) was added to a mixture of 1.5 g (2.17 mmol) **26**, 61 mg CuI, 126 mg PPh_3 and 123 mg $Pd(PPh_3)_2Cl_2$. TMS-acetylene (632.7 mg, 6.50 mmol) was added to this solution. The solution was stirred for four hours at 50˚C. Diethylether and 10% sulfuric acid(aq) were added to the reaction mixture. The organic layer was separated, washed with water and brine and dried with $MgSO_4$. The obtained brown solid was further purified using column chromatografie using a DCM/PE 1/1 eluence. The eluence of the column was switched to $CHCl_3$ to release the product form the column. 475 mg (0.75 mmol, 35%) of a pure yellow solid and 961 mg of an impure brown solid were obtained. ^{1}H-NMR (400 MHz, $CDCl_3$, 25˚C): 8.23 ($s^{(broad)}$, 2H), 7.63 (s, 2H), 7.60 (d, ^3J(HH) = 8.27 Hz, 2H), 7.48 (d, ^3J(HH) = 8.43 Hz, 2H), 7.30 (d, ^3J(HH) = 8.19 Hz, 4H), 7.00 (d, ^3J(HH) = 8.10 Hz, 4H), 6.82 ($s^{(broad)}$, 2H), 1.36 (s, 9H).

Synthesis of **32**.

400 mg (0.63 mmol) **31**, 1.88 g (13.63 mmol) K_2CO_3 and 20 ml of MeOH were stirred for 3.5 hours at room temperature under an N_2 atmosphere (no Schlenck techniques used). Water and chloroform were added. The organic layer was separated and washed with water and brine. The aqueous layer was extracted with chloroform and diethylether. The organic layers were combined and solvent was removed under vacuum. ^{1}H-NMR showed an incomplete reaction.

The reaction was repeated over 16 hours. Water and chloroform were added. The organic layer was separated and washed with water and brine. The aqueous layer was extracted with chloroform and diethylether. The obtained brown solid was further purified using column chromatografie using a DCM eluence. The eluence of the column was switched to chloroform to release the product from the column. The column was repeated using a chloroform eluence. The eluence was switched to chloroform with 1% TEA to release the product from the column. The product was obtained as a yellow solid (264 mg, 0.54 mmol, 85%). ^{1}H-NMR (400 MHz, $CDCl_3$, 25˚C): 8.27 (d, ^3J(HH) = 5.98 Hz, 2H), 7.65 (s, 2H), 7.61 (d, ^3J(HH) = 8.66 Hz, 2H), 7.50 (d, ^3J(HH) = 8.51 Hz, 2H), 7.34 (d, ^3J(HH) = 8.25 Hz, 4H), 7.06 (d, ^3J(HH) = 8.51 Hz, 4H), 6.78 (d, ^3J(HH) = 6.19 Hz, 2H), 1.36 (s, 9H). ^{13}C-NMR (100 MHz, $CDCl_3$, 25˚C): 151.2, 149.1, 147.4, 141.5, 141.4, 141.3, 136.8, 134.7, 131.8, 129.7, 128.5, 126.9, 126.5, 126.0, 120.7, 83.3, 77.8, 34.6, 31.3. MS (ESI-MS): *m/z* 488.2379 g/mol [M^++H].

Synthesis of **33**.[50]
Under an N_2 atmosphere 49 mg (0.1 mmol) **32** and 110 mg **30** were dissolved in 4 ml of TEA in a dry Schlenck flask. To this solution 4 mg CuI and 6.5 mg $Pd(PPh_3)_2Cl_2$ were added. The mixture was stirred for 17.5 hours at 50˚C. After the reaction mixture cooled down to room temperature water and diethylether were added. A white solid was observed which was filtrated off. The organic layer was separated and washed with water, 10% acetic acid, water and brine. The organic layer was dried using $MgSO_4$ and the solvent was removed using vacuum. 90 mg of **30** was obtained.

Synthesis of iodine derivative of **30**.[51]
Under an N_2 atmosphere, 90 mg (0.23 mmol) **30** were dissolved in 2 ml of THF and the solution was cooled to -78˚C. To the solution 0.15 ml 1.6 M *n*-BuLi (0.24 mmol) in *n*-hexane were added (this turned the solution purple). The solution was stirred at -78˚C for 30 minutes before 68.3 (0.25 mmol) mg I_2 were added. The solution turned brown and was stirred for another 2 hours at -78˚C and 1 hour at room temperature. 10 ml saturated Sodiumthiosulfate(aq) and diethylether was added. The aqueous layer was separated and extracted with diethylether. Organic layers were combined and dried over $MgSO_4$. Solvent was removed under vacuum. Crude ^{1}H-NMR did not show the product.

Synthesis of 1-bromo-4-*tert*-butyl-2,6-diiodobenzene.[52]
Under an N_2 atmosphere, 971 mg (5.8 mmol) potassium iodine were added to a solution of 442 mg (1.9 mmol) periodic acid in 2 ml sulfuric acid. A crust formed on the surface of the mixture. The mixture was cooled to 0˚C and 1-bromo-4-*tert*-butylbenzene was added. This was stirred at 0˚C for 40 min. The mixture was added to ice and the precipitate formed was filtrated off. The solid was dissolved in THF and concentrated under vacuum. Methanol and water were added. A black solid was obtained. A ^{1}H-NMR spectrum was obtained.

Synthesis of **34**.[43]

Synthesis and purification of **34** was done like **19**. 3.41 g (5.6 mmol, 35%) of a yellow solid was obtained. The compound was used without further purification.

Synthesis of **35**.[43]

640 mg (16 mmol) NaOH were dissolved in 32 ml methanol and stirred for 15 minutes. Solvent was removed under vacuum and 1.22 g (2 mmol) **34** and 6 ml acetic anhydride was added. This mixture was stirred at 140˚C for 2.5 hours. It was stirred overnight at room temperature over 16 hours. Water was added and the mixture was filtrated. The residue was washed with ca. 150 ml water and ca. 30 ml of methanol. The obtained brown solid was further purified using column chromatografie using chloroform with 1% TEA as an eluence (Rf = 0.36). Product was obtained as a slightly yellow powder (1.02 g, 1.74 mmol, 87%). ^{1}H-NMR (400 MHz, $CDCl_3$, 25˚C): 8.31 (d, ^{3}J(HH) = 6.10 Hz, 2H), 7.66 (s, 2H), 7.62 (d, ^{3}J(HH) = 8.39 Hz, 2H), 7.51 (d, ^{3}J(HH) = 8.55 Hz, 2H), 7.38-7.33 (m, 4H), 7.03 (t, ^{3}J(HH) = 7.80 Hz, 2H), 6.93 (d, ^{3}J(HH) = 7.95 Hz, 2H), 6.81 (d, ^{3}J(HH) = 6.18 Hz, 2H), 1.38 (s, 9H). ^{13}C-NMR (100 MHz, $CDCl_3$, 25˚C): 151.3, 148.4$^{(broad)}$, 142.8, 141.5, 140.7, 136.6, 134.7, 132.6, 130.1, 129.4, 128.6, 128.5, 126.9, 126.7$^{(broad)}$, 126.0, 122.2, 34.8, 32.9. MS (ESI-MS): *m/z* 598.0571 g/mol [M^{+}+H].

Synthesis of **36**.[54]

Under an N_2 atmosphere, 60 ml TEA/THF 1/1 were added to a mixture of 714 mg (1.20 mmol) **35**, 88 mg $Pd(PPh_3)_2Cl_2$, 157 mg PPh_3 and 22 mg CuI. 272 mg (2.77 mmol) TMS-acetylene were added and the reaction mixture was heated to 90˚C. Upon reaching 90 ˚C the reaction temperature was lowered to 77˚C. Another 167 mg (1.70 mmol) TMS-acetylene were added and the reaction was stirred at 77˚C for 60 hours. After the solution was cooled to room temperature diethyl ether and water were added. The organic layer was separated, washed with water, 10% acetic acid(aq), water and brine and dried over $MgSO_4$. The solvent was removed using vacuum. The obtained yellow solid was further purified using three successive columns using chloroform with 1% TEA as an eluence (Rf = 0.30). The product was obtained as a slightly yellow powder (301 mg, 0.48 mmol, 40%). ^{1}H-NMR (400 MHz, $CDCl_3$, 25˚C): 8.51 (d$^{(broad)}$, ^{3}J(HH) = 4.06 Hz, 2H), 7.65 (s, 2H), 7.62 (d, ^{3}J(HH) = 8.72 Hz, 2H), 7.49 (d, ^{3}J(HH) = 8.72 Hz, 2H), 7.44 (s$^{(broad)}$, 2H), 7.31 (d, ^{3}J(HH) = 7.67, 2H), 6.80-6.49 (m, 4H), 1.37 (s, 9H), 0.24 (s, 18H).

Synthesis of **37**.

Under an N_2 atmosphere (without using Schlenck techniques), 231 mg (0.37 mmol) **36**, 1.09 g (7.89 mmol) K_2CO_3, 5 ml MeOH and 5 ml THF (used without drying or degassing steps) were stirred for 20 hours in a round bottom flask. The reaction mixture was extracted with chloroform and diethylether. Organic layers were combined and solvent was removed under vacuum The obtained brown solid was further purified using column chromatografie using chloroform with 1% TEA as an eluence. Product was obtained as a yellow solid (115 mg, 0.24 mmol, 65%). (1.02 g, 1.74 mmol, 87%). ^{1}H-NMR (400 MHz, $CDCl_3$, 25˚C): 8.27 (dd, 6.18Hz and 1.66 Hz, 2H), 7.66 (s, 2H), 7.62 (d, ^{3}J(HH) = 8.44 Hz, 2H), 7.50 (d, ^{3}J(HH) = 8.44 Hz, 2H), 7.38 (t, 1.34 Hz, 2H), 7.34 (dt, 7.69 Hz and 1.43 Hz, 2H), 7.10 (t, ^{3}J(HH) = 7.76 Hz, 2H), 6.96 (dt, 7.99 Hz and 1.66 Hz, 2H), 6.80 (dd, 6.10 Hz and 1.73 Hz, 2H), 3.04 (s, 2H), 1.38 (s, 9H). ^{13}C-NMR (100 MHz, $CDCl_3$, 25˚C): 151.2, 149.0, 149.0, 147.3, 141.2, 141.2, 136.8, 134.9, 133.2, 130.6, 130.4, 128.5, 127.9, 126.9, 126.5, 125.9, 122.0, 83.23, 34.9, 31.5. MS (ESI-MS): *m/z* 488.2363 g/mol [M^{+}+H].

Synthesis of **38**.
Under and N_2 atmosphere, 30 ml piperidine were added to a mixture of 110 mg (0.23 mmol) **37**, 68.4 (0.15 mmol) of 1,3,5-triiodobenzene, 16 mg CuI, 30 mg PPh_3 and 32 mg $Pd(PPh_3)_2Cl_2$. Vacuum was applied directly followed by addition of N_2 and this cycle was repeated 3 more times. The mixture was stirred for 20 hours at 45˚C. Water and diethylether were added and a precipitate was observed. This precipitate was filtrated off and washed with water three times. It was attempted to dissolve the brown solid in chloroform. The sample partially dissolved leaving a white solid. The sample in the chloroform solution was recrystallized using methanol and was washed with more methanol. The obtained brown solid (ca. 15 mg) could not be identified as the product.

Under an N_2 atmosphere, 80 ml TEA and 80 ml THF were added to a mixture of 100.6 mg (0.17 mmol) **35**, 127 mg CuI, 850 mg PPh_3 and 495 mg $Pd(PPh_3)_2Cl_2$. It was attempted to dose 16.8 mg of 1,3,5-triethynylbenzene in 9 ml of TEA/THF (1/1) over 24h. However this failed and after 16 hours it was aborted (none of the solution had been dosed to the reaction mixture). The apparatus was reset and a new solution was made of 16.9 mg (0.11 mmol) of 1,3,5-triethynylbenzene in 4 ml of TEA/THF (1/1). The solution was dosed to the reaction mixture over 6 hours. The reaction mixture was stirred at 77˚C for 72 hours. After the reaction cooled to room temperature, diethyl ether and water were added. A solid was obtained and a small amount of this solid could be dissolved in chloroform (ca. 3 mg). ^{1}H-NMR was obtained.

Synthesis of **39**.[55]
Under an N_2 atmosphere, 2 ml dioxane were added to a mixture of 0.53 mg (0.86 mmol) **35**, 0.52 mg (3.48 mmol) NaI, 12 mg CuI and 25 mg N,N-dimethylethelynediamine. The solution was stirred at 110˚C for 19 hours. After the reaction cooled to room temperature, 5 ml 30% NH_3(aq) were added to the reaction mixture and the obtained solution was added to 25 ml of water. The solution was extracted three times with DCM. The organic layers where combined and dried over $MgSO_4$. Solvent was removed under vacuum and an ESI-MS spectrum was obtained.

Synthesis of **40**.
Under an N_2 atmosphere, 14 ml of dioxane was added to a mixture of 0.78 mg (2.51 mmol) 4,4'-dibromobiphenyl, 1.70 g (17.33 mmol) potassium acetate and 1.99 g (7.87 mmol) bispinacolatodiboron. The mixture was stirred at 80˚C for 42 hours. After the reaction cooled to room temperature, water was added and the solution was extracted three times using DCM. The organic layer were combined and dried using $MgSO_4$ and concentrated under vacuum. The obtained white solid was further purified using column chromatografie using a DCM eluence. The product was obtained as a white solid (509 mg, 1.25 mmol, 50%). ^{1}H-NMR spectra of the sample matched known literature values[56]. ^{1}H-NMR (400 MHz, $CDCl_3$, 25˚C): 7.88 (d, ^3J(HH) = 8.16 Hz, 4H), 7.63 (d, ^3J(HH) = 8.24 Hz, 4H), 1.36 (s, 24H).

Synthesis of **41**.
Under an N_2 atmosphere, 100 ml $THF^{(technical)}$ and 10 ml water were added to mixture of 113.6 mg (0.19 mmol) **35** and 3,74 g K_2CO_3. The mixture was degassed for 20 minutes and 284 mg $Pd(PPh_3)_2Cl_2$ were added. The reaction mixture was heated to 70˚C and 77 mg (0.19 mmol) **40** in 3.4 ml of THF/water (10/1) were dosed over 3 hours to the reaction mixture. The mixture was stirred at 70˚C for 16 hours. After the reaction cooled to room temperature, water was added to the reaction

mixture. Solids were filtrated off. The solids could partially be dissolved in DCM (50 mg). However no pure product could be obtained.

Synthesis of **42**.[57]
Under an N_2 atmosphere, 20 ml THF(technical) and 2 ml water were added to mixture of 100.7 mg (0.17 mmol) **35**, 272 mg (0.67 mmol) **40** and 333 mg K_2CO_3. The mixture was degassed for 15 minutes and 32 mg $Pd(PPh_3)_2Cl_2$ was added. This was stirred at 70˚C for 16 hours. After the reaction cooled to RT, water was added to the reaction mixture. The mixture was extracted three times with DCM. The remaining solids were filtrated off and the combined organic layer was dried with $MgSO_4$. The solvent was removed under vacuum and 80 mg of a brown solid was obtained. A TLC test was done and with a DCM eluence spots were observed at an R_f value of: 0.02, 0.11, 0.23, 0.32, 0.48, 0.75 and 0.91. No further purification was attempted.

Synthesis of **43**.
Under an N_2 atmosphere, 30 ml TEA and 30 ml THF were added to a mixture of 2.19 mg (12 mmol) 4-bromo-styrene, 116 mg CuI and 790 mg PPh_3. Vacuum was applied followed by addition of nitrogen gas. 422 mg $Pd(PPh_3)_2Cl_2$ and 2.59 mg TMS-acetylene (26 mmol) were added and the setup was wrapped in aluminum foil to reduce the exposure to light. The reaction mixture was stirred at 77˚C for 16 hours. After the mixture cooled to room temperature it was filtrated and the filtrate was concentrated under vacuum. The obtained brown solution was further purified using column chromatografie using *n*-hexane (R_f = 0.43). The product was obtained as a clear solution in *n*-hexane (489 mg(determined with proton-NMR) in *n*-hexane (37%), 2.44 mmol, 20%). ^{1}H-NMR spectrum matched known literature values[58]. ^{1}H-NMR (400 MHz, $CDCl_3$, 25˚C), 7.42 (d, ^3J(HH) = 8.57 Hz, 2H), 7.33 (d, ^3J(HH) = 8.20 Hz, 2H), 6.69 (dd, 11.0 Hz and 17.5 Hz, 1H), 5.78(d, ^3J(HH) = 17.6 Hz, 1H), 5.29 (d, ^3J(HH) = 11 Hz, 1H), 0.251 (s, 9H).

7. Acknowledgements

I came to the university looking to test my academic and practical skills and was not disappointed. At no point was this more so than during my master thesis in the Organic Chemstry and Catalysis group. It was my genuine pleasure to undertake this challenge with the aid of all the members of the group. The various discussions, these being work related or otherwise, were invaluable for my project, my academic development and maintaining my sanity trough the daily 4 hour commute.

There are some people I would like to thank especially. Starting with professor Bert Klein Gebbink for giving me the opportunity to do my master thesis at his group.
Also I would like to especially thank doctor Matthias Otte for the daily supervision and reacquainting me with the practical life of an organic chemist. Also I would like to thank him for the various serious talks we had: about my project, the educational system and chemistry in general, but also for the less serious talks about being rich and famous and the poetic depth of lyrics in music.

The same gratitude extends to Thom Klein, Annet Vliegenthart, Desmond Eefting and Martine Tiddens for our more close cooperation, be that as a fellow student under Matthias or as my neighbor in “The Office”.

I would also like to thank the technical staff: doctor Johann Jastrzebski, Henk Kleijn and Jord van Schaik for their aid in obtaining my analytical data and other practical problems Matthias could not help me with. I also would like to thank doctor Martin Lutz for measuring the crystal structure of my compound.

Finally I would like to extend my thanks to the remainder of the OCC group for an awesome year of chemistry. The productive atmosphere and close nit group really made the last year a joy.

Literature

[1] P.G. Jessop, F. Joó, CC. Tai, *Coordination Chemistry Reviews* **2004**, *248,* 2425–2442.

[2] W. Wang, S. Wang, X. Ma, J. Gong, *Chem. Soc. Rev.* **2011**, *40*, 3703–3727.

[3] W.R. Cullen, M.D. Fryzuk, B.R. James, J.P. Kutney, GJ. Kang, G. Herb, I.S. Thorburn, R. Spogliarich, *Journal of Molecular Catalysis* **1990**, *62*, 243-253.

[4] P. Jochmann, D.W. Stephan, *Chem. Eur. J.* **2014**, *20*, 8370 – 8378.

[5] R. Waymouth, P. Pino, *J. Am. Chem. Soc.* **1990**, *112*, 4911-4914.

[6] G.D. Frey, V. Lavallo, B. Donnadieu, W.W. Schoeller, G. Bertrand, *Science* **2007**, *314*, 439-441.

[7] C. Walling, L. Bollyky, *J. Am. Chem. Soc.* **1964**, *86*, 3750-3752

[8] M.W. Haenel, J. Narangerel, U. Richter, A. Rufinska, *Angew. Chem. Int. Ed.* **2006**, *45*, 1061 – 1066.

[9] K. Ravindra, L. Bencs, R. Van Grieken, *The Science of the Total Environment* **2004**, *318*, 1–43.

[10] G. Agiorgitis, R. Wolf, *Chemical Geology* **1984**, *42*, 277-286.

[11] L.J. Cabri, D.C. Harris, T.W. Weiser, *Explor. Mining Geol.* **1996**, *vol. 5 no. 2,* 73-167.

[12] J. Seayad, B. List, *Org. Biomol. Chem.* **2005**, *3*, 719–724.

[13] P.I. Dalko, L. Moisan, *Angew. Chem. Int. Ed.* **2004**, *43*, 5138 – 5175.

[14] K.A. Jørgensen, *Angew. Chem. Int. Ed.* **2000**, *39*, 3558 – 3588.

[15] G. N. Lewis, *Valence and the Structure of Atoms and Molecules*, Chemical Catalogue Company, New York, **1923**.

[16] H. C. Brown, H. I. Schlesinger, S. Z. Cardon, *J. Am. Chem. Soc.* **1942**, *64*, 325 – 329

[17] H. C. Brown, B. Kanner, *J. Am. Chem. Soc.* **1966**, *88*, 986 – 992.

[18] G. Wittig, E. Benz, *Chem. Ber.* **1959**, *92*, 1999 – 2013.

[19] W. Tochtermann, *Angew. Chem. Int. Ed. Engl.* **1966**, *5*, 351 – 371.

[20] G.C. Welch, R. R. S. Juan, J. D. Masuda, D. W.Stephan, *Science* **2006**, *314*, 1124 – 1126.

[21] L.L. Zeonjuk, N. Vankova, A. Mavrandonakis, T. Heine, G. Röschenthaler, J. Eicher, *Chem. Eur. J.* **2013**, *19*, 17413 – 17424.

[22] G.C. Welch, D.W. Stephan, *J. Am. Chem. Soc.* **2007**, *129*, 1880-1881.

[23] P. Spies, G. Erker, G. Kehr, K. Bergander, R. Fröhlich, S. Grimme, D.W. Stephan, *Chem. Commun.* **2007**, 5072–5074.

[24] S. Schwendemann, R. Fröhlich, G. Kehr, G. Erker, *Chem. Sci.* **2011**, *2*, 1842–1849.

[25] D. J. Scott, M.J. Fuchter, A.E. Ashley, *Angew. Chem. Int. Ed.* **2014**, *53*, 1 – 6.

[26] P.A. Chase and D.W. Stephan, *Angew. Chem. Int. Ed.* **2008**, *47*, 7433–74.

[27] H. Wang, R. Fröhlich, G. Kehr, G. Erker, *Chem.Commun*. **2008**, 5966–5968.

[28] K.V. Axenov, G. Kehr, R. Fröhlich, G. Erker, *Organometallics* **2009**, *28*, 5148–5158.

[29] P. A. Chase, T. Jurca, D. W. Stephan, *Chem.Commun*. **2008**, 1701–1703.

[30] T. Mahdi, D.W. Stephan, *J. Am. Chem. Soc.* **2014**, *136 (45)*, 15809–15812.

[31] S.J. Geier, A.L. Gille, T.M. Gilbert, D.W. Stephan, *Inorg. Chem.* **2009**, *48*, 10466–10474.

[32] S.J. Geier, D.W. Stephan, *J. Am. Chem. Soc.* **2009**, *131*, 3476–3477

[33] C.B. Caputo, K. Zhu, V.N. Vukotic, S.J. Loeb, D.W. Stephan, *Angew. Chem. Int. Ed.* **2013**, *52*, 960 –963.

[34] L.J. Hounjet, C. Bannwarth, C.N. Garon, C.B. Caputo, S. Grimme, D.W. Stephan, *Angew. Chem.* **2013**, *125*, 7640 –7643.

[35] C. Yu, Y.Jin, W Zhang, *Chem. Rec.* **2015**, *15*, 97-106.

[36] J. Vollmeyer, U. Baumeister, S. Höger, *Beilstein J. Org. Chem.* **2014**, *10*, 910–920.

[37] M. Mastalerz, *Angew. Chem. Int. Ed.* **2010**, *49*, 5042 – 5053.

[38] R.L.E. Furlan, S. Otto, J.K.M. Sanders, *PNAS* **2002,** *vol. 99 no. 8*, 4801–4804.
[39] H.R. Kricheldorf, *Macromolecules* **2003**, *36*, 2302-2308.
[40] K. Matsui, Y. Segawa, K. Itami, *J. Am. Chem. Soc.* **2014**, *136*, 16452−16458.
[41] W. Huang, M. Wang, C. Du, Y. Chen, R. Qin, L. Su, C. Zhang, Z. Liu, C. Li, Z. Bo, *Chem. Eur. J.* **2011**, *17*, 440 – 444.
[42] S. Lei, A. Ver Heyen, S. De Feyter, M. Surin, R. Lazzaroni, S. Rosenfeldt, M. Ballauff, P. Lindner, D. Mössinger, S. Höger, *Chem. Eur. J.* **2009**, *15*, 2518 – 2535.
[43] N. Shabelina, S. Klyatskaya, V. Enkelmann, S. Höger, *C. R. Chimie* **2009**, *12*, 430-436.
[44] A. Britze, J. Jacob, V. Choudhary, V. Moellmann, G. Grundmeier, H. Luftmann, D. Kuckling, *Polymer* **2010**, *51*, 5294-5303.
[45] M. Yamashita, Y. Yamamoto, K. Akiba, D. Hashizume, F. Iwasaki, N. Takagi, S. Nagase, *J. Am. Chem. Soc.* **2005**, *127*, 4354-4371.
[46] T. Ishiyama, N. Matsuda, N. Miyaura, A. Suzuki, *J. Am. Chem. Soc.* **1993**, *115*, 11018-11019.
[47] Y. Hirano, S. Kojima, Y. Yamamoto, *J. Org. Chem.* **2011**, *76*, 2123–2131.
[48] L. Chen, B.E. Lemma, J.S. Rich, J. Mack, *GreenChem.* **2014**, *16*,1101–1103.
[49] A. Elangovan, YH. Wang, TI. Ho, *Org. Lett.* **2003**, *vol. 5 No. 11,* 1841-1844.
[50] J.H. Park, S.V. Bhilare, S.W. Youn, *Org. Lett.* **2011**, *Vol. 13 No. 9*, 2228-2231.
[51] HK. Chang, S. Datta, A. Das, A. Odedra, RS. Liu, *Angew. Chem. Int. Ed.* **2007**, *46*, 4744–4747.
[52] M.B. Goldfinger, K.B. Crawford, T.M. Swager, *J. Am. Chem. Soc.* **1997**, *Vol. 119 No. 20*, 4578-4593.
[53] M. Lehmann, A. Schulz, A. Villinger, *Angew.Chem.Int.Ed.* **2009**, *48*, 7444 –7447.
[54] CC. Huang, YC. Lin, PY. Lin, YJ. Chen, *Eur. J. Org. Chem.* **2006**, 4510–4518.
[55] A. Klapars, S.L. Buchwald, *J. Am. Chem. Soc.* **2002**, *124*, 14844-14845.
[56] CJ. Zhao, D. Xue, ZH. Jai, C. Wang, J. Xiao, *Synlett* **2014**, *25*, 1577–1584.
[57] D. Gudeika, R.R. Reghu, J.V. Grazulevicius, G. Buika, J. Simokaitiene, A. Miasojedovas, S. Jursenas, V. Jankauskas, *Dyes and Pigments*, **2013**, *99*, 895-902.
[58] S.E. Denmark, L. Neuville, M.E.L. Christy, S.A. Tymonko, *J. Org. Chem.* **2006**, *71*, 8500-8509.

Appendix

^{1}H-NMR of **20**

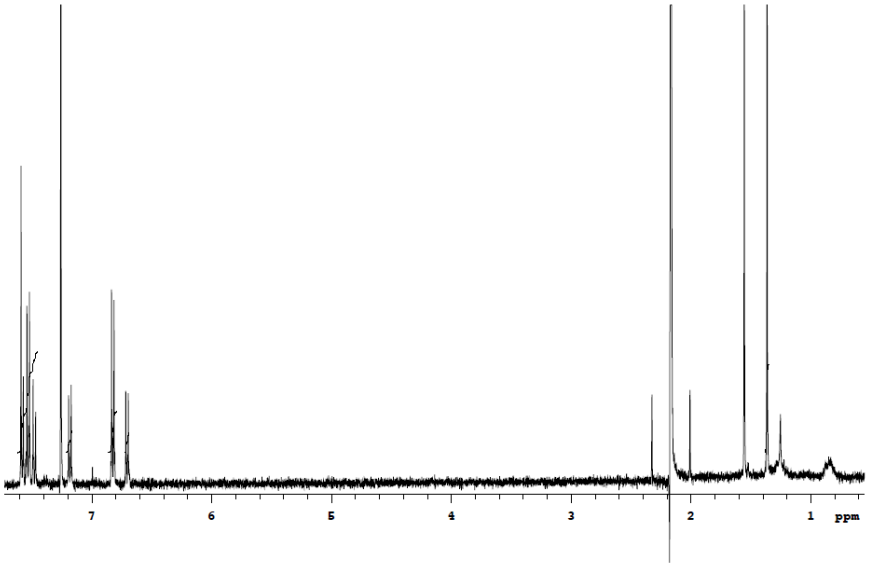

^{1}H-NMR of failed reaction of **21** attempt 1

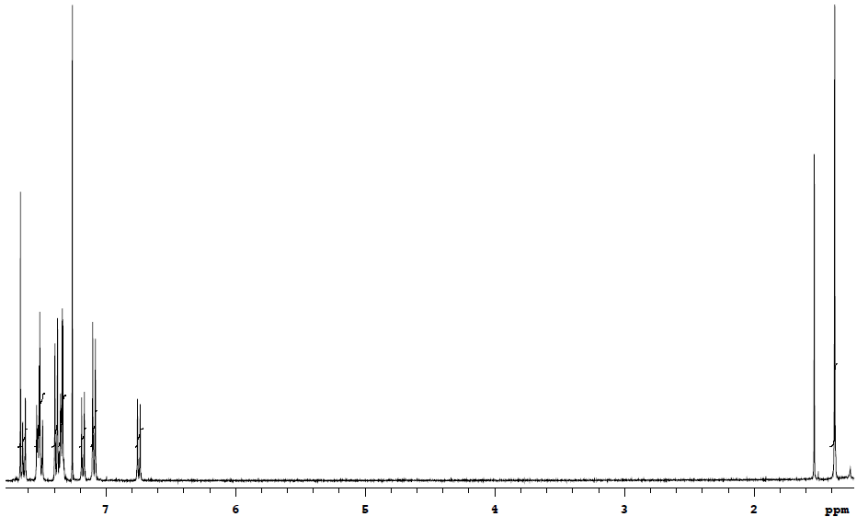

^{1}H-NMR of failed synthesis of **23** attempt 2

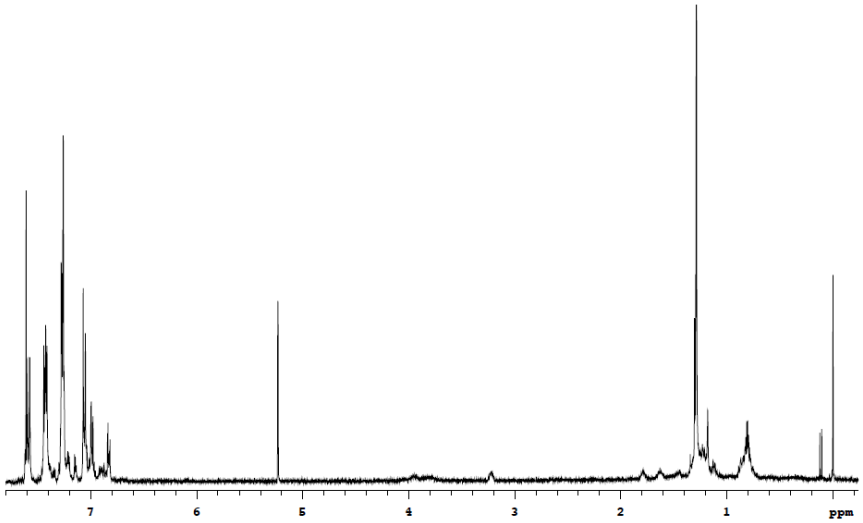

^{1}H-NMR of failed synthesis of **25** attempt 1

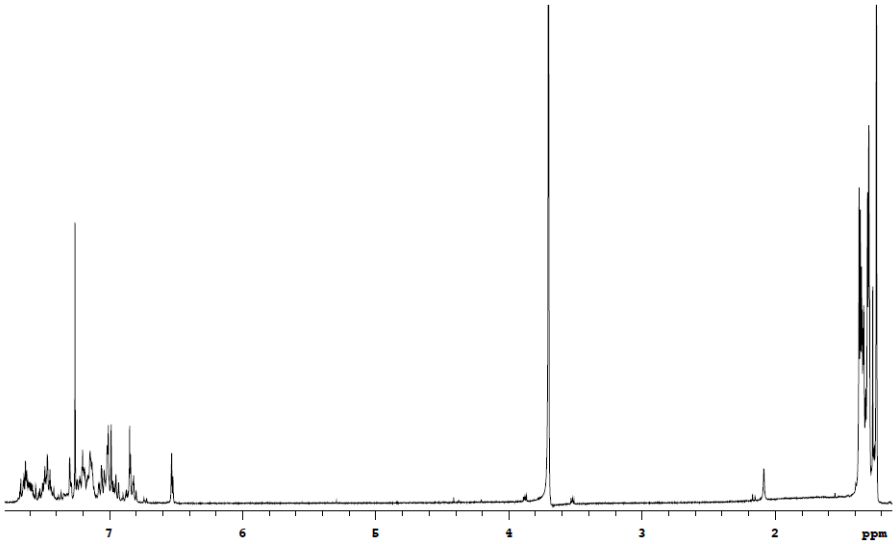

^{1}H-NMR of failed synthesis of **25** attempt 2

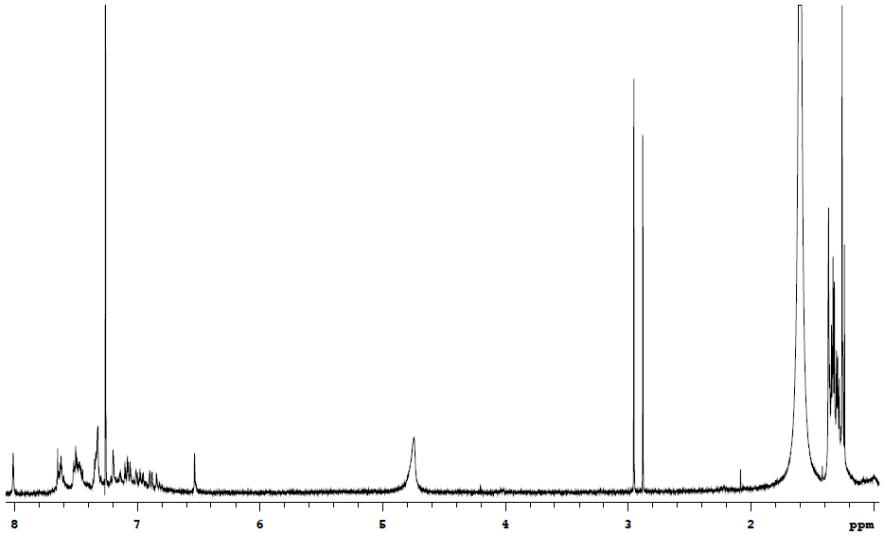

^{1}H-NMR of failed synthesis of **25** attempt 3

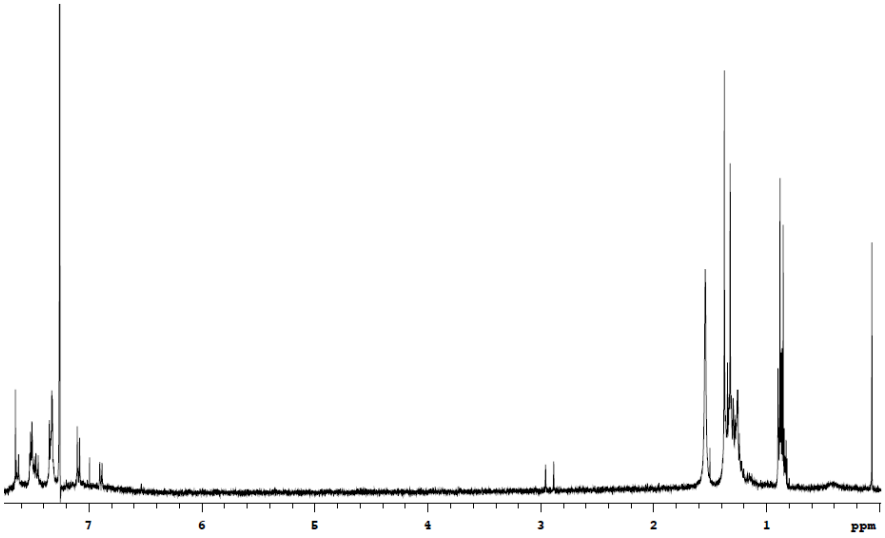

^{1}H-NMR of **26**

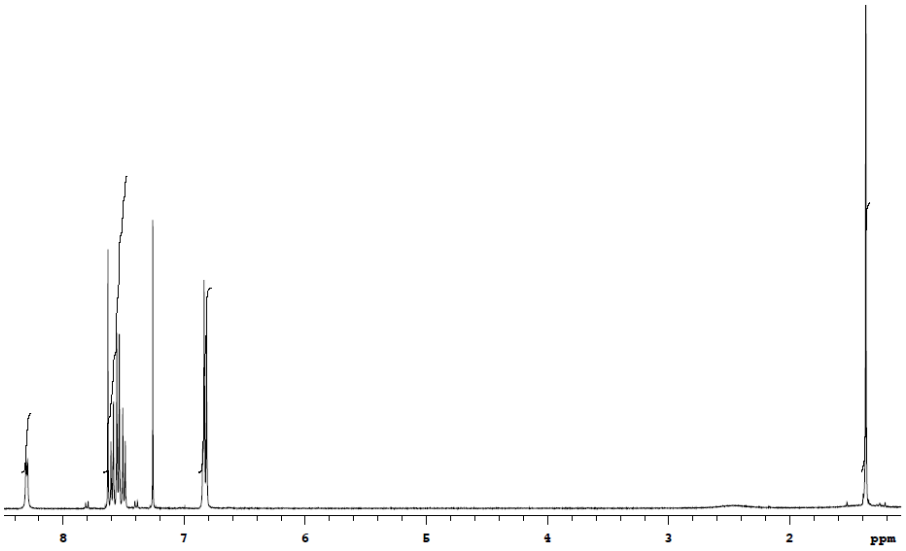

^{1}H-NMR of **27** in $CDCL_3$

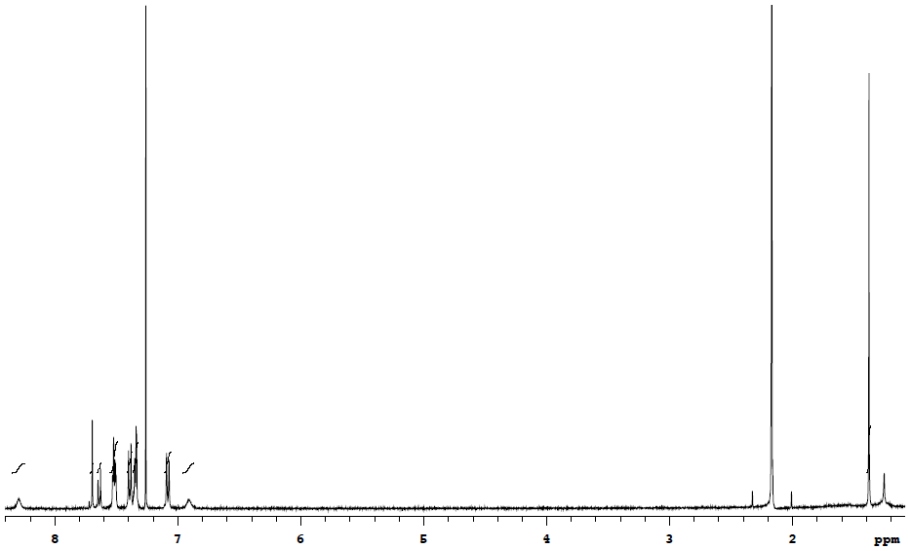

^{1}H-NMR of **27** in toluene-d8

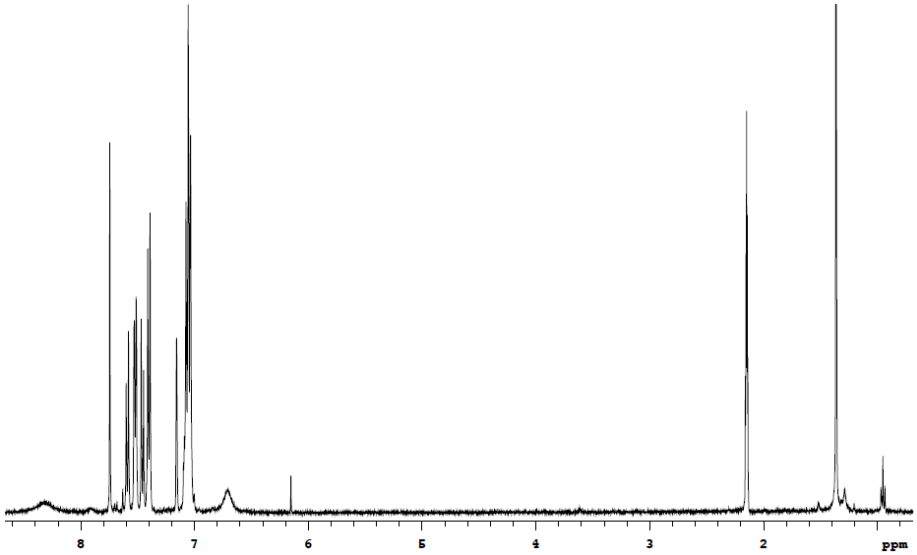

^{1}H-NMR of **27** in CD_2Cl_2

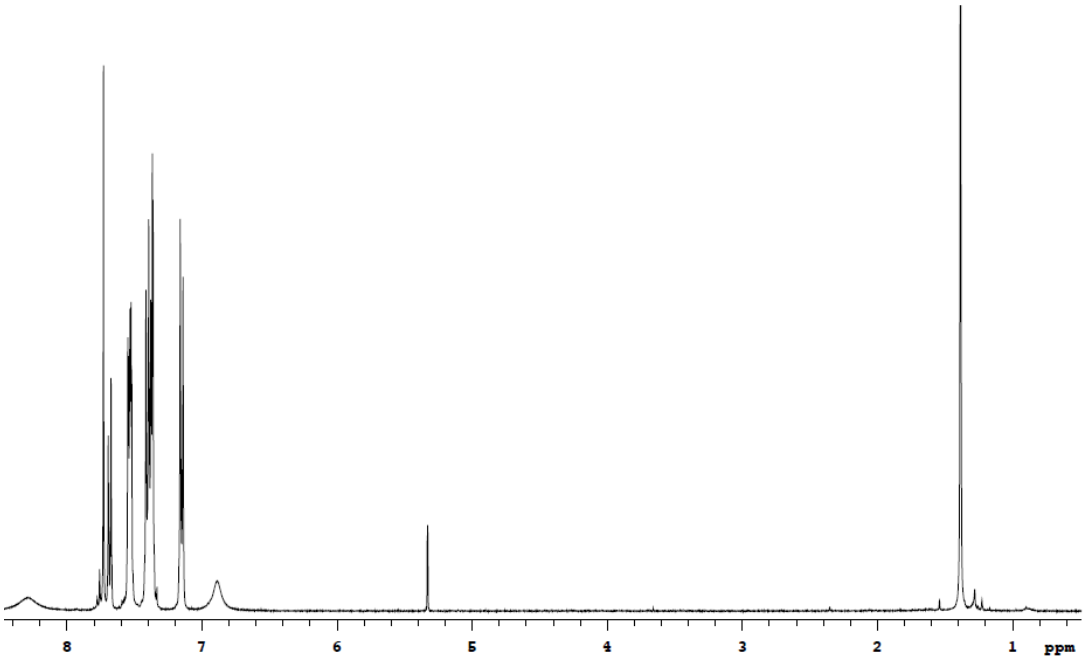

^{1}H-NMR of **28**

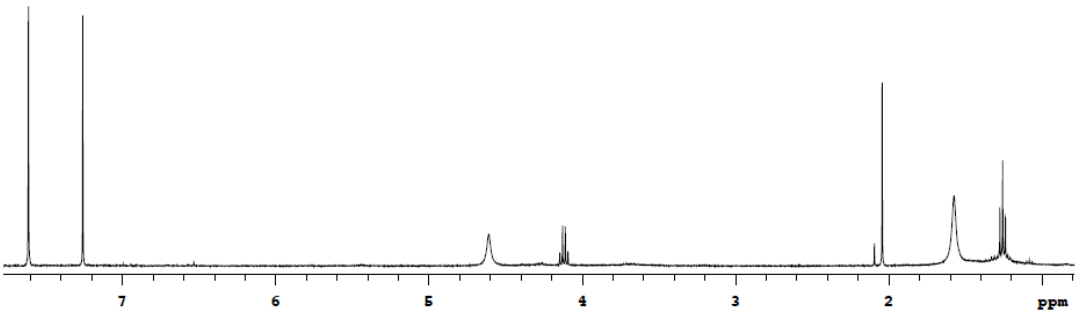

^{1}H-NMR of **29**

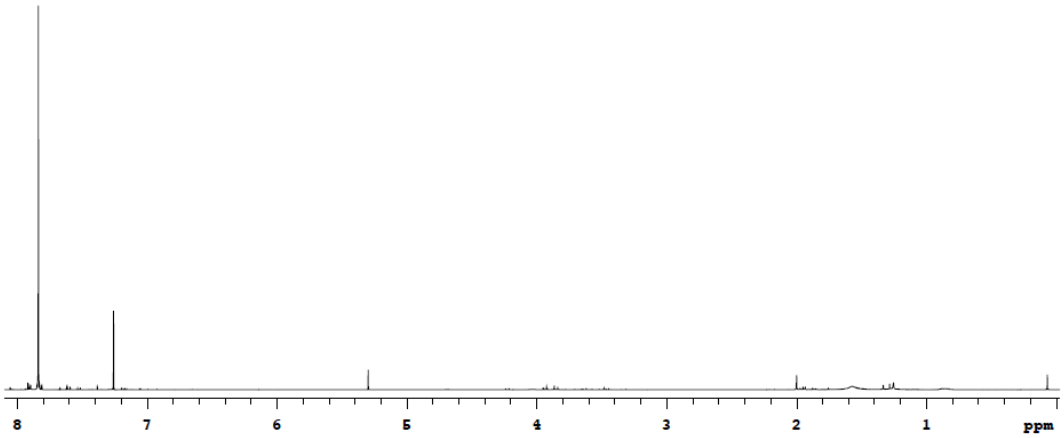

^{1}H-NMR of **30** (impure)

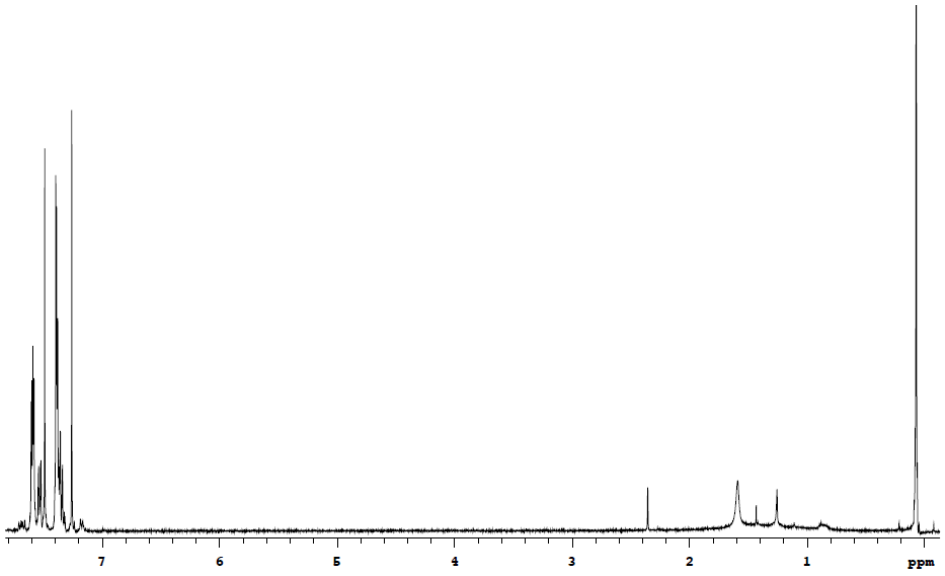

^{1}H-NMR of **31**

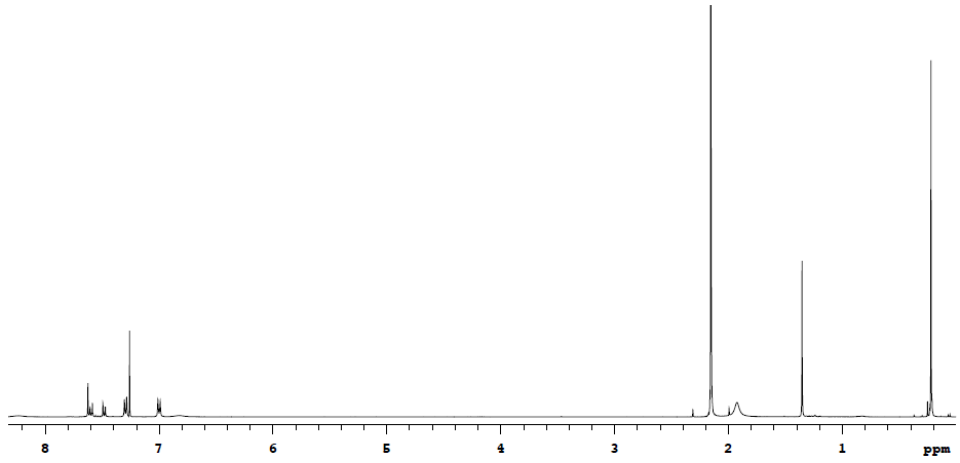

^{1}H-NMR of **32**

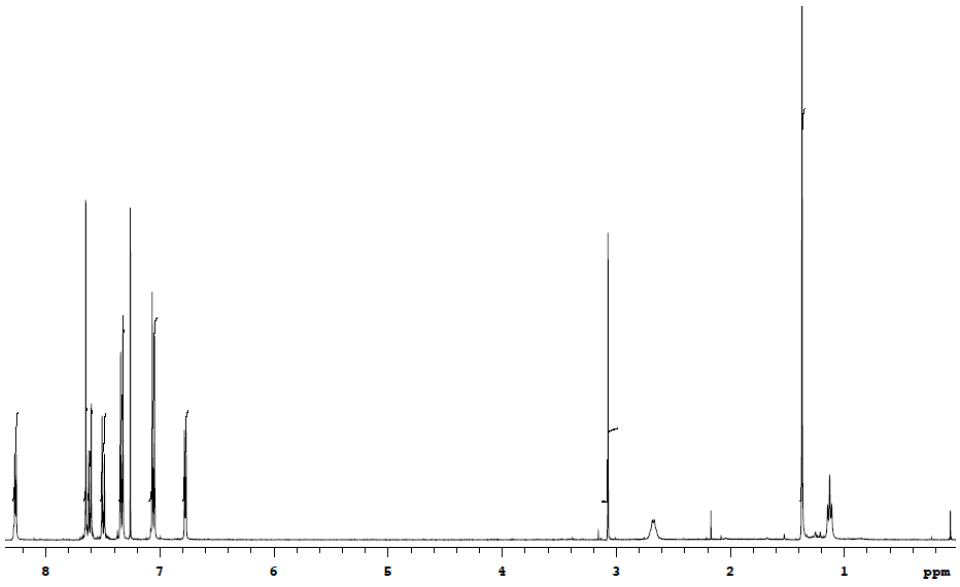

^{1}H-NMR of failed synthesis of **33**

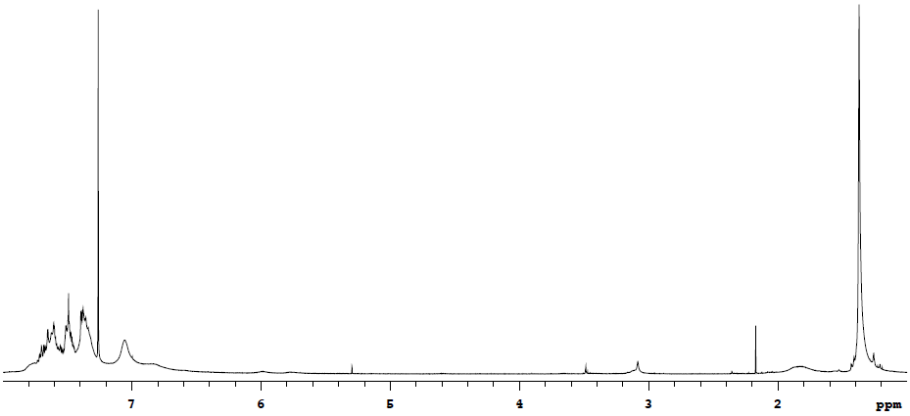

^{1}H-NMR of failed synthesis of 4-*tert*-butyl-2,6-diiodo-bromobenzene

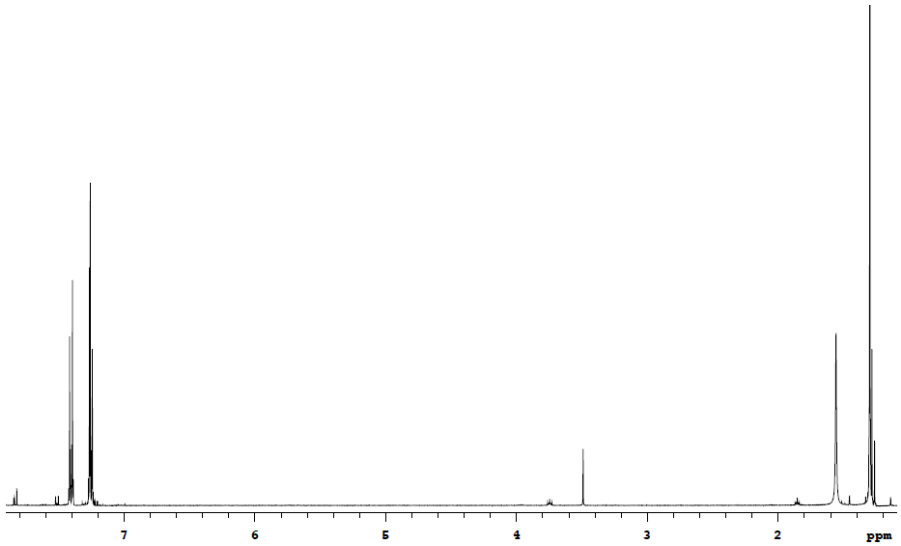

^{1}H-NMR of failed synthesis of **30** with bromine substituted for iodine

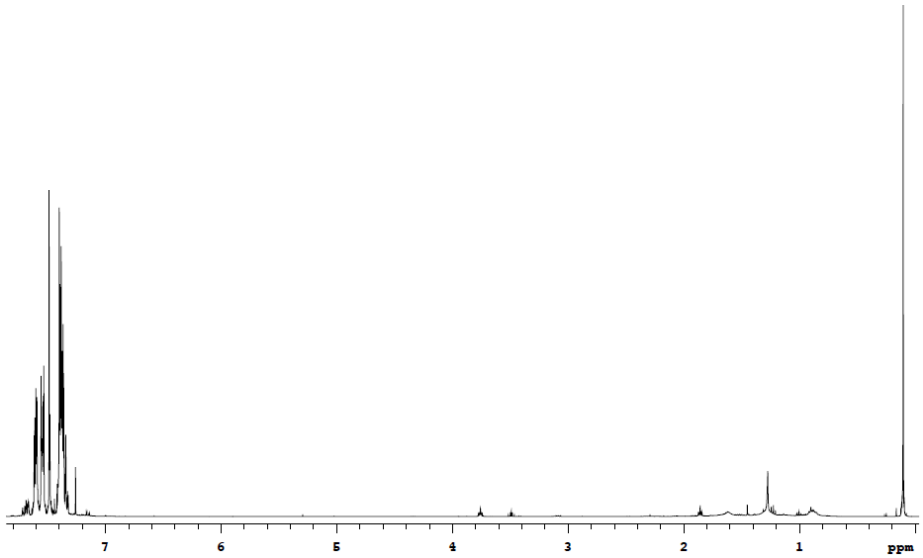

^{1}H-NMR of 35

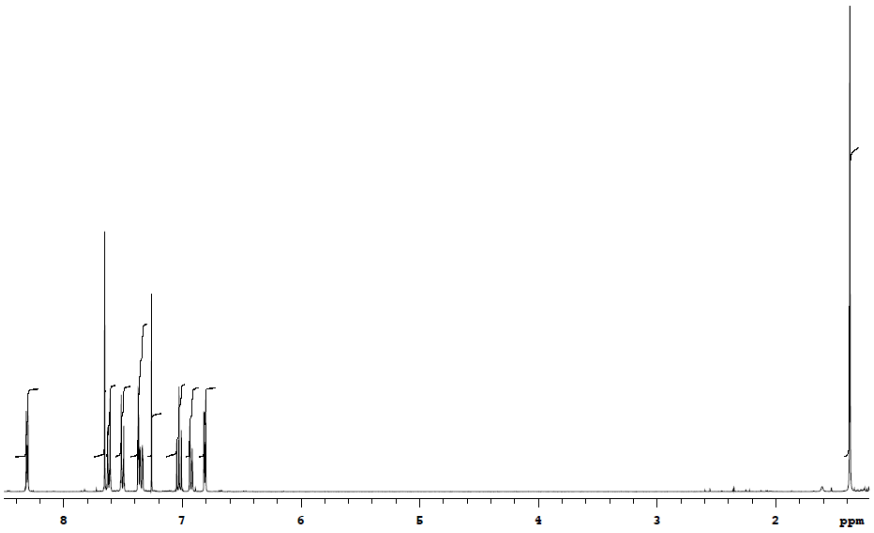

^{1}H-NMR of 36

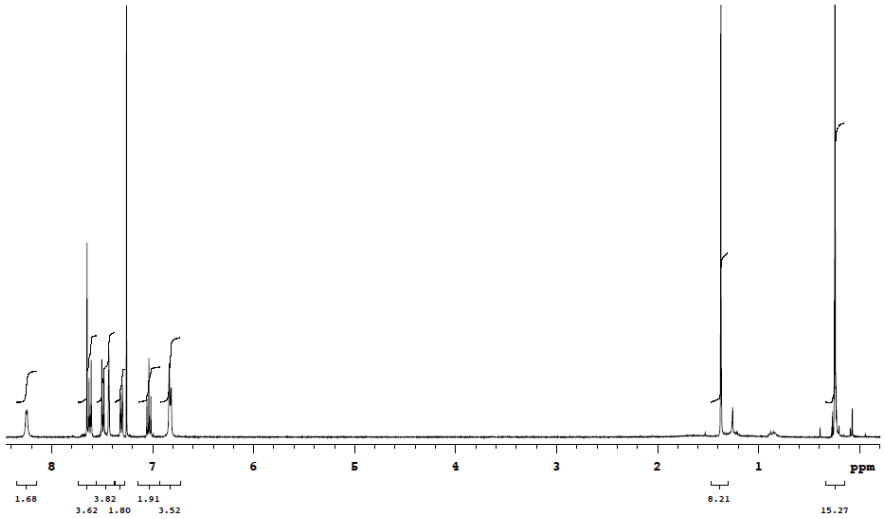

^{1}H-NMR of 37

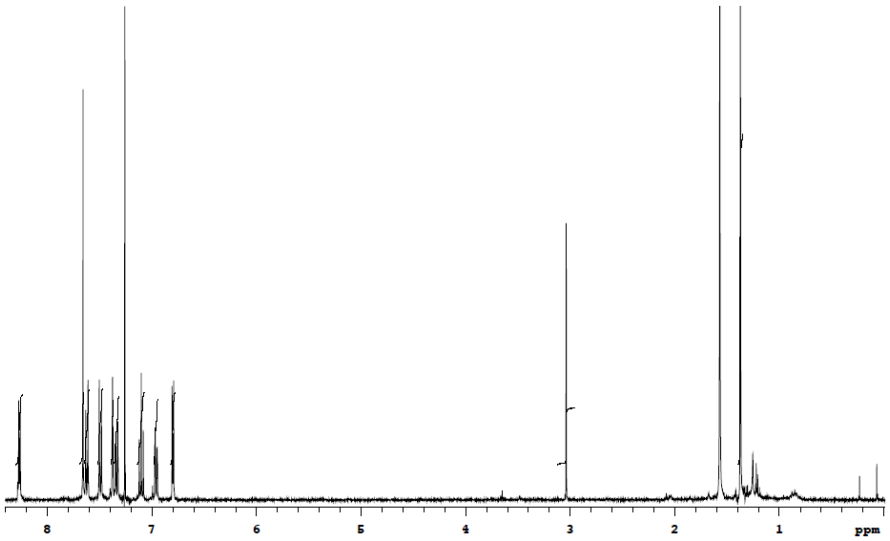

^{1}H-NMR of failed synthesis of **38** attempt 1

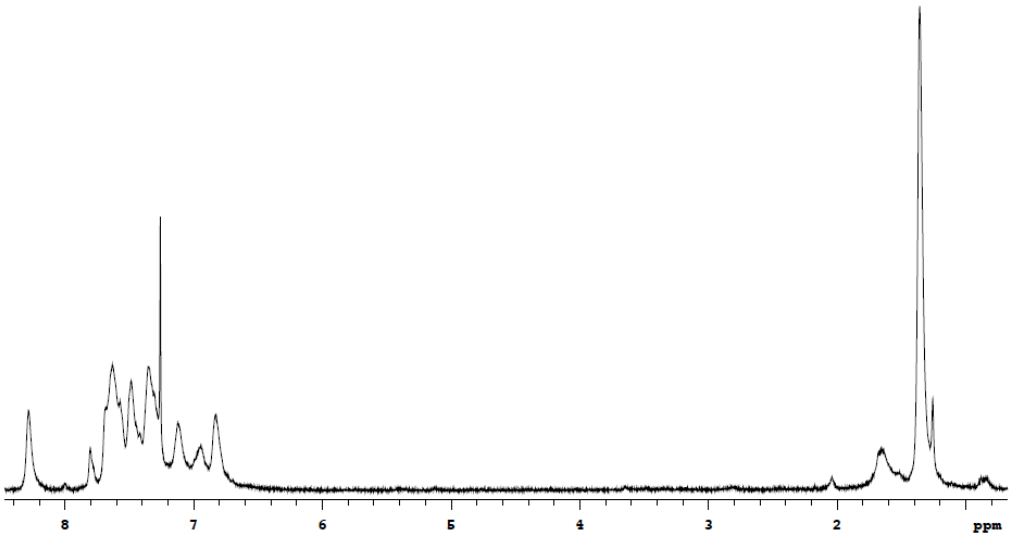

^{1}H-NMR of failed synthesis of **38** attempt 2

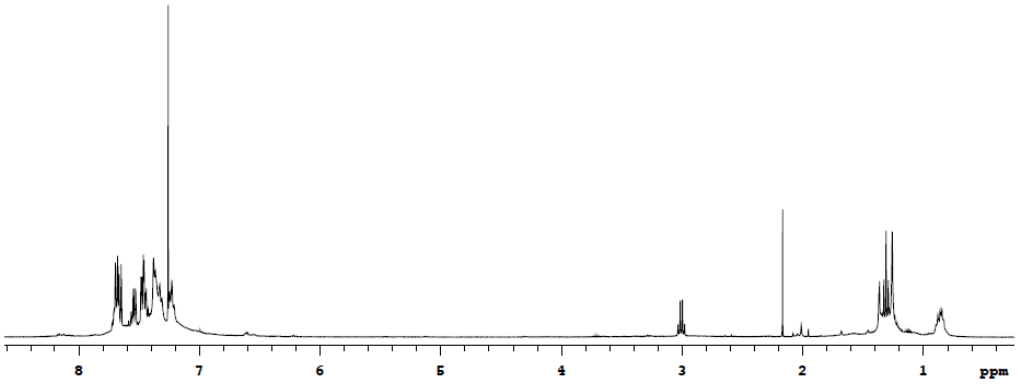

^{1}H-NMR of **39**

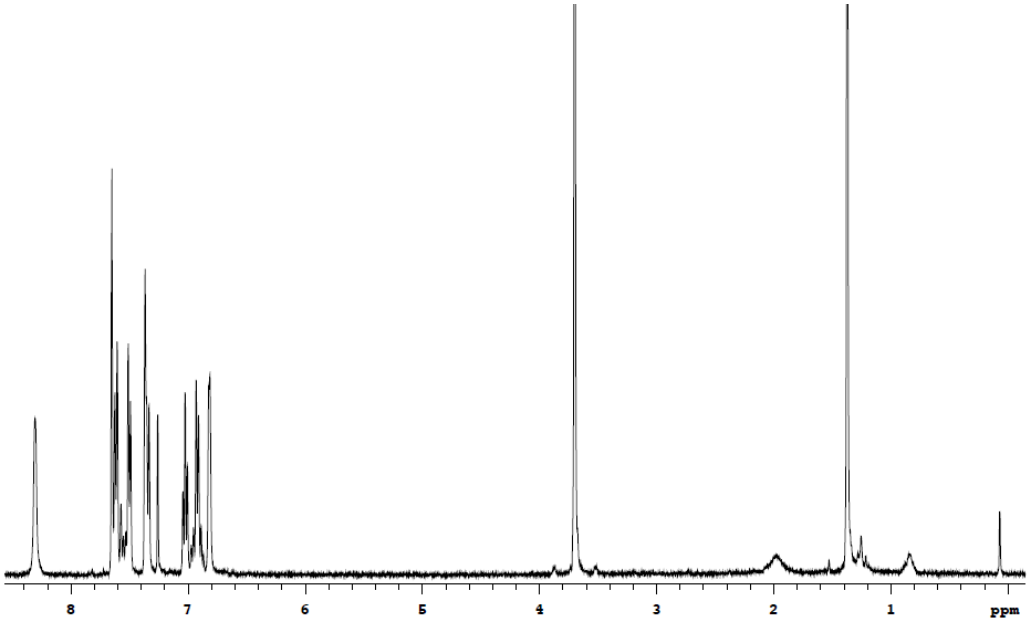

^{1}H-NMR of **40**

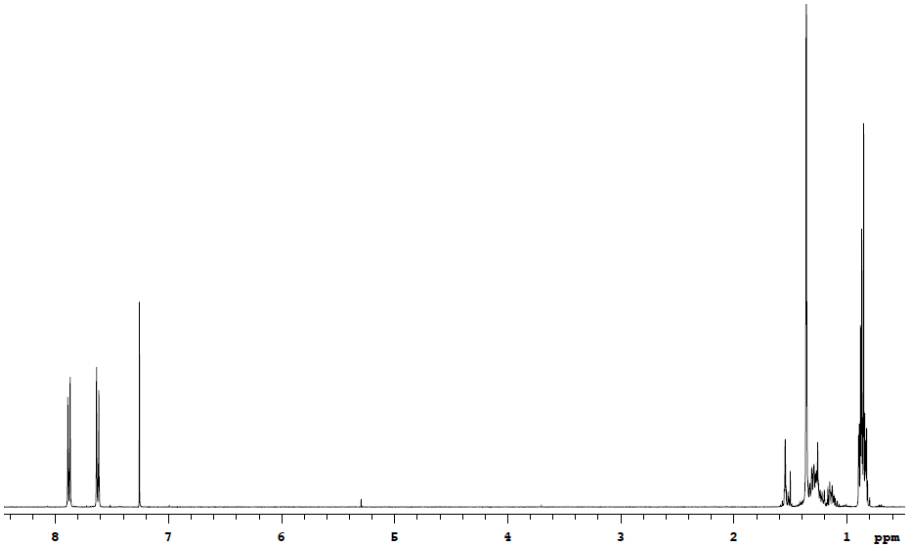

^{1}H-NMR of failed synthesis of **41**

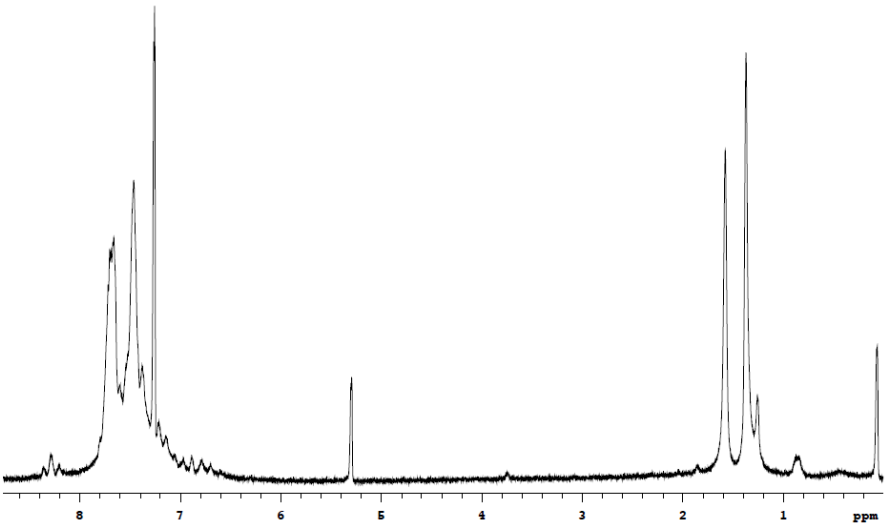

^{1}H-NMR of failed synthesis of **42**

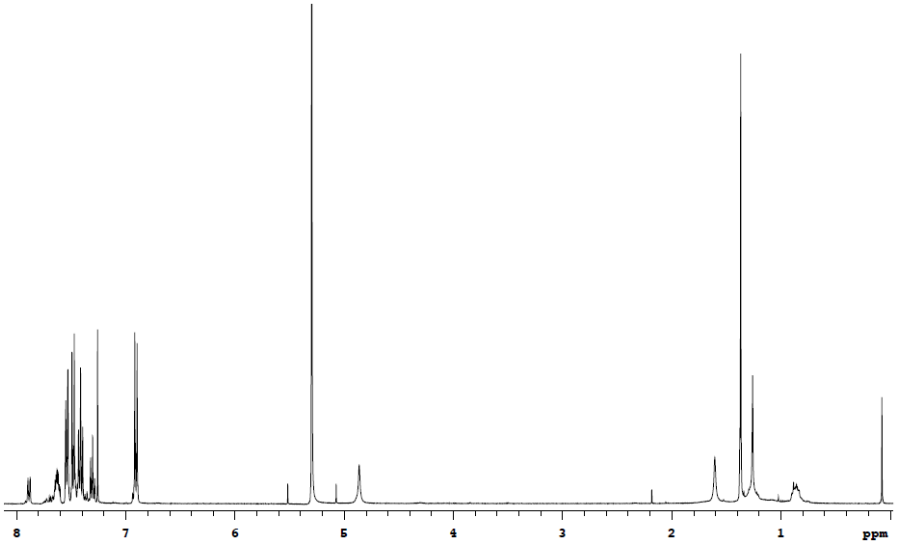

^{1}H-NMR of **43**

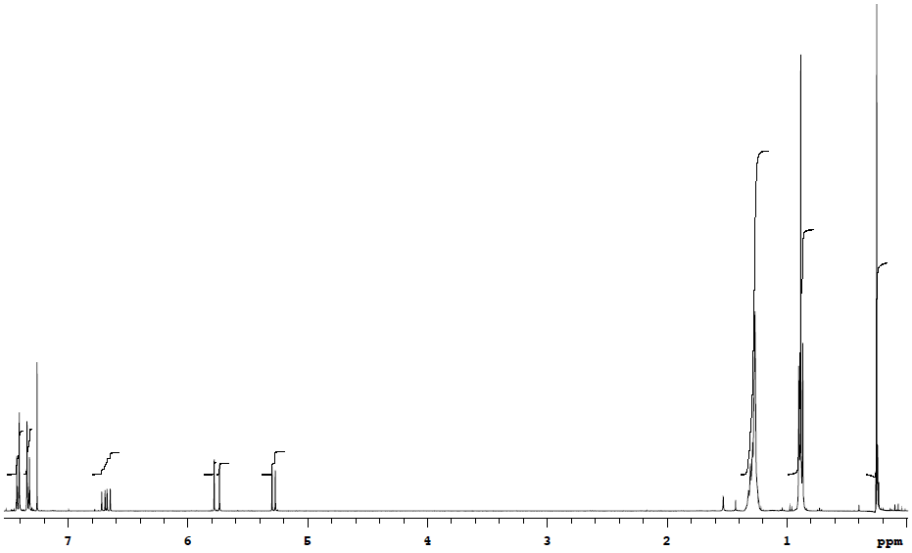

^{1}H-NMR of **10** mixed with **27** in toluene-d8

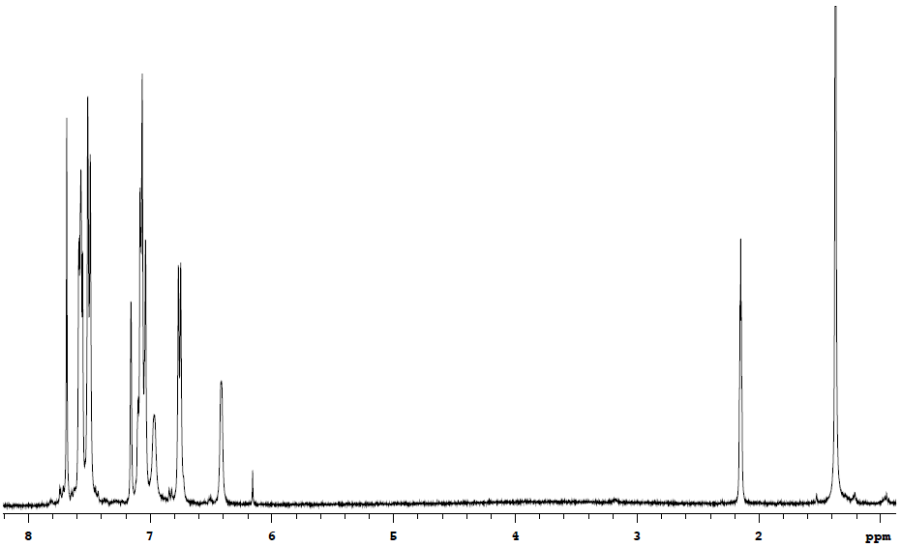

^{1}H-NMR of **10** mixed with **27** in CD_2Cl_2

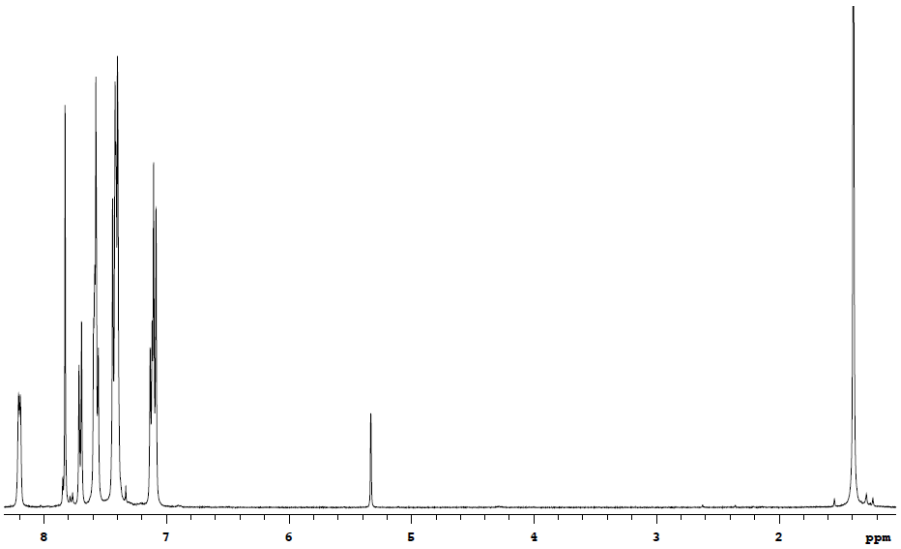

^{1}H-NMR of **10** mixed with **27** in CD_2Cl_2 with H_2

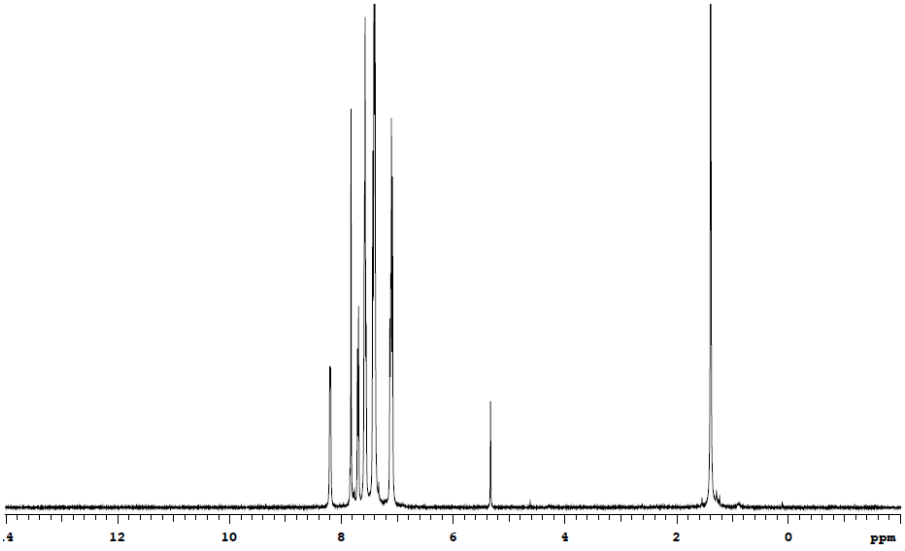

^{13}C-NMR of **21**

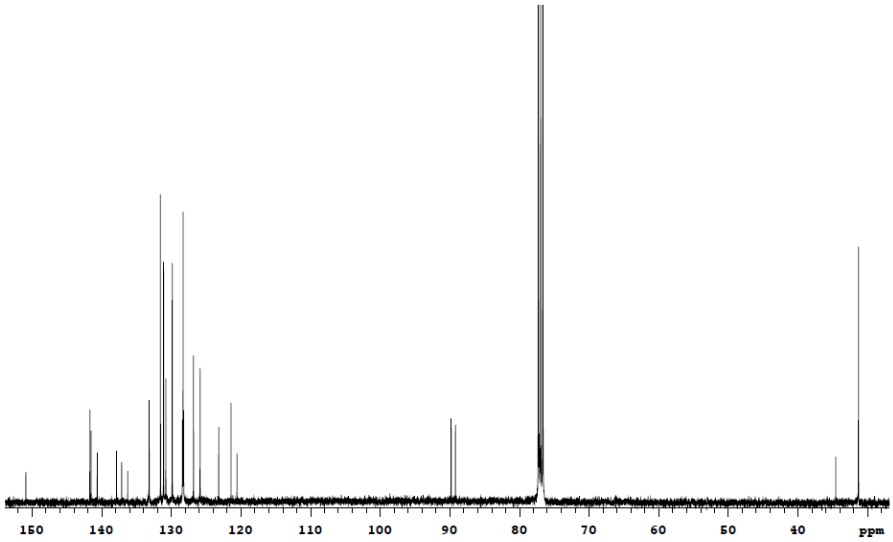

^{13}C-NMR of **27**

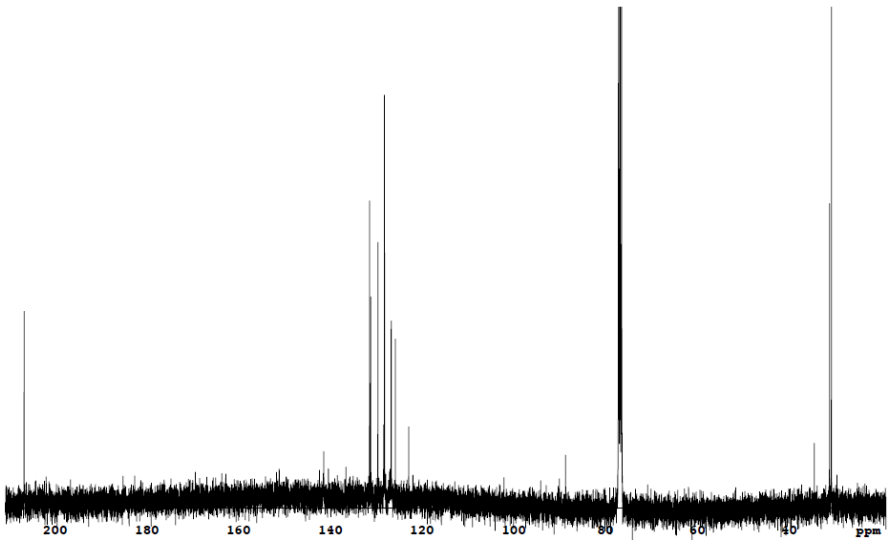

^{13}C-NMR of 29

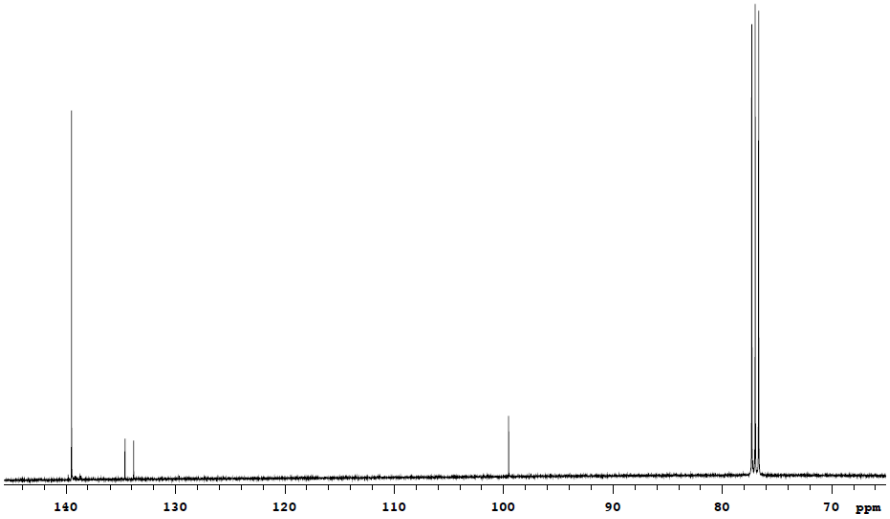

^{13}C-NMR of 30

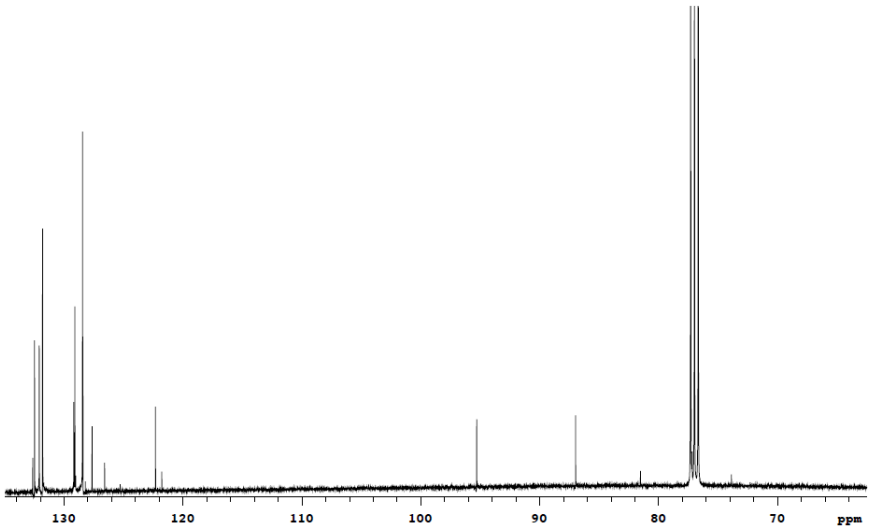

^{13}C-NMR of 31

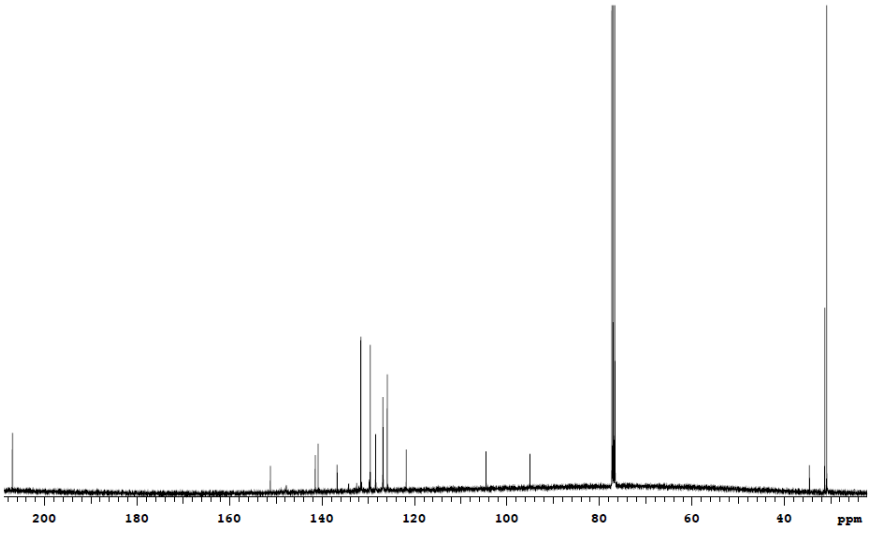

^{13}C-NMR of 32

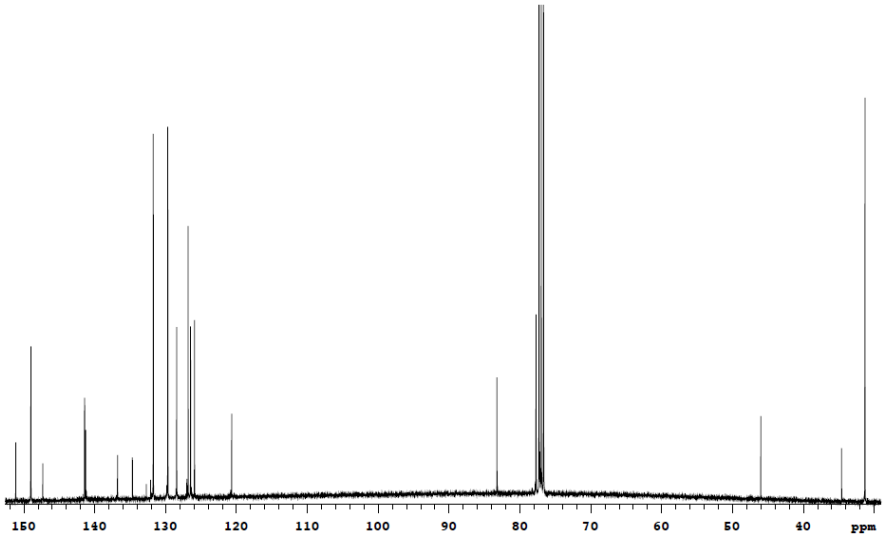

^{13}C-NMR of 35

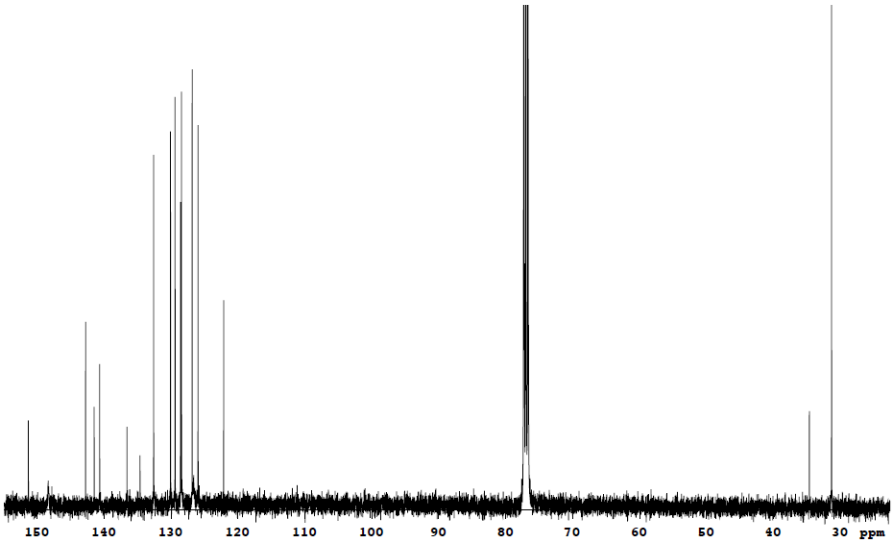

^{13}C-NMR of 37

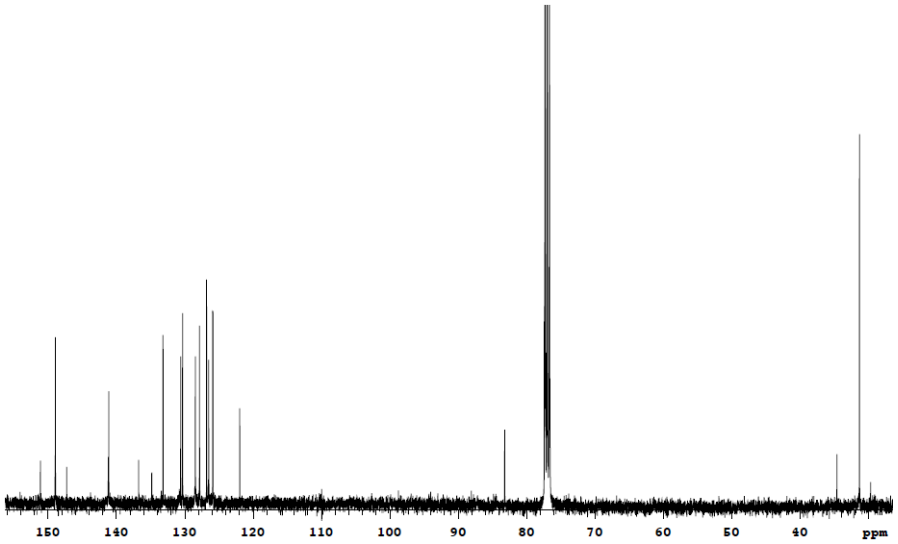

^{13}C-NMR of **40**

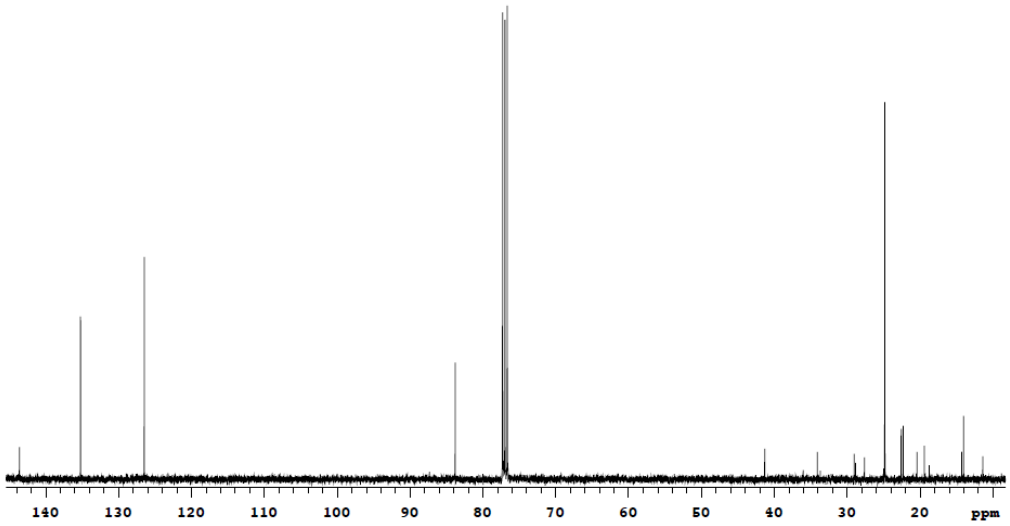

^{19}F-NMR of **10** in toluene-d8 (impure)

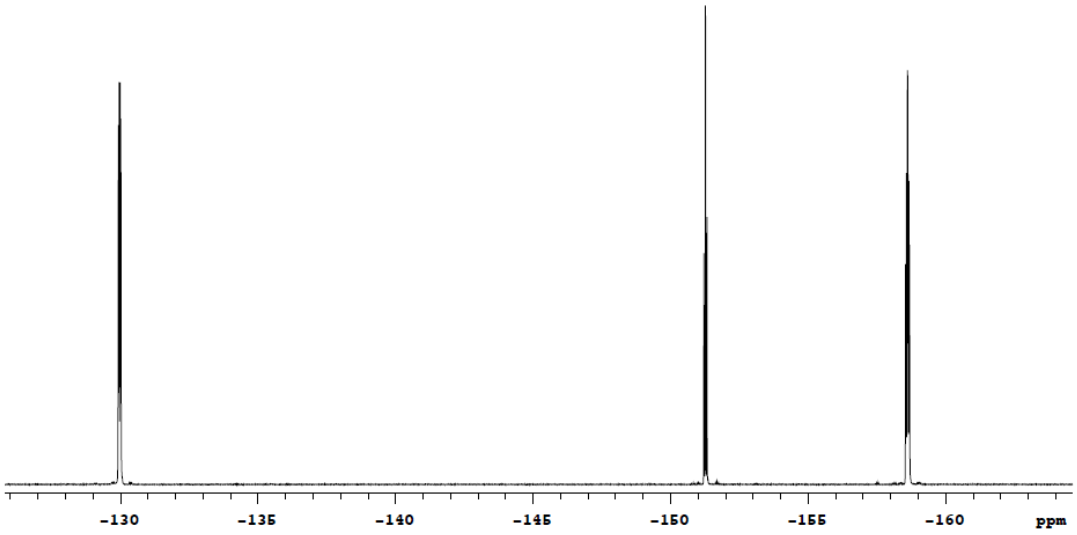

^{19}F-NMR of **10** in CD_2Cl_2

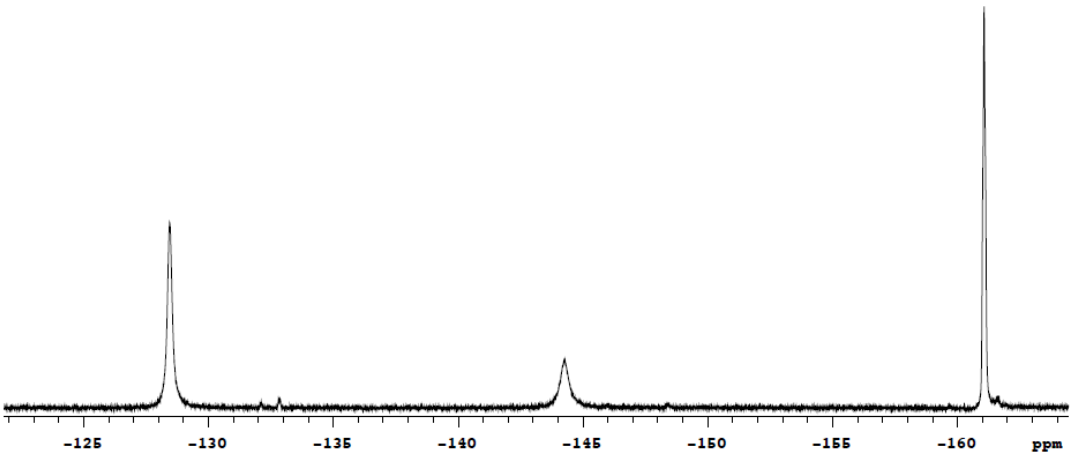

^{19}F-NMR of **10** mixed with **27** in toluene-d8

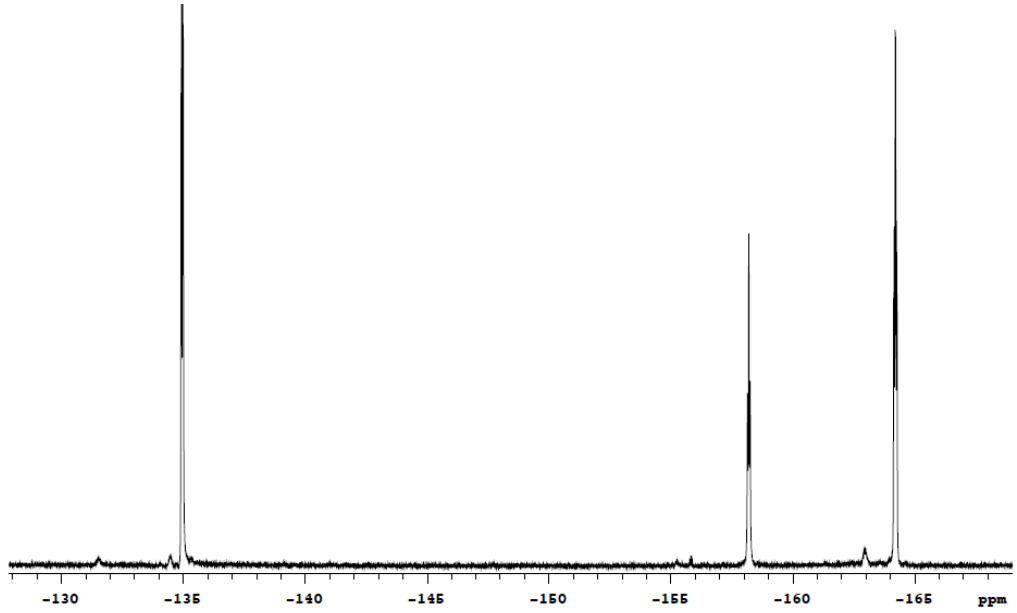

^{19}F-NMR of **10** mixed with **27** in toluene-d8 after 16 hours

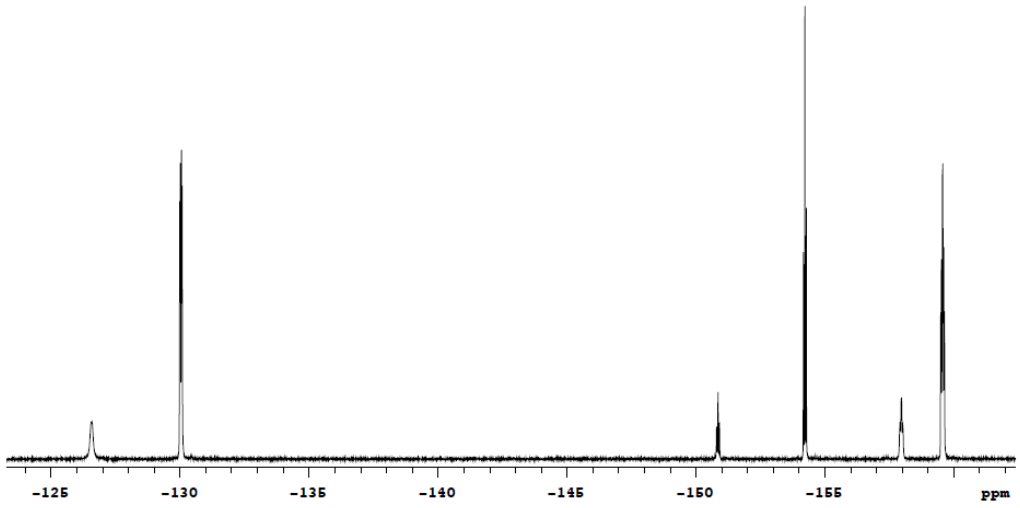

^{19}F-NMR of **10** mixed with **27** in toluene-d8 after 40 hours

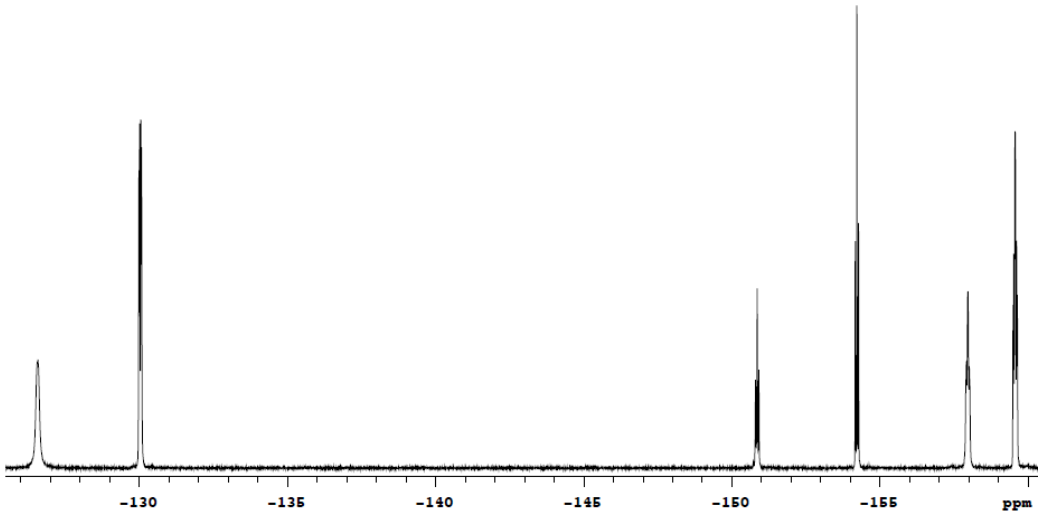

^{19}F-NMR of **10** mixed with **27** in toluene-d8 after 12 days

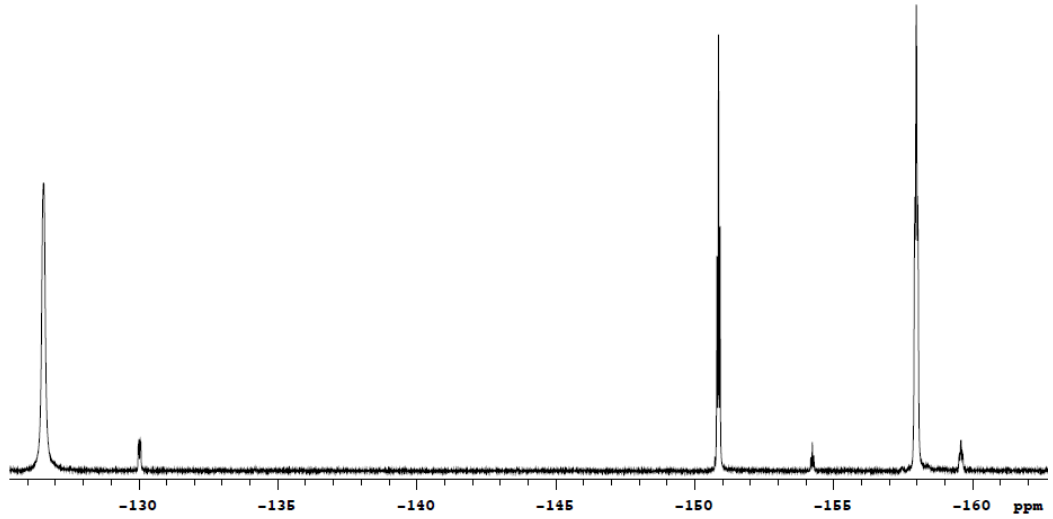

^{19}F-NMR of **10** mixed with **27** in toluene-d8 without hydrogen after 1 day

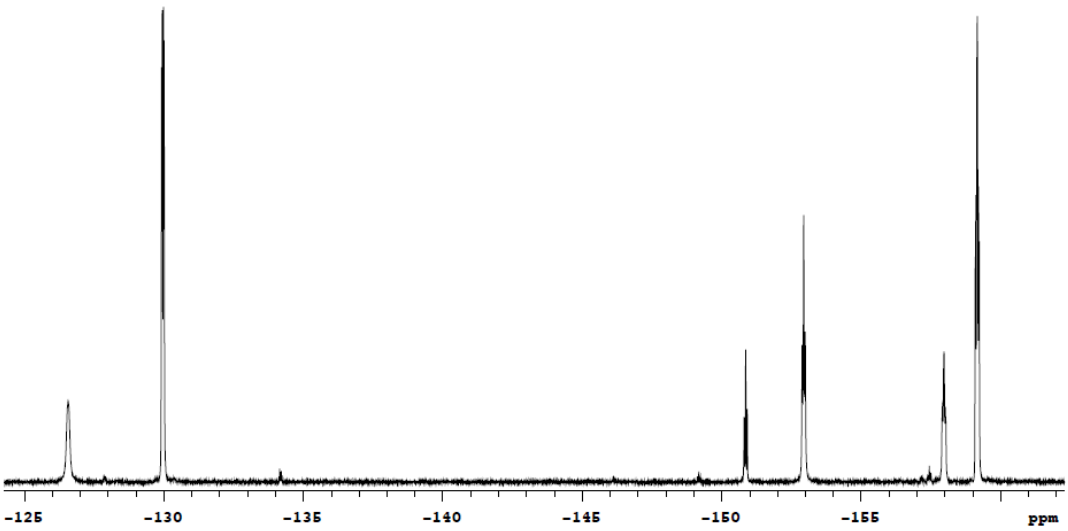

^{19}F-NMR of **10** mixed with **27** in CD_2Cl_2

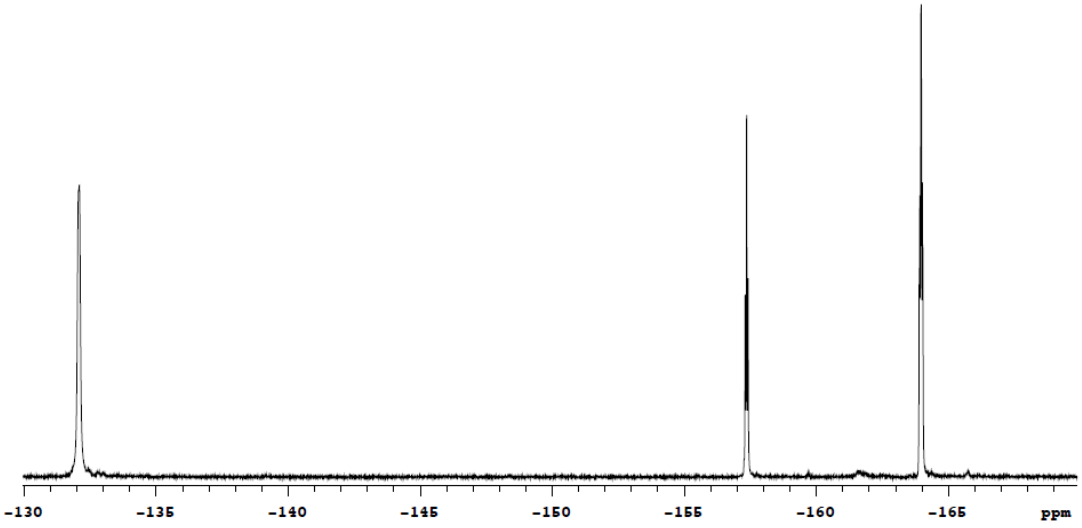

^{19}F-NMR of **10** mixed with **27** in CD_2Cl_2 after two days

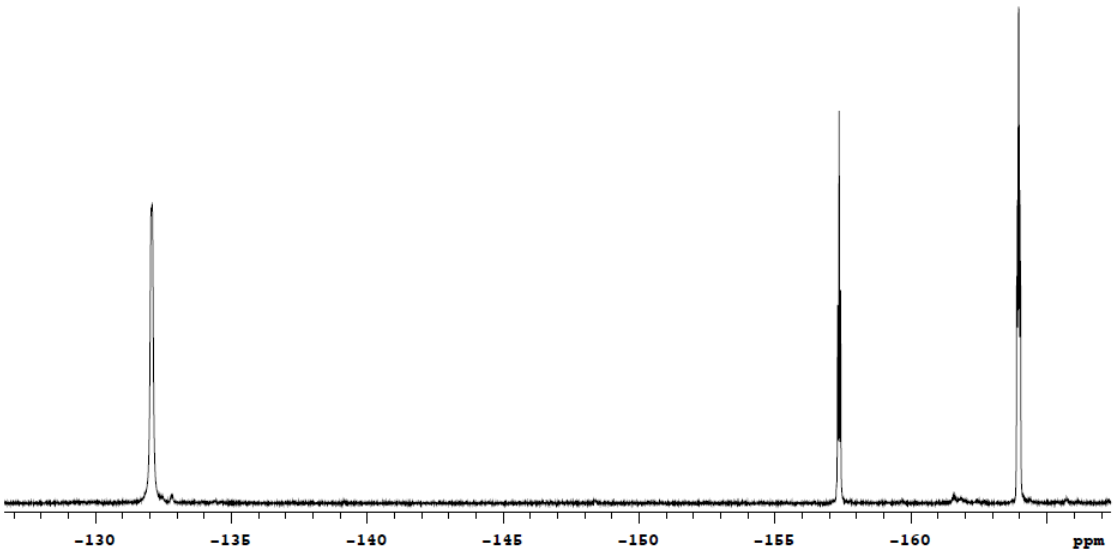

^{19}F-NMR of **10** mixed with **27** in CD_2Cl_2 with H_2

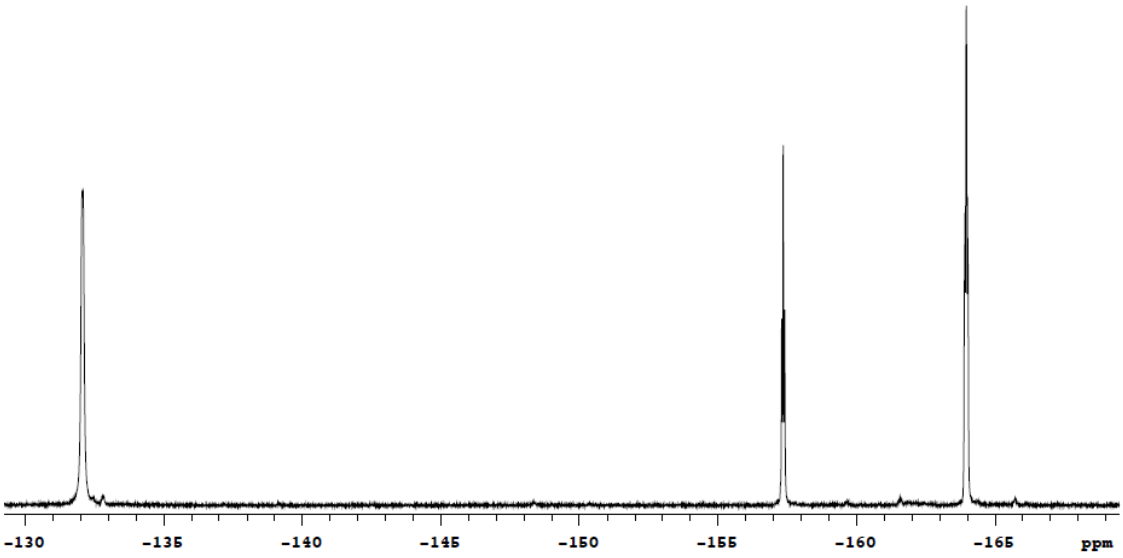

^{11}B-NMR of **10** in toluene-d8 (impure)

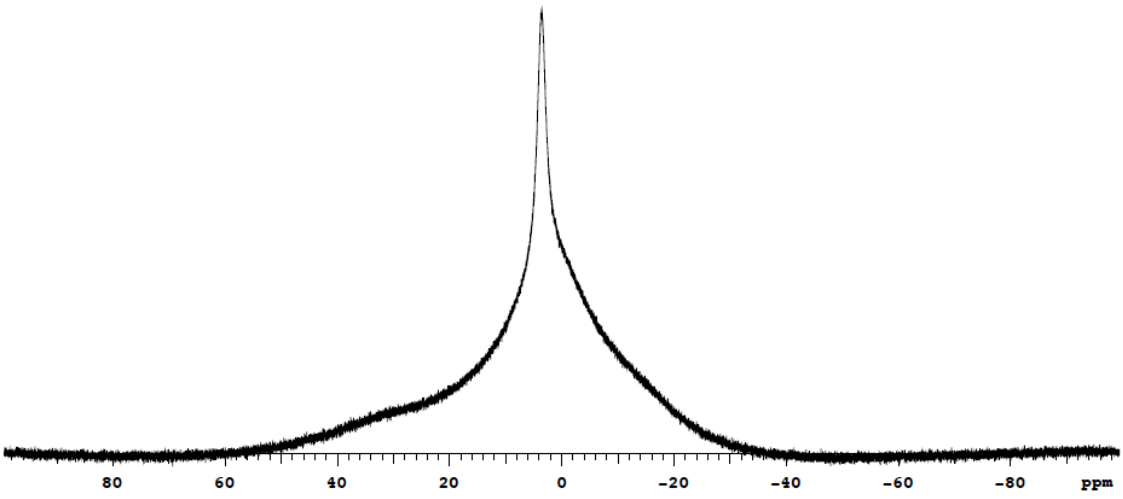

^{11}B-NMR of **10** in CD_2Cl_2

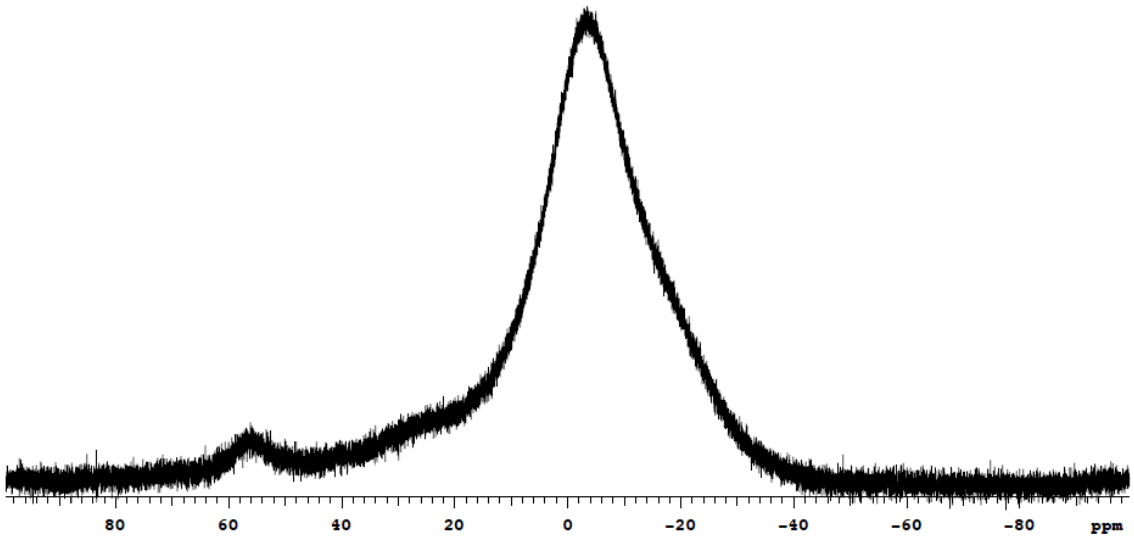

^{11}B-NMR of **10** mixed with **27** in CD_2Cl_2

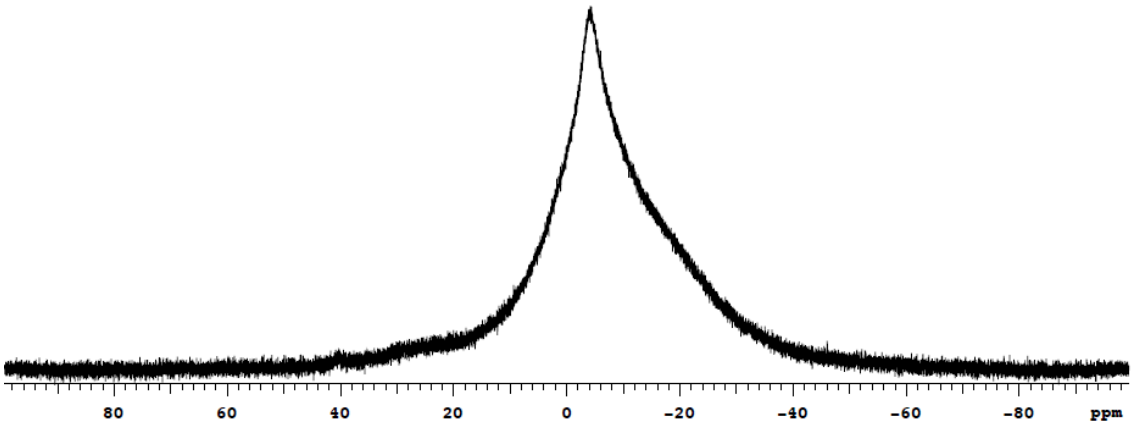

APT-NMR of **21**

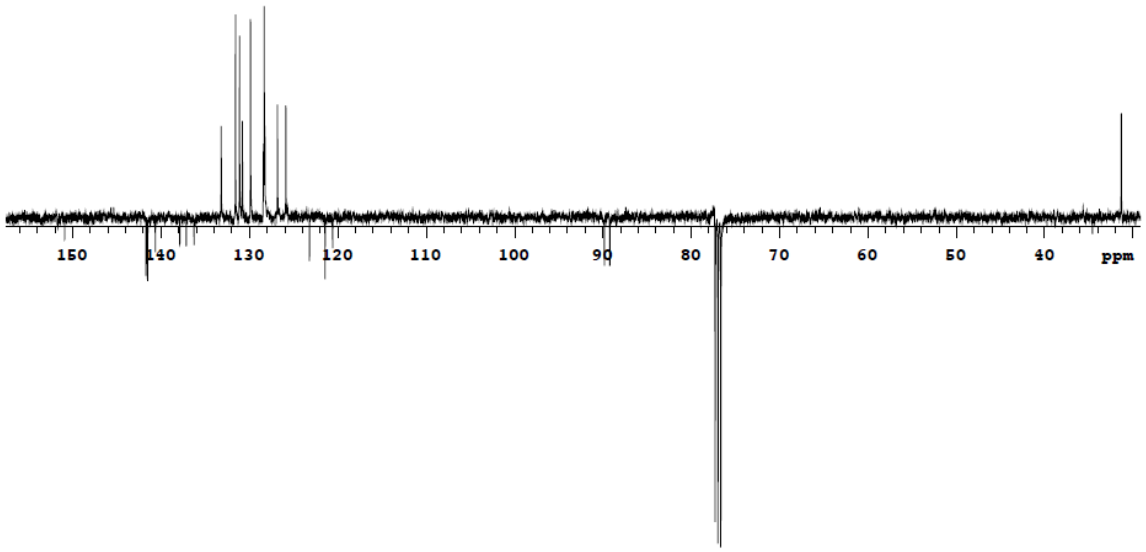

COSY-NMR of 21

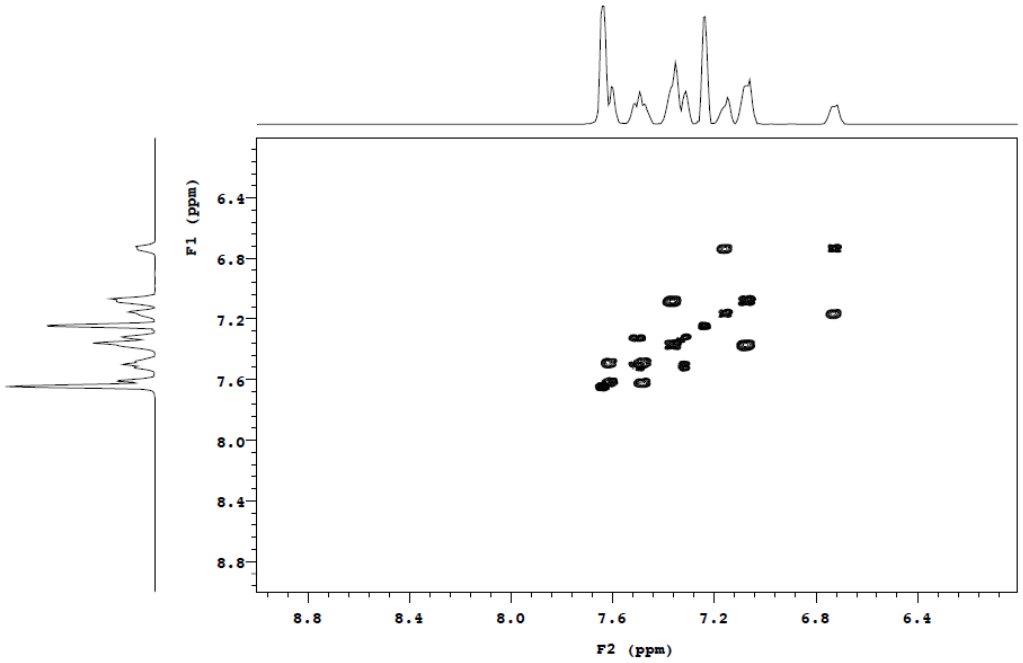

HMQC-NMR of 21

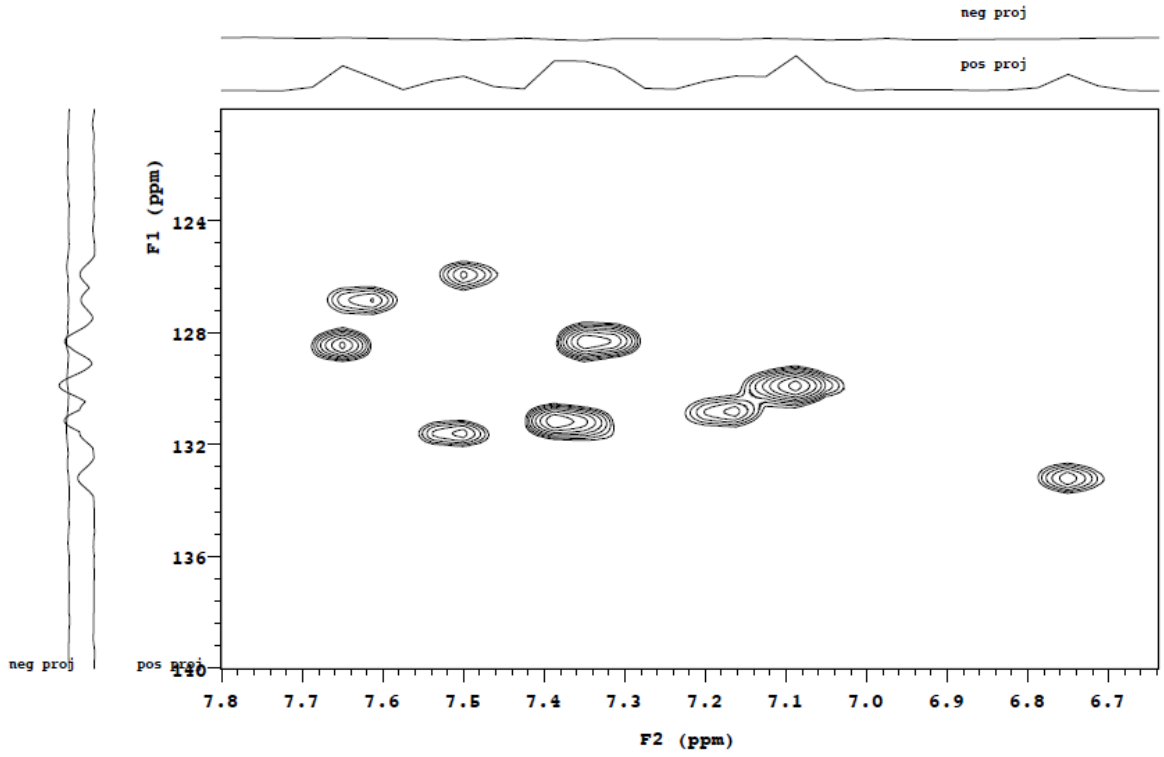

ESI-MS of 21

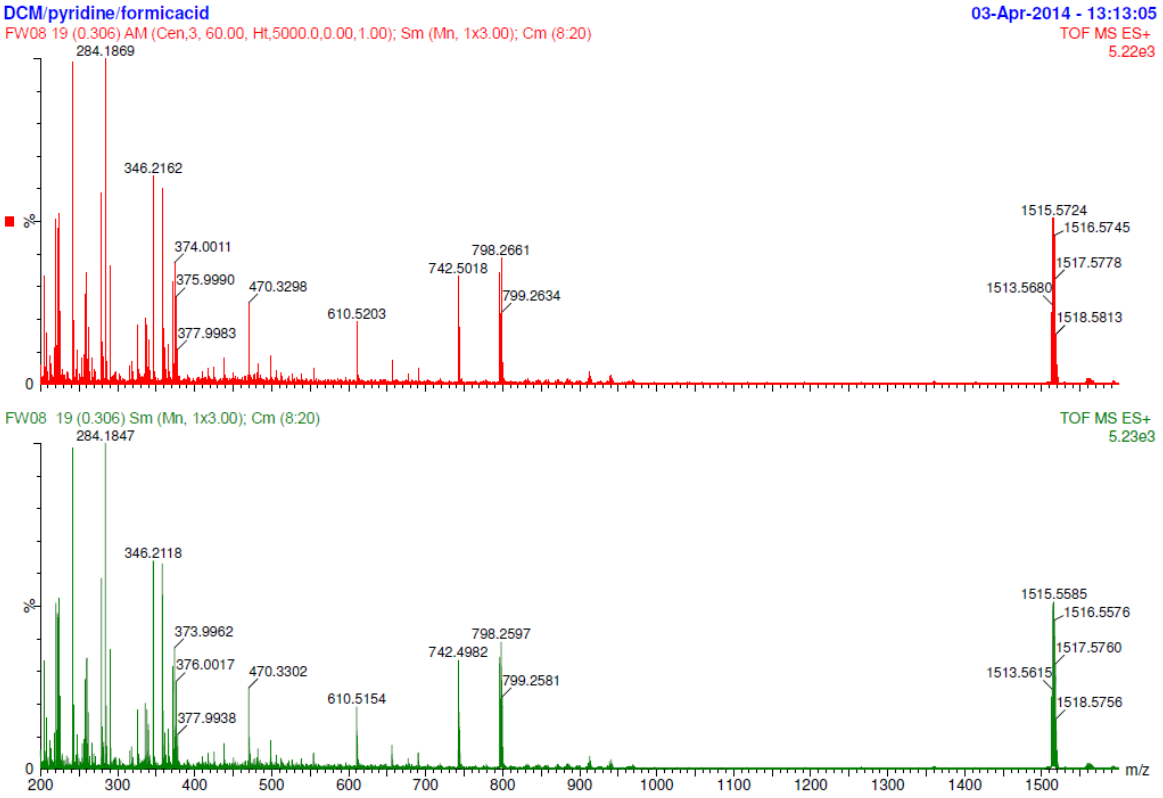

ESI-MS of 27

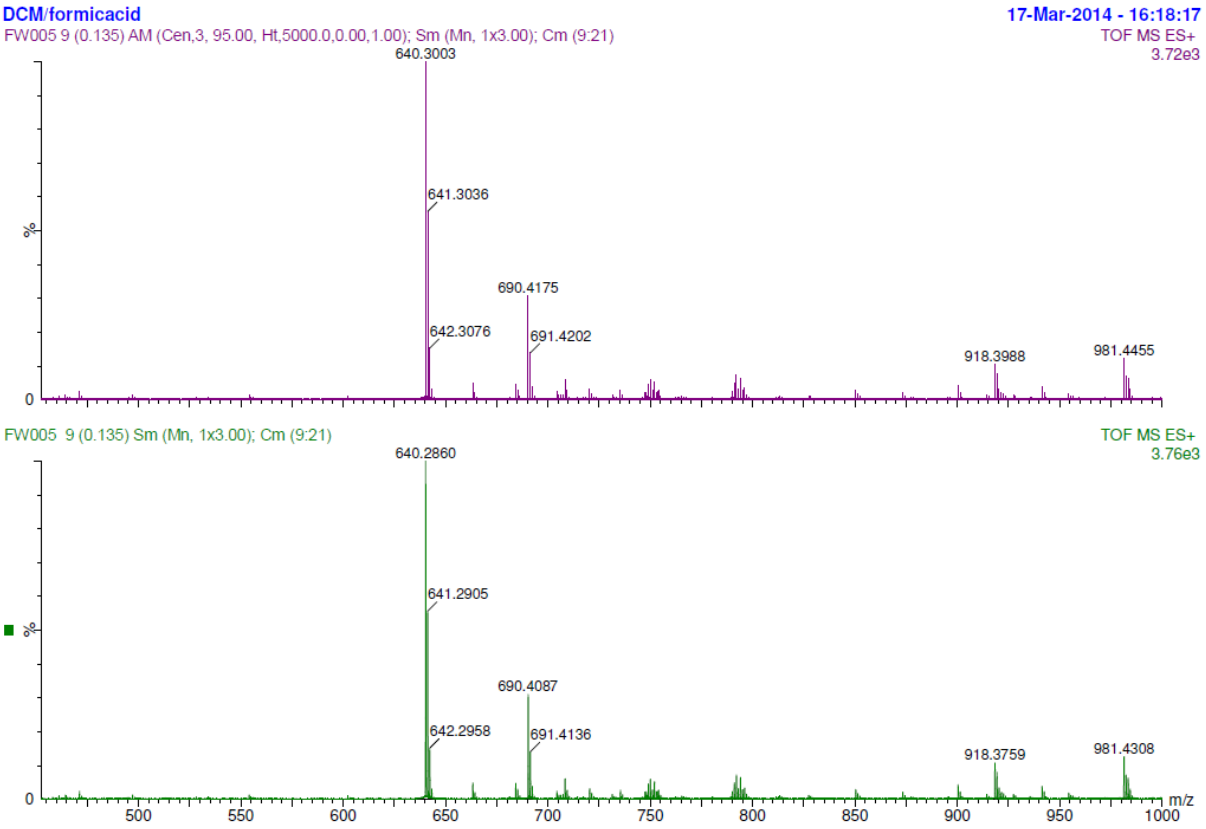

ESI-MS of 32

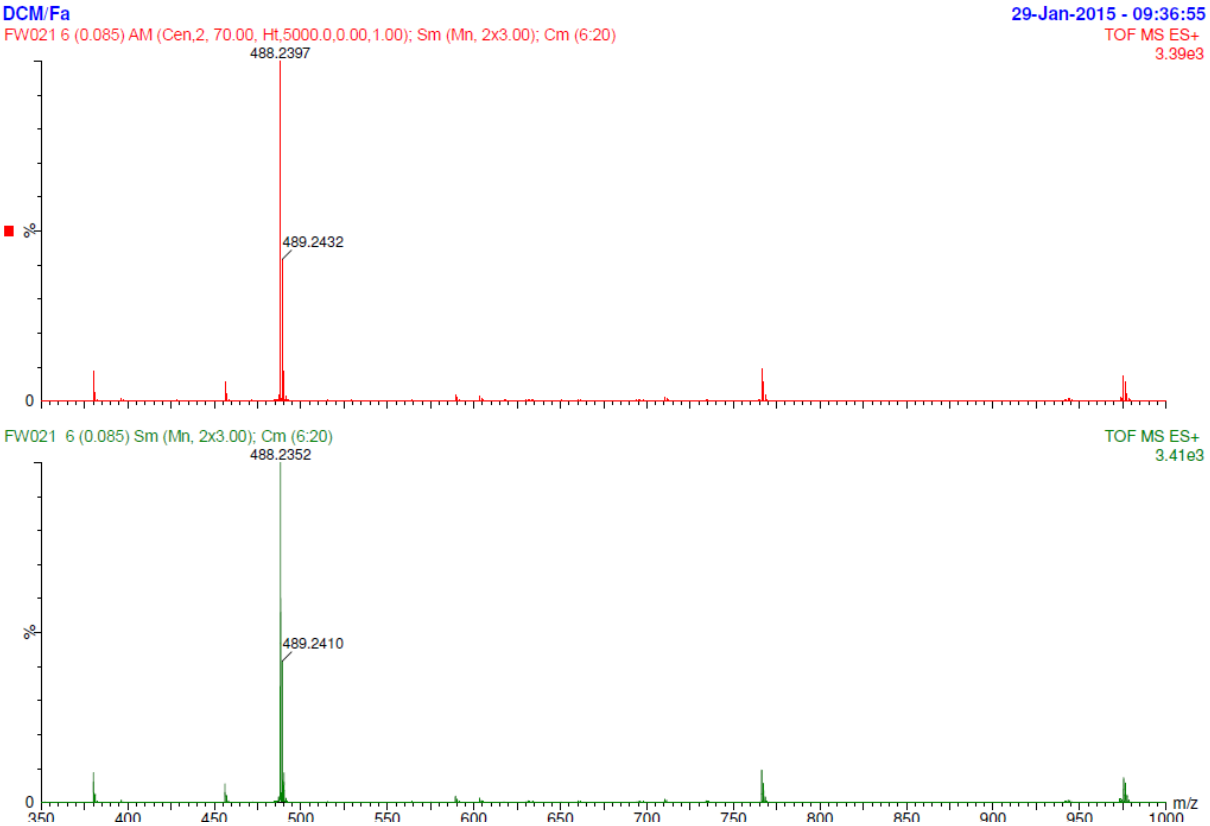

ESI-MS of 35

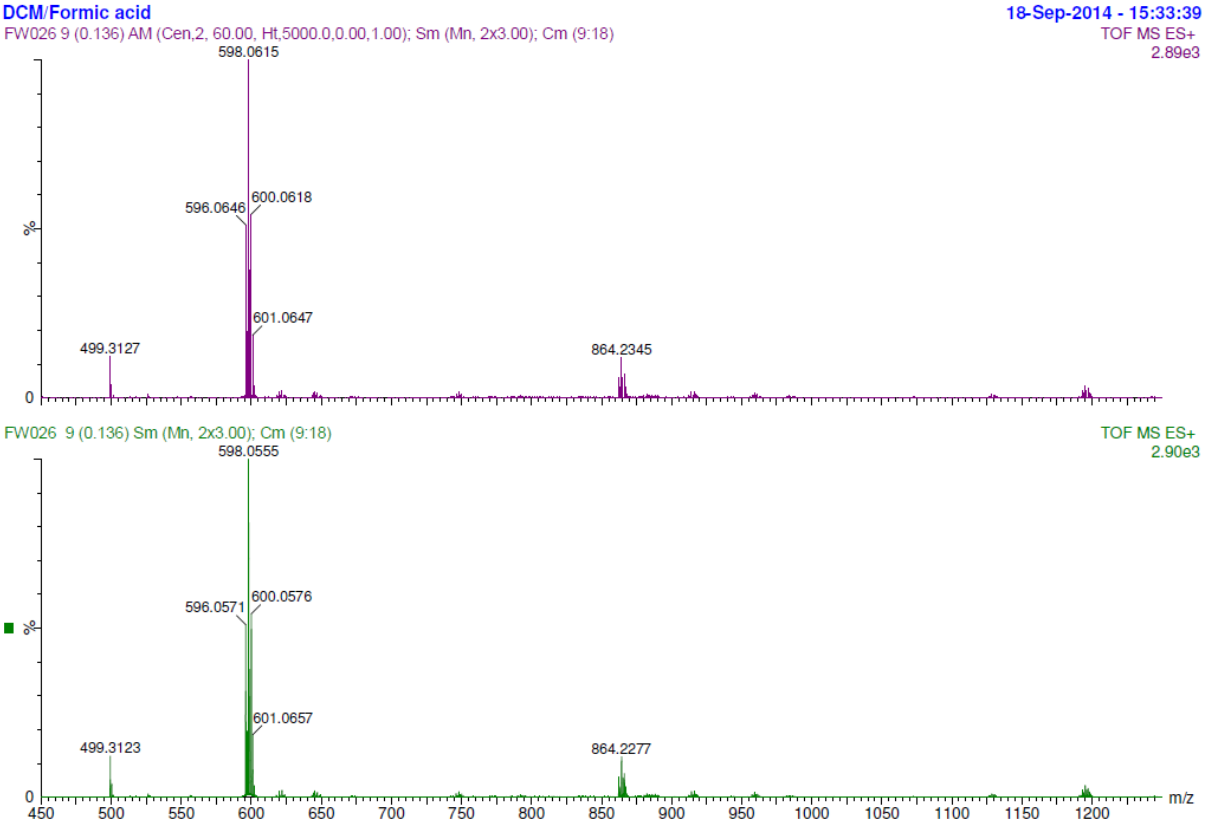

ESI-MS of 37

ESI-MS of 39

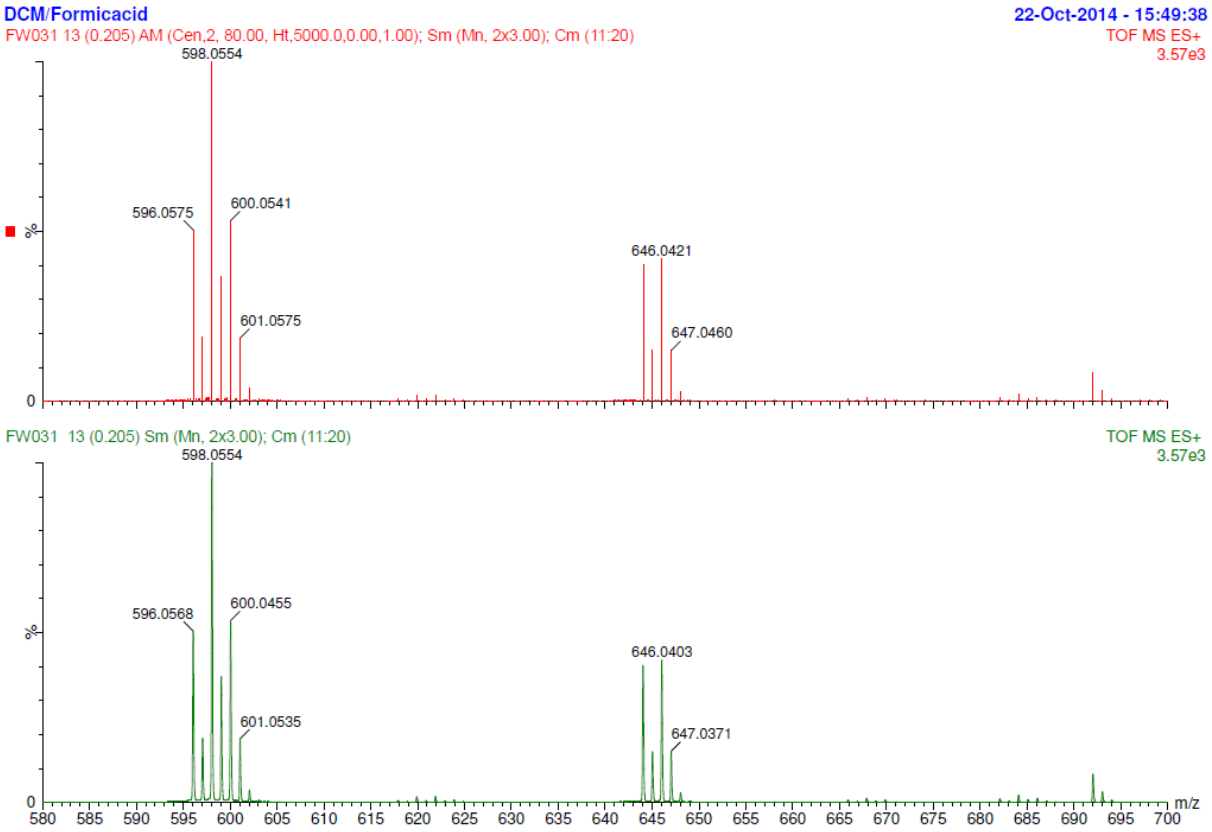

ESI-MS of 41

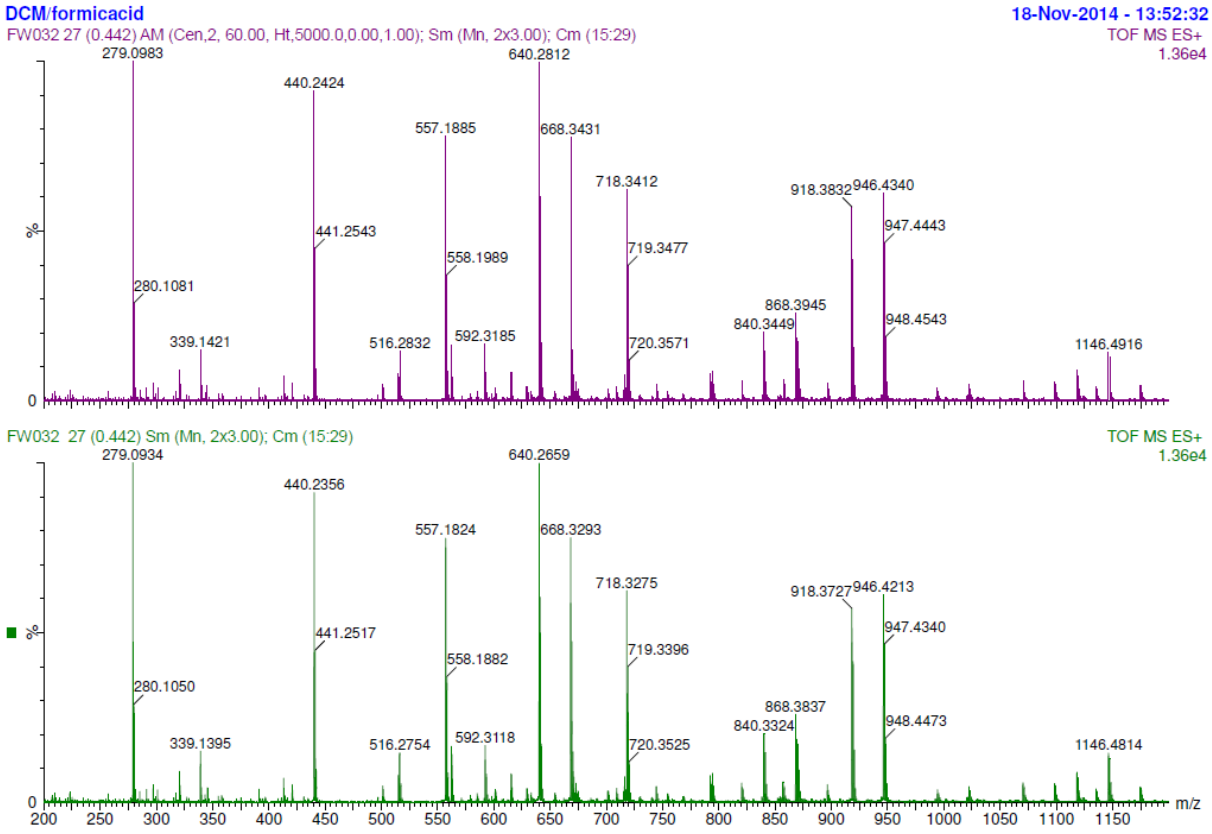
DCM/formicacid
18-Nov-2014 - 13:52:32
FW032 27 (0.442) AM (Cen,2, 60.00, Ht,5000.0,0.00,1.00); Sm (Mn, 2x3.00); Cm (15:29)
TOF MS ES+
1.36e4
279.0983
640.2812
440.2424
557.1885
668.3431
718.3412
918.3832
946.4340
947.4443
441.2543
719.3477
558.1989
280.1081
868.3945
840.3449
948.4543
339.1421
516.2832
592.3185
720.3571
1146.4916
%
0
FW032 27 (0.442) Sm (Mn, 2x3.00); Cm (15:29)
TOF MS ES+
1.36e4
279.0934
640.2659
440.2356
557.1824
668.3293
718.3275
918.3727
946.4213
947.4340
441.2517
719.3396
558.1882
280.1050
868.3837
840.3324
948.4473
339.1395
516.2754
592.3118
720.3525
1146.4814
%
0
200 250 300 350 400 450 500 550 600 650 700 750 800 850 900 950 1000 1050 1100 1150
m/z

FTIR of 21

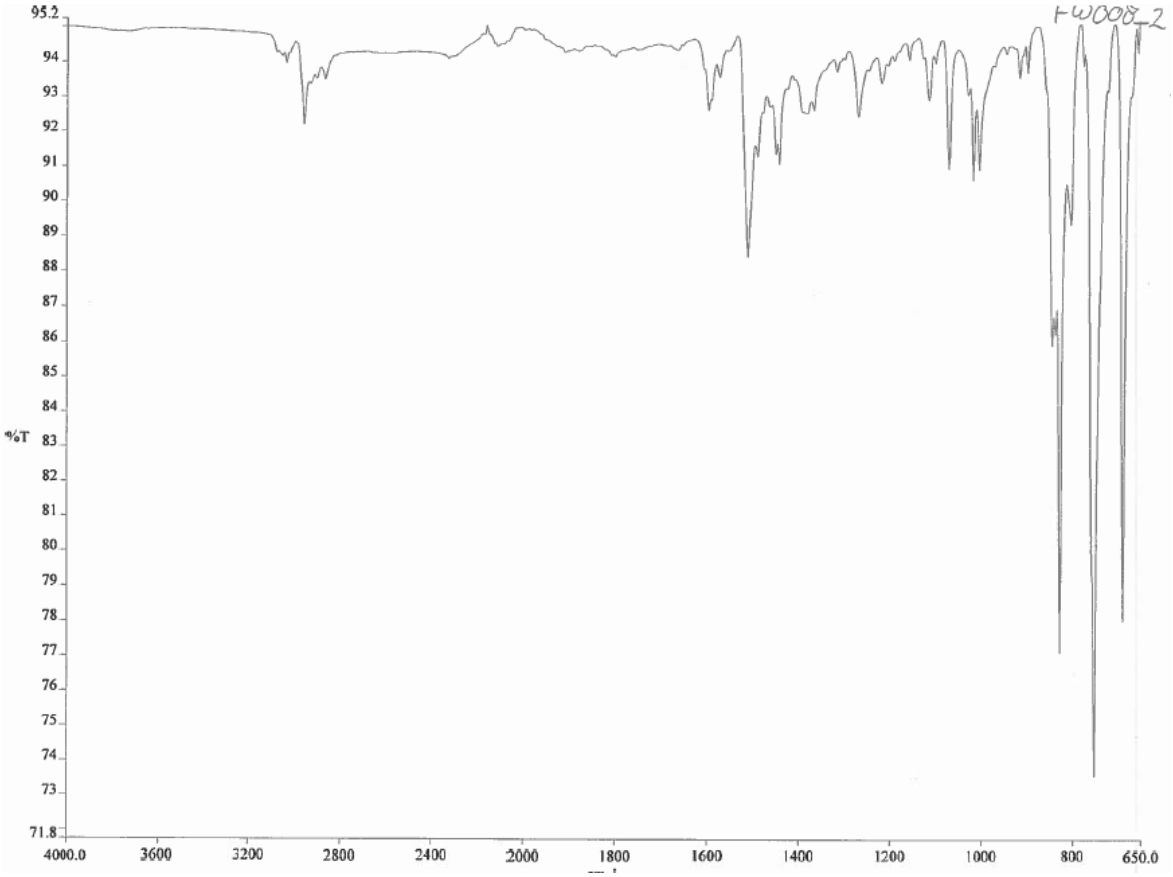

FTIR of 27

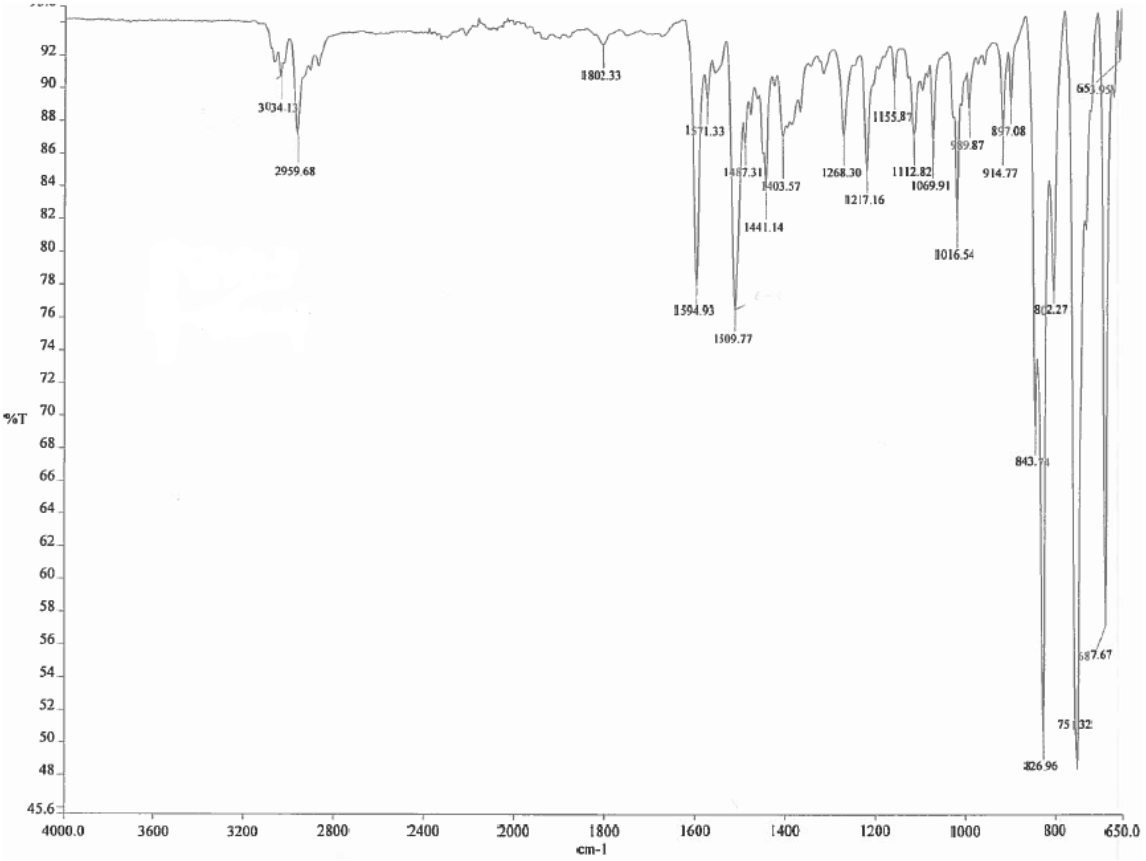

FTIR of 32

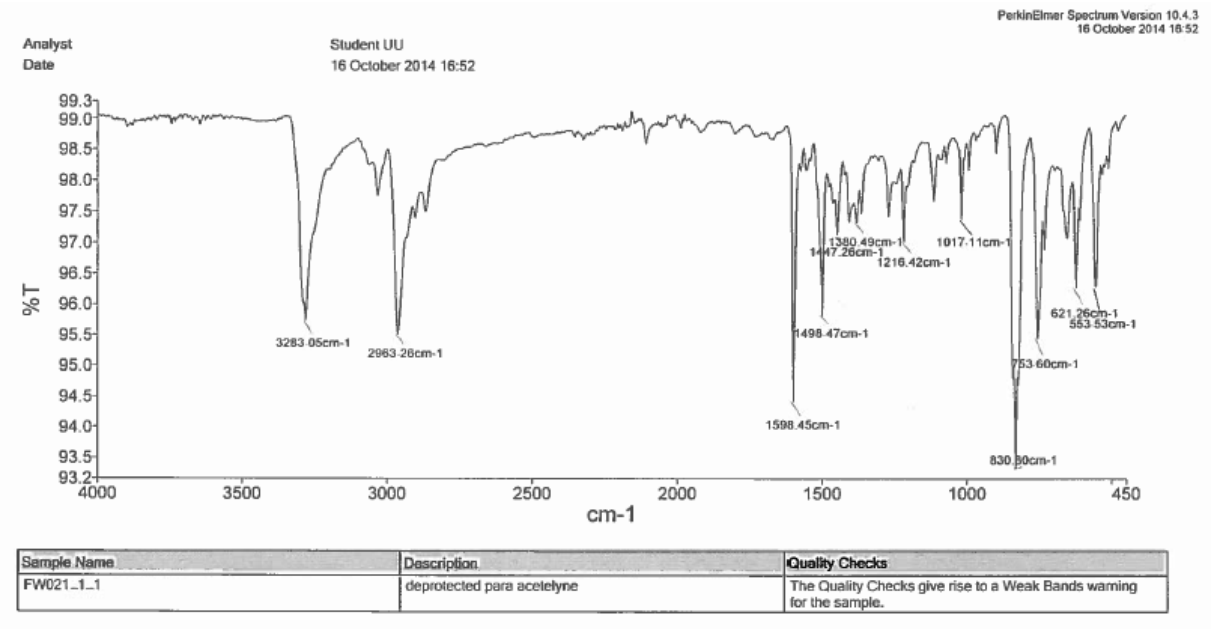

Sample Name	Description	Quality Checks
FW021_1_1	deprotected para acetelyne	The Quality Checks give rise to a Weak Bands warning for the sample.

FTIR of 35